

A fault kinematic and geomorphological study of the Late Cenozoic Ilgin
Basin, Central Anatolia, Turkey

MSc. Thesis

by

Marijn Koopman

*Earth Science Department, Utrecht University,
Budapestlaan 4, 3584 CD Utrecht*

September 2011

Abstract

The Ilgin Basin in Central Anatolia is the southeastern extension of the Akşehir-Afyon Basin, situated at the eastern periphery of the Isparta Angle region. The basin geometry, its patterns of sediment infill and its kinematics are controlled by the interference between Late Cenozoic (i.e. neotectonic) overprints and re-activation of old, largely pre-Cenozoic, structures. This thesis provides new structural and geomorphological data aiming to understand the structural complexities involved with such interference and a critical note about the relevance of outcrop-scale observations for regional-scale interpretations of the associated kinematics. The interconnectivity and interaction between intersecting faults and the presence of pre-existing basement structures in the Ilgin Basin and adjacent basin regions are major complications to the application of the stress inversion method. An integration of outcrop-based fault slip data and structural analysis using a Digital Elevation Model is therefore essential to reconstruct their meaning in terms of kinematic evolution of the Ilgin Basin. Fault geometries and their kinematic analysis indicate that transtension in the Ilgin basin is influenced by a small but geometrically significant, left-lateral shear component. This kinematic model inferred for the Ilgin Basin is not in line and therefore difficult to correlate with the deformation kinematics of Late Cenozoic fault zones to the north and northeast.

Contents

Introduction	2
1. Regional geological history of Anatolia	5
Early evolution.....	5
Collision and collapse.....	6
Neogene basin development	7
2. Regional structural setting.....	9
Isparta Angle.....	11
Previous studies on the Akşehir-Afyon Basin	12
3. Stratigraphy and structural framework of the Ilgin Basin.....	14
Methods	15
Stratigraphy of the Ilgin Basin.....	21
<i>Early and Middle Miocene</i>	21
<i>Middle- Late Miocene</i>	22
<i>Pliocene-Quaternary</i>	22
General structural characteristics of the Ilgin Basin.....	24
Fault orientations and structural trends.....	27
~ <i>E-W to WNW-ESE fault trends</i>	29
<i>NNE-SSW fault trends</i>	29
<i>NE-SW fault trends</i>	29
Akşehir Fault Zone	36
Derbent Fault Zone	42
Çhavuşgöl Fault Zone.....	45
4. Basin geometry and kinematics: discussion.....	55
5. Implications of present study	64
Implications for the stress Inversion Method	64
Regional implications of the Ilgin basin kinematics.....	65
6. Conclusions	69
Acknowledgements	69
References	70

Introduction

The Ilgin Basin is a relatively small (~50x50 km) Neogene to recent, fault-controlled depression in the Central Anatolian region of Turkey (Figure 1). It is situated at approximately 38° 8.700' N latitude and 31° 51.800 E longitude, between the main towns of Konya (at 60 km to the southeast) and Akşehir (at 45 km to the northwest). The geomorphology is controlled by a major NW-SE trending fault zone, known as the Akşehir Fault zone. The Sultandağı is a mountainous upthrown region to the SW of the basin, elevated to nearly 2000 m, and characterized by exposed metamorphic rocks of largely Cambrian to Permian age.

The Ilgin Basin is a neotectonic fault-controlled basin, filled with Miocene to Quaternary lacustrine sediments on top of a Cambrian to Mesozoic basement. Details on the evolution of the Ilgin Basin are relatively unknown and poorly documented (General Directorate of Mineral Research and Exploration, Ankara/Turkey, 2009), while literature about the region on the early-plate tectonic history (e.g., Robertson, 2000; van Hinsbergen et al 2009) and the neo-tectonic setting (e.g., Sengör et al., 1985; Bozkurt , 2001) is substantial.

The Ilgin Basin shares its Late Cenozoic development and sediment infill with a number of larger and somewhat better known fault-controlled basins in Central Anatolia, such as the basins of the inner Isparta Angle (i.e., Lycian, Aksu, Köprü and Manavgat basins; Flecker et al., 2004), Akşehir-Afyon (Koçyiğit et al., 2003), Tuzgözü (e.g. Çemen et al., 1999) and Sivas (e.g., Yılmaz et al., 2006). The primary structure of the basement in these analogue basin settings is different and is associated with variable histories of deformation. Moreover, the Late Cenozoic to present-day basin evolution is laterally non-uniform, time-transgressive and controlled by local kinematics.

Late Cenozoic deformation in the Ilgin Basin seems to be controlled by interference between the regional-scale basement structure (i.e. the paleo-structural setting), and the currently active neo-tectonic setting. The basin geometry, its patterns of sediment infill and its kinematics are controlled by Late Cenozoic overprints and re-activation of old (largely pre-Cenozoic) anisotropic structures. A contribution to understand structural complexities involved with this interference, based on new fault-kinematic and geomorphological field observations is the main objective of this thesis.

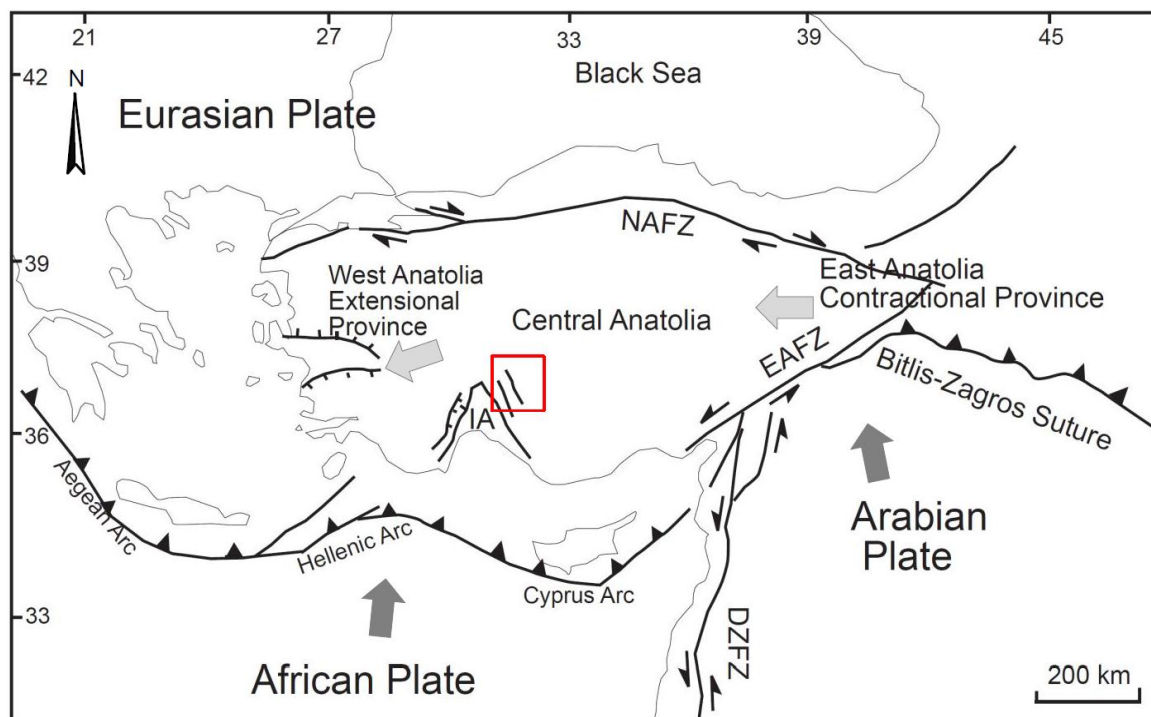


Figure 1. Simplified tectonic map of Anatolia showing the major neotectonic structures and provinces (modified from Bozkurt, 2001). NAFZ – North Anatolian Fault Zone, EAFZ – East Anatolian Fault Zone, DSFZ – Dead Sea Fault Zone, IA – Isparta Angle. Heavy lines with half arrows are the major strike-slip zones, heavy lines with triangles indicate the active subduction zone at the Aegean, Hellenic and Cyprus arcs. Other heavy lines with triangles indicate the major fold and thrust belt at the Bitlis-Zagros Suture. Red box is the location of the study area. Dark arrows indicate relative direction of movement of the Arabian and African plates; light grey arrows indicate relative movement of Anatolia.

Research Objective

The main objective of this study is to understand the structural history of the Late Cenozoic Ilgin Basin and to elucidate the tectonic history of Central Anatolia, with emphasis on (sub) recent faulting. The Ilgin Basin in Central Anatolia is located in a transition zone between two regional-scale tectonic domains. East Anatolia forms an easterly domain showing a tectonic evolution dominated by collision of Arabia and Eurasia. Western Anatolia on the other hand is severely affected by back-arc extension associated with roll-back of the African Plate. In the transition zone between these two domains, terrestrial basins including the Ilgin Basin were associated with and modified by transtensional deformation. Structural studies in this basin setting are crucial to understand the interaction between the above mentioned dynamic processes and their kinematic consequences. With the aim to link the basin-scale observations with the regional structural setting, this thesis proposes a plausible kinematic scenario for the evolution of the Ilgin Basin using new fault-slip and geomorphological data as well as a detailed DEM (Digital Elevation Model) analysis.

Outline of this thesis

Section 1 provides a short summary of the regional geological history and (plate-tectonic) framework of Anatolia to present the paleo-setting of the basin substratum and its major structures.

In **Section 2** the focus will be on the regional setting of major structures and fault zones in Anatolia. I will zoom in on the Isparta Angle and Ilgin Basin setting.

The newly acquired data of the Ilgin Basin and their analysis are presented in **section 3**. This includes fault-slip measurements from several outcrops in the basin and a structural DEM analysis of the region.

In **section 4**, an integration of the new structural data and regional evaluations of section 1, 2, and 3 are presented, with the aim to give an explanation for the relationship between the fault orientations and kinematics and basin geometry.

In **section 5** I will discuss the interpretations and implications of the proposed kinematic basin model and integrate the results with the regional geology of Central Anatolia. **Section 6** provides a brief summary of the main conclusions of this thesis.

1. Regional geological history of Anatolia

Early evolution

In the Early Cretaceous (~110 Ma) the Tethys Ocean separated the Supercontinent Gondwana in the South from the Eurasian assembly in the North. Instead of a single ocean, the Tethys Ocean consisted of several oceanic seaways, separated by island arcs and microcontinents. This seaway formed a gateway, connecting what is now known as the Indian Ocean through the Mediterranean Sea to the Atlantic Ocean. From the Early Cretaceous onward, the progressive closure of the Tethys resulted in the accretion and amalgamation of continental fragments, followed by continent-continent collision, forming the single landmass of Anatolia in the course of the Cenozoic. Generally two branches of Neotethys are recognized in the present-day configuration, a northern Neotethys, and a southern Neotethys. Northern regions, called the Strandja, Istanbul and Sakarya terranes are parts of the Pontides. The Anatolide-Tauride terranes are located in the southern Anatolia. Although still heavily debated what affinities the northern and southern terranes of Anatolia have, it is generally thought that the Pontides show affinity with Laurussia while the Anatolide-Tauride terrane has a Gondwana affinity. In the Late Cretaceous oceanic closure was followed by continent-continent collision between the northern and the southern terranes. Intra-oceanic subduction resulted in widespread ophiolite emplacement and high-pressure metamorphism (Robertson et al 2009; van Hinsbergen et al., 2009). The subduction thrusts between the terranes were relocated northward during the Paleocene-Eocene, leading to the final continent-continent collision between the Taurides and Pontides (Robertson et al 2009; Kaymakci et al 2009; van Hinsbergen et al., 2009). By Oligocene time, Anatolia was largely a single landmass, highly non-uniform by inheritance from the terrane amalgamation during its preceding structural history. Inevitably, a multitude of strength anisotropies must have played a prominent role in the Late Cenozoic to neo-tectonic evolution and basin development. Re-activation of pre-existing structures has influenced the structural style, the tectono-stratigraphy, and the kinematics of deformation in the Ilgin Basin, the objective of this study.

Collision and collapse

The northward movement of Africa and Arabia towards Eurasia is at present still active and ongoing. In the Anatolian region major embayments along the converging continental margins have a prominent influence on lateral changes in structural setting from east to west. In the east, continent-continent collision between Arabia and Anatolia is followed by break-off of the subducted Arabian slab in the Miocene (Keskin 2003; Faccenna et al. 2006; Hafkenscheid et al. 2006; Hüsing et al. 2009; van Hinsbergen et al., 2009). This is in line with the study of Hüsing et al. (2009), who studied the youngest foreland basin deposits associated with the collision of Arabia with the Anatolide-Tauride region and suggested that these sediments with an age of 11 Ma are linked to slab break-off, marking the end of subduction of the Arabian plate. In the west, at the Hellenic and Cyprus arcs, subduction of the African slab under Anatolia is associated with roll-back of the subducting slab, slab break-off and activity of Subduction Transform Edge Propagation faults (STEPS; Govers & Wortel, 2005). During and in response to these processes, Anatolia is laterally extruding westward, accommodated along major strike-slip fault zones, i.e. the North Anatolian Fault Zone and the East Anatolian Fault Zone (Dewey & Sengör, 1979; Sengör et al., 1985, 2005; Hubert-Ferrari et al., 2002; 2009). This is in line with the study of Hubert-Ferrari et al. (2002, 2009) who suggest an age of 12-10 Ma for the onset of the activity of the North Anatolian Fault Zone. The development of the NAFZ and the EAFZ together with the westward movement of Anatolia are associated with the relative difference in velocity between the overall northward migrating Arabian and African plate. The Arabian plate moves to the N to NW at a rate of 25 mm/yr (Reilinger et al., 1997; Oral et al., 1995; DeMets et al., 1990, 1994; Barka et al., 1997) and Africa has a northward movement at a rate of 10 mm/yr (Oral et al., 1995; Barka et al., 1997). The relative difference in velocity is accommodated by left-lateral strike-slip displacement along the Dead Sea Fault Zone. As a consequence to these processes of slab-break off, roll-back and westward lateral extrusion, Anatolia is divided into partly overlapping domains of exhumation, deformation and sedimentation (Hinsbergen et al., 2009). It is likely that during and in response to these tectonic processes, pre-existing structures or strength anisotropies are easily reactivated and may play a significant role in the orientation and kinematics of newly developed structures. These 'weak' zones are present as a basement fabric, associated with variable histories of deformation. The transition between these two tectonic domains of collision in the east and ~N-S back-arc extension due to roll-back in the west, is located at the Aegean and western Anatolian regions. These regions are affected by continental extension

and exhumation of metamorphic core complexes (e.g., the Menderes Metamorphic Core Complex. Lister et al. 1984; Gautier et al. 1993; Gautier & Brun 1994; Bozkurt & Oberhänsli 2001; Gessner et al. 2001; Jolivet 2001; Ring & Reishmann 2002; Jolivet et al. 2003; Edwards & Grasemann 2009; Papanikolaou et al. 2009; Sen & Seyitoğlu 2009; Tirel et al. 2009; van Hinsbergen & Boekhout 2009; van Hinsbergen et al., 2009) and a lateral change in type of volcanism (Pe-Piper & Piper 2002; Dilek & Altunkaynak 2009). The onset of widespread volcanism at 13-11 Ma is associated with a rapid uplift of eastern Anatolia (Dewey et al. 1986; Pearce et al. 1990; Keskin 2003; Şengör et al. 2003; Hüsing et al., 2009), related to detachment of the northward dipping subducted lithosphere at the Arabian-Eurasian convergence zone (Keskin 2003; Faccenna et al. 2006; Hafkenscheid et al. 2006; Hüsing et al., 2009). Dilek & Altunkaynak (2009) studied the igneous and metamorphic rocks of Anatolia and found a southward migration and compositional variation of volcanism and magmatism since the Eocene. Van Hinsbergen summarized the main findings of Dilek & Altunkaynak (2009) as follows: volcanism was initiated by slab-break-off and changed its composition southward due to asthenospheric flow as a consequence of lithospheric delamination. Volcanism in the Middle Miocene is related to lithospheric extension and the formation of the Menderes metamorphic core complex. In the Quaternary, volcanism in western Anatolia changed to an alkaline composition, related to uncontaminated mantle flow.

Neogene basin development

During the Miocene to Quaternary, intramontane, extensional/transensional and fault bounded basins developed mainly in the western and central regions of Anatolia. (Şengör and Yilmaz, 1981; Robertson and Dixon, 1984; Şengör et al., 1985; Zanchi et al., 1993). In mid-Pliocene to recent times, several of these young, neotectonic basins are connected and characterized by marine sedimentation. These include the Aksu, Köprü, Manavgat, Adana, Mut and Ermenek basins in southern Anatolia (e.g., Flecker et al., 1995, 2004; Glover and Robertson, 1998a; Tanar and Gokçen, 1990; Karabıyıkoglu et al., 2000; Satur et al., 2000; Ilgar and Nemeç, 2004; Alçiçek et al., 2005). Other basins, such as the inner Büyük Menderes Basin, Burdur, Alaşehir/Gediz, Simav, Akşehir-Afyon, Ilgin and Çameli basin, remained fully terrestrial and are characterized by alluvial and lacustrine sedimentation (e.g., Price and Scott, 1991; Seyitoğlu and Scott, 1996; Seyitoğlu, 1997; Koçyiğit et al., 2000a; Bozkurt, 2000; Alçiçek, 2001). The development of many of these Neogene to Quaternary basins are often related to multiple episodes or pulses of extension (e.g. Koçyiğit et al., 2000a; 2003), but

several basins experienced tectonic inversion, related to pulses of post-orogenic compression or transtension during the mid-Miocene and/or Pliocene (Flecker et al., 1995, 2004; Koçığıt et al., 1999, 2000; Karabıyıkoglu et al., 2000). Many studies on these basins are focused on the lithological and stratigraphic characteristics (e.g., Becker-Platen, 1970; Erakman et al., 1982; MeYhur and AkpVnar, 1984; Sfbilir and Emre, 1990; Xenel, 1997a, b, c) but little is known about the sedimentation patterns and deformation structures such that the subsidence and fault kinematic history of the basins remained unconstrained. Moreover, the Ilgin Basin is documented in terms of its lithological and stratigraphic character, but a structural study is lacking. The Ilgin Basin is located next to, and connected with the Akşehir-Afyon Basin to the northwest. The Sultandağı Mountain range, and its parallel-trending Akşehir Fault zone, forms the southwestern boundary for both basins. Based on similarities in lithological character, their common NW-SE trend and western bounding margin, the Ilgin and Akşehir-Afyon basins may have experienced a similar early evolution in deformation and deposition. The boundary between both basins is therefore, not clearly defined.

2. Regional structural setting

The active dextral North Anatolian Fault Zone (NAFZ) and the sinistral East Anatolian Fault Zone (EAFZ) are considered as the main tectonic boundary zones of the Central Anatolia highland (Figure 2). These major structures are, together with the Dead Sea Fault Zone (DSFZ) and the subduction-related processes at the Hellenic and Cyprus arcs, responsible for a broad region of distributed and overlapping zones of active deformation in Anatolia (Görsöy 2003; see also paper from Bozkurt 2001). Secondary faults bifurcate off from the NAFZ and EAF Fault zones, and divide Central Anatolia in smaller domains of more local deformation. These faults form patterns of smaller, en-echelon relaying fault segments, extending hundreds of kilometers into Central Anatolia. These segmented zones are characterized by both left and right-lateral strike-slip components. Moreover, in eastern Central Anatolia, most E-W trending zones are characterized by strike-slip with reverse components, while the NE- to NNE trending fault zones generally have a normal oblique-slip character (e.g. Bozkurt and Koçyigit 1996; Bozkurt, 2001) Major active fault zones include the NE-SW-trending left lateral Central Anatolian Fault zone (CAFZ), the NW-SE trending right-lateral Tuzgölü Fault zone (TFZ), the WNW-ESE-trending Eskişehir, and NNW-SSE-trending Akşehir oblique-slip normal fault zones.

The CAFZ extends ~730 km from east Anatolia to the Eastern Mediterranean Sea, parallel along the East Anatolian Fault zone. NE-SW trending, left-lateral strike-slip faults are associated with reactivation of NE-SW extending, paleotectonic structures (i.e. the Ecemiş Corridor or Ecemiş Fault; Bozkurt, 2001) during the Plio-Quaternary. Pull-apart basins located within the CAFZ indicate significant amounts of extension associated with left-lateral transtension. Paleomagnetic data from 1-2 Ma volcanics located in the same region indicate ~10° anticlockwise rotation during the last 1 Ma (Tatar et al., 2000), suggesting relatively recent fault activity.

The Tuzgölü Fault zone is a prominent geomorphological structure that trends 200 km to the NW-SE. The Tuzgölü pull-apart basin, located along this zone indicates that right-lateral transtension is associated with a significant component of normal-slip.

Deformation in the NW-SE trending Eskişehir Fault zone is associated with minor components of right-lateral displacement (Ocakoglu 2007). The NW-SE Akşehir Fault zone along the Sultandağı Mountain range is a normal-oblique fault zone, located at the outer eastern flank of the Isparta Angle (Blumenthal, 1963). Displacements along this fault zone are associated with transtension with a minor left-lateral component (this study). The Akşehir-Afyon and Ilgin Basins are located at the hanging-wall side of the Akşehir Fault, along the NW-trending Sultandağı Mountain range that forms the footwall. This prominent mountain range forms the eastern outer flank of the triangular-shaped Isparta Angle. In order to place the studied Ilgin Basin in a regional structural context, the structural and geomorphological characteristics of the Isparta Angle will be described in the next section.

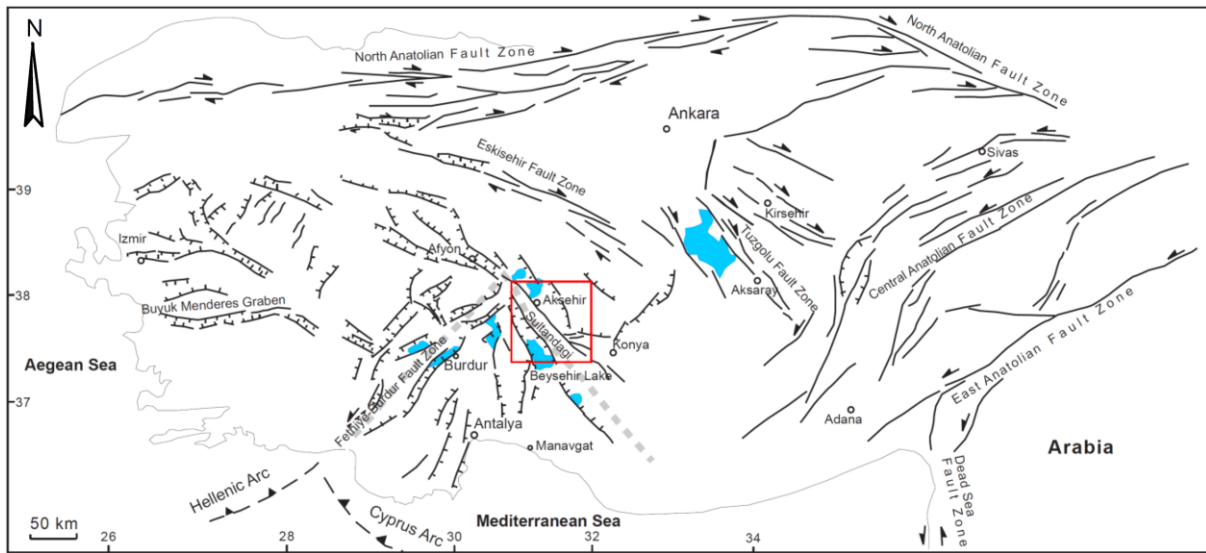


Figure 2. Simplified map showing the main structural elements of Anatolia (modified from Bozkurt, 2001). Heavy lines with half arrows are the major strike-slip zones, heavy lines with hachures are normal-oblique faults. Blue areas are lakes. Dashed line indicates the Isparta Angle region. Red box indicates the location of the Akşehir-Afyon and Ilgin Basin.

Isparta Angle

The Isparta Angle (Blumenthal, 1963) is located at the inland boundary between the Cyprus Arc to the east and the Hellenic Arc to the west, and is considered as a transition zone between domains of different plate tectonics and associated regional deformation. The Isparta Angle (IA) is approximately 120 km long and 50 km wide at its southern end, and extends offshore into the Antalya basin (Verhaert et al., 2006). It forms an important key boundary structure between active extensional deformation in the Aegean to West Anatolia, and uplift of the Anatolian plateau in Central Anatolia (Flecker et al., 2004). The NE-SW trending, left-lateral Fethiye-Burdur fault zone can be considered as the westernmost outer margin of the Isparta Angle, and the NW- trending Akşehir Fault zone forms the boundary at the eastern outer flank of the angle. The Isparta Angle is characterized by a basin and range type morphology and records the emplacement of large-scale carbonate platforms and ophiolites during the opening and partial closure of the Neotethyan ocean in the Mesozoic-Early Tertiary (Poisson, 1977, 1984; Poisson et al., 2003a; Woodcock and Robertson, 1977; Robertson and Woodcock, 1982; Waldron, 1984; Robertson et al., 1991; Robertson, 1993; Flecker et al., 2005). Pliocene to Quaternary (i.e. neotectonic) deformation in the IA records both extension and compression (e.g. Poisson, 1977; Dupoux, 1983; Price and Scott, 1994; Frizon de Lamotte et al., 1995; Glover and Robertson, 1998a,b; Temiz et al., 1997; Flecker et al., 2005; Verhaert et al., 2006). During the Miocene, roll-back related extension behind the Cyprus-Hellenic arcs is active. Little is known about how this regional tectonic context affected sedimentation and deformation within the Isparta Angle during the Miocene.

Flecker et al. (2005) studied the facies patterns and structural trends of four Miocene basins located in the inner parts of the Isparta Angle: Lycian, Aksu, Köprü and Manavgat basins. Their palaeogeographic reconstructions suggest that during the Early Miocene, the western Lycian basin and adjacent Aksu basin experienced flexural subsidence, related to the southeastward thrusting and loading of the Lycian Nappes. As a consequence of nappe emplacement, a forebulge formed and caused uplift in the Aksu and Köprü basins, initiating half-graben formation. The Manavgat basin was little influenced by these processes. Only the margins of this basin were influenced by flexure due to Lycian Nappe emplacement. Further development and deformation of these basins is not linked to the Lycian flexure, but is associated with the influence of tectonic evolution of the intersecting Cyprus and south Aegean arcs. The Köprü and Aksu basins are kinematically linked with the Kyrenia

lineament, which forms a part of the Cyprus arc (Flecker et al., 2005). The western outer flank of the IA includes the NE-trending Fethiye-Burdur fault zone, and is interpreted at the landward continuation of the Pliny Strabo trench (ten Veen and Kleinspehn, 2002; ten Veen, 2004).

The eastern flank of the Isparta angle comprises mainly NW-trending, elongated and fault-bounded basins, including the Yalvaç, Apa, Beyşehir, Akşehir-Afyon Graben and Ilgin Basin (Figure 3) which are separated by mountain ranges of deformed and partly metamorphosed Paleozoic and Mesozoic rocks. The Akşehir-Afyon Graben and the Ilgin Basin are located at the outer eastern flank of the Isparta Angle, along the Sultandağı mountain range. The bounding Akşehir Fault was initially interpreted as a thrust (also referred to as the Sultandağı thrust) instead of a normal fault, and the neotectonic deformation structures were linked to compressional deformation after the early Messinian (Boray et al. 1985; Barka et al. 1995; Uysal 1995; Altunel et al. 1999). Koçyiğit (1996, 2000) and Koçyiğit et al. (2000a, 2003) suggests that the northeastern part of the Akşehir-Afyon Basin is related to NE-SW extension, based on fault-slip data and focal mechanism solutions of mainly the northern region along the Akşehir Fault and the Akşehir-Afyon Basin. The study of IA in terms of its geometry and its neotectonic (i.e. Neogene) deformation structures can provide more insights on the Late Cenozoic deformation history of the IA and thereby on the kinematics of different overlapping tectonic domains in Central Anatolia. While the stratigraphy and structures of the northern part of the Akşehir-Afyon Basin and the Akşehir Fault have been studied mainly by Koçyiğit (1996, 2000) and Koçyiğit et al. (2000a, 2003), the southern region of the Akşehir-Afyon Basin and the Ilgin basin are less well-documented and field data are scarce.

Previous studies on the Akşehir-Afyon Basin

Previous studies of the northern part of the Akşehir-Afyon Basin record extensional, syn-sedimentary deformation structures, identified in the Pliocene to Quaternary basin sediments (Koçyiğit et al., 2000a, 2003). The older, middle Miocene sediments are folded and thrust and are therefore associated with an early phase of compressional deformation in the northern part of the Akşehir-Afyon Basin (Koçyiğit et al., 2000a, 2003). Several studies focused on the sense of displacement along the northern part of the Akşehir Fault that forms the eastern boundary of the Sultandağı Mountain range. Boray et al. (1985) suggests that the fault is an active, dextral strike-slip fault and mentions its significance to the development of the Isparta

Angle. Şaroğlu et al. (1987) and Barka et al. (1995) consider the Isparta Angle as a compressional structure, and Şaroğlu et al. (1987) suggests a change in fault movement from dextral strike-slip to a presently active reverse fault. More recent studies identified a normal-oblique sense of recent fault displacement and show that these findings correlate well with focal mechanisms of two recent seismic events: the 2000 December 15th Sultandağı Earthquake with a $M_w = 6.0$ (Taymaz and Tan, 2001), and the 2002 February the 3rd Çay Earthquake, with a $M_w = 6.5$ (Koçyiğit et al., 2000; 2003; Ergin et al., 2009). However, the lateral slip component is not well constrained by seismological data. GPS data modeling provides insights on present-day surface displacements and verifies a normal sense of displacement and a left-lateral slip for the Çay Earthquake on a nearly E-W orientated fault segment (Aktuğ et al., 2010).

3. Stratigraphy and structural framework of the Ilgin Basin

The Ilgin Basin is the southeastern continuation of the Akşehir-Afyon Basin (also referred to as the Akşehir-Afyon Graben (AAG) by Koçyiğit et al.(2003)). The Ilgin Basin and Akşehir-Afyon Basin form an elongated topographic depression, approximately 100 km long and ~50 km wide, which trend parallel along the Akşehir Fault zone and Sultandağı Mountain range (Figures 3-5). The basin region is surrounded by the Paleozoic and Mesozoic metamorphic mountains of the Sultandağı Stratigraphic Unit to the west and by several blocks of the Gavurdağı and Teknedağı to the north and northeast and by the Doğanışar Unit southeast (Geological map of Ilgin, scale 1:100.000, MTA, General Directorate of Mineral Research and Exploration, 2009). The basin is connected by a NE trending corridor with the Çhavuşgöl basin to the northeast and, via a narrow passage to the southeast with the Apa basin. The basin sediments are best exposed in the central part of the Ilgin Basin, while in the north to northwest, they are covered with recent alluvial fan deposits and paleosoils. Most of the sediments are of middle to late Miocene, Pliocene and Quaternary age, deposited mainly in a lacustrine environment. Intercalations of alluvial fan deposits indicate tectonic disturbances in an overall lacustrine depositional environment. The Ilgin basin becomes progressively younger towards the north, as evident by the relative ages of the basin sediments. The ages change from mainly early to middle Miocene in the Ilgin basin to late Miocene, Pliocene and Quaternary towards the north, into the Akşehir-Afyon basin. The stratigraphy has been studied in the southeastern part of the AAG and the Ilgin basin and, partially, in the Çhavuşgöl sub-basin. More in particular, Lower to Upper Miocene sediments are mostly studied in the center and south of the Ilgin basin. The youngest, Pliocene to Quaternary sediments are mostly studied in the Çhavuşgöl basin. The basin sediments lie unconformably on pre- early Miocene, mainly metamorphic rocks of the Sultandağı, Gavurdağı, Teknedağı and Doğanışar mountains (Geological map of Ilgin, scale 1:100.000, MTA, General Directorate of Mineral Research and Exploration, 2009). The rocks of the ~100 km long, NW-trending Sultandağı mountain range are mainly Cambrian to Upper Devonian quartzites and dolomitized limestones, which are partly overthrust by NW-SE trending stacks of Devonian to Permian schists and recrystallized limestones.. These NW-SE basement trends are also present in the Ilgin basin sediments. The relatively smaller basement

blocks of Gavurdağı, Teknedağı and Doğanışar consist of mainly Carboniferous to Jurassic recrystallized limestones, dolomite, and red sandstones (Geological map of Ilgin, scale 1:100.000, MTA, General Directorate of Mineral Research & Exploration, 2009). Unlike the Sultandagi Mountain range at the western basin margin, the eastern and southeastern margin of the Ilgin basin consists of three separated and fault-bounded basement blocks. Faults within and along the margins of these basement blocks, identified in the field and on the DEM, are NW and NE to ENE trending. Similar trends are also identified in the basin sediments. The contact between the basement blocks and basin sediments are steeply dipping and most likely normal faults, confirmed by slickensides and striations on fault plane exposures of basement blocks adjacent to basin sediments. These tectonic contacts are studied to some extent, but there is no control on the timing of faulting between basin sediments and the basement. Focus lies therefore on the structures – preferably syn-sedimentary structures - within the Late Miocene to Quaternary basin sediments. The variable orientations of active oblique-normal faults in the basin sediments indicate that extension is accommodated into multiple directions. Study on the origin and deformation history of the metamorphic basement rocks is beyond the scope of this thesis.

Methods

Stratigraphic analysis

The stratigraphy is studied the southern part of the Akşehir-Afyon Basin and the Ilgin Basin. Geological maps and stratigraphic data from previous studies (Geological map of Turkey, scale: 1/500.000. Geological map of Ilgin, scale: 1/100.000, MTA, General Directorate of Mineral Research & Exploration, 2009) are used mainly to determine the relative age of the stratigraphy and the studied deformation structures found in different outcrops. The Ilgin Basin continues laterally towards the northwest Akşehir-Afyon Basin and the stratigraphy of both basins is comparable. The stratigraphy of the Akşehir-Afyon Basin, studied most recently by Koçyiğit et al. (2000a, 2003), is comparable with the stratigraphic observations of present study of the Ilgin Basin. Kazancı et al. (1997) and Koçyiğit et al. (2000a, 2003) defined the relative ages of several important key horizons based on fossil content, such as *Dreissensia* sp. and gastropods, and by C^{14} dating. Some of these lateral overlapping key horizons are also identified during present study of the southern part of the Basin and are therefore, assumed to be of similar age.

Fault-slip data and DEM analysis

Two SW-NE cross-sections are constructed on the basis of new outcrop and published map data and a Digital Elevation Model (DEM) of the basin. Fault orientations and fault patterns observed in the field are combined with structural and geomorphological observations from the Digital Elevation Model (DEM) and maps of the study area to identify the main fault orientations and structural patterns. The fault-slip data for this study were collected from key areas and sections of the Miocene to Recent sediments of the Ilgin basin. Slip directions were mainly determined by slickensides and striations on fault planes. In most cases, the relative timing of displacements between intersecting faults could not be determined, which is the result of the interconnected patterns of faults and joints that do not reveal any cross-cutting relationships. This suggests coeval fault development. In other outcrops, the inter-relationships are obscured by the presence of incoherent and brecciated fault zones. In outcrops with clear fault planes or displaced beds, the relative timing of fault displacement was determined by the relative age of the faulted stratigraphic horizons. Due to limited exposure in the southern part of the Ilgin Basin, fault measurements are concentrated mainly in the northern part of the studied area.

Paleo-stress Inversion Method

The fault-slip data obtained from the field are analyzed by using a similar approach as that of Kaymakci et al. (2000, 2003b), who studied the paleo-stress evolution of the Çankiri Basin in Central Turkey and Kaymakci (2006) who studied the Denizli Basin in West Turkey. Most sampling sites are spatially separated by more than 50 meter, exceeding the maximum desirable diameter to keep structural homogeneity (Hancock, 1985). These sites were therefore subdivided and analysed as separate subareas. The fault-slip data of each subarea and similar age were grouped together and used to determine the local stress field, using the direct paleo-stress inversion method of Angelier (INVDIR program, 1984, 1990, 1994). This paleo-stress inversion method gives an estimation for the orientation of the principal stress axes (i.e. the maximum, intermediate and minimum stress axes, σ_1 , σ_2 and σ_3 , respectively) of each subarea by calculating the best-fit stress tensor for a given fault slip data set. The method assumes that the direction of slip along a fault records the direction of maximum resolved shear stress along the measured fault surface (Carey and Brunier, 1974; Etchecopar et al., 1981; Angelier, 1979, 1984, 1990, 1994; Petit and Laville, 1985; Means, 1987; Reches, 1987; Krantz, 1988; Lisle, 1987; Doblas, 1998). Together with the relative timing of fault

displacement, the inversion technique is typically used to determine the paleostress field of each subarea (i.e. the orientations of the minimum (σ_3) and maximum principle stress axes (σ_1)). To determine the best stress tensor that fits the fault sets, a numerical method is used to minimize the sum of the angular misfits. After processing the data, the faults with a misfit angle larger than 15° are separated manually from the data set and the procedure was repeated for the 'misfitting' data set. The misfit angle for each separated data set is checked again and if needed, the data was separated again. The direct inversion method (Angelier, 1979) requires a minimum number of four fault-slip measurements. Data sets with less than four slickenside measurements or faults with no slickensides are not used in the final construction of the stress tensors. The orientation of the principal stress axes of each of the subareas are compared and, if similar in orientation, correlated. The fault data are plotted in lower-hemisphere equal area projections, including the remaining fault populations for which no stress tensor could be calculated.

The initial approach was to combine the results with the stratigraphy of the area in an attempt to determine the relative order and orientations of the different paleo-stresses and to thereby arrange the different stress tensors into ordered deformation phases. This method is typically used for paleostress analysis for many areas worldwide (e.g. Kaymakci et al., 2000, 2003b). However, this approach was not applicable for present study area because for most of the faults it turned out to be impossible to assess a relative timing. Another complication associated with the application of the paleo-stress inversion method is the presence of pre-existing structural basement anisotropies and the interference of intersecting faults that may have had a significant influence on the orientations of newly developing faults.

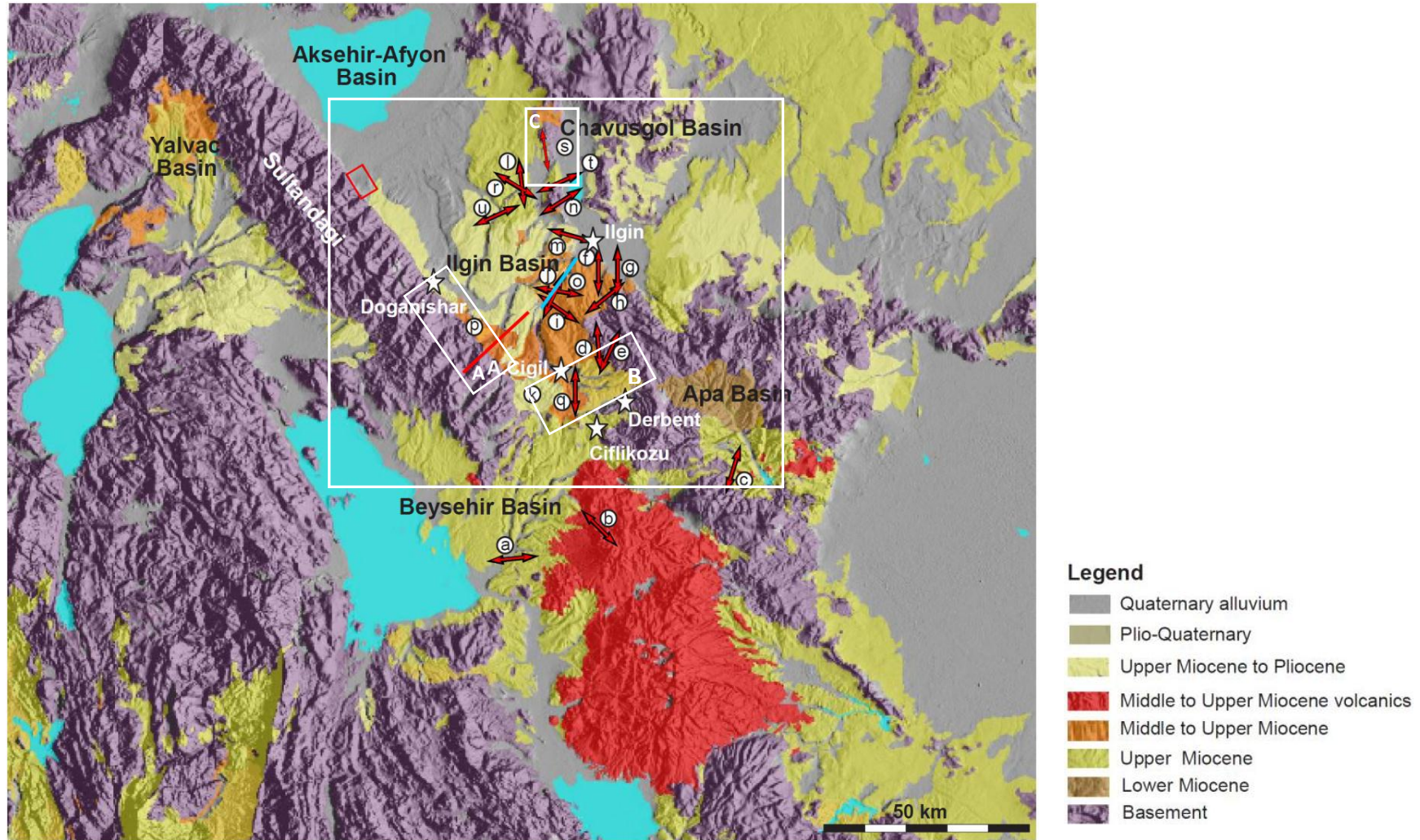


Figure 3. Geological map showing the main Miocene to Quaternary sediments of the Ilgin , Akşehir-Afyon , Apa, Beyşehir and Yalvaç Basins and Pre-Cenozoic metamorphic basement. Arrows indicate the orientation of minimum principle stress axis (σ_3) obtained from the measured faults at different localities (roman letters). More detailed view of the outlined area is represented in figure 14. Smaller white boxes indicate the studied areas of the Akşehir (A), the Derbent (B) and Chavusgöl (C) Fault Zone. Red and blue lines show locations of two cross-sections. Main towns are indicated by stars. Red square is the location of figure 16.

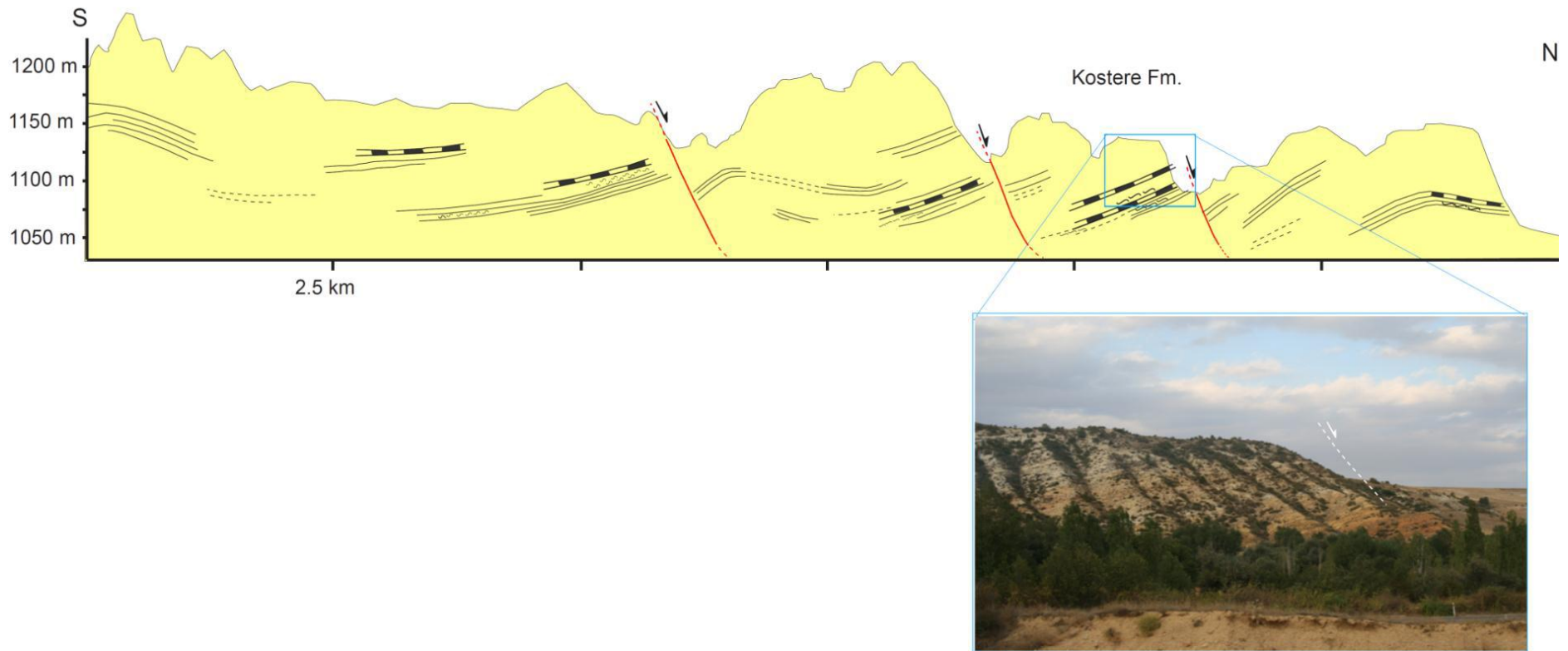


Figure 4. Cross-section through the Middle to late Miocene lacustrine deposits of the central part of the Ilgin Basin (blue line in figure 3). Photo shows yellow, coarse grained sands in lower section and intercalating lacustrine white limestones progressively towards the top of the section. Bedding dips to the southeast.

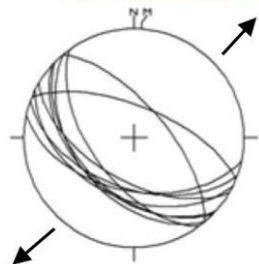
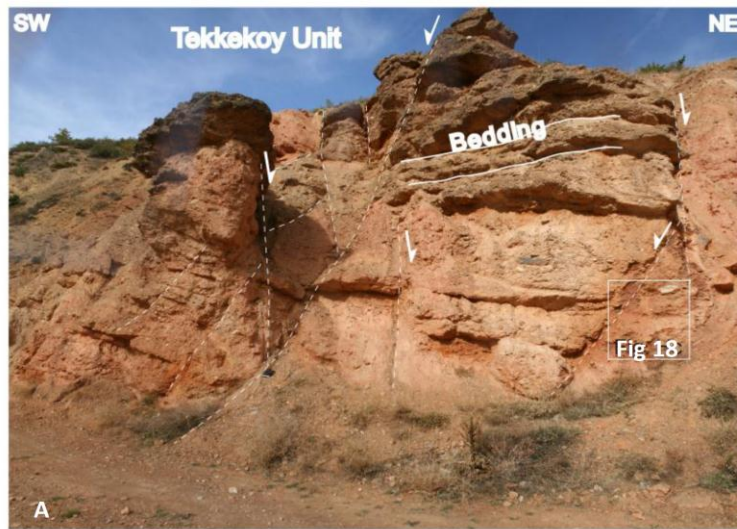
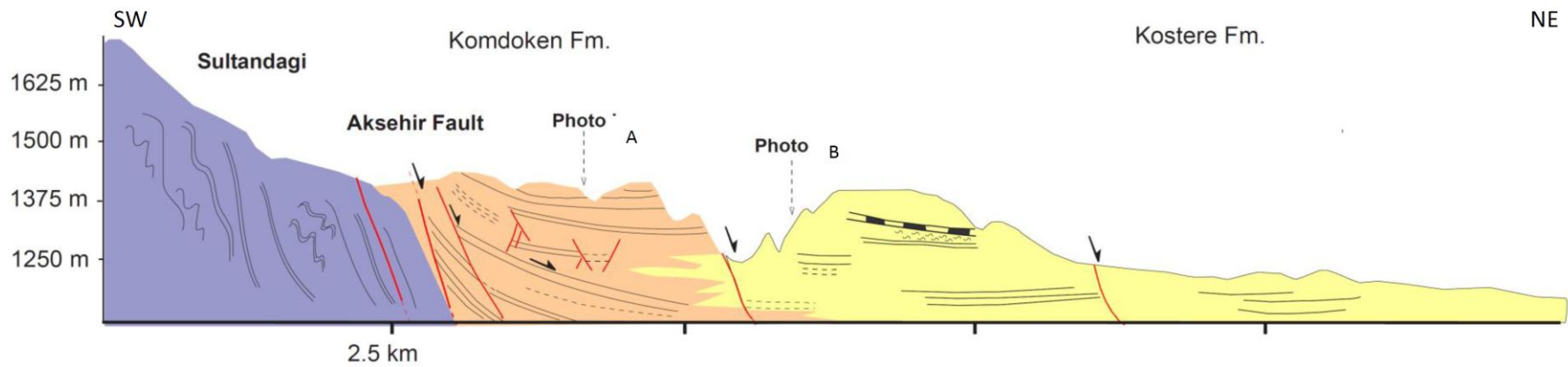


Figure 5. Cross-section (red line in figure 3) through the Sultandađı mountain range and Middle – Upper Miocene alluvial fans and lacustrine sediments in the southwest of the Igin Basin showing NE dipping faults of the Akşehir Fault Zone and parallel dipping faults towards the center of the basin (i.e. to the NE). b: High angle normal faults in Middle –Upper Miocene mass flow conglomerates of the Tekkekoy unit. Faults dip NE and SW. Stereographic projection (equal area, lower hemisphere) showing orientations of normal faults, indicating NE-WS direction of extension. c: horizontal dipping lacustrine limestone bed.

Stratigraphy of the Ilgin Basin

Early and Middle Miocene

The lower to middle Miocene basin sediments are exposed at several outcrops in the Ilgin Basin. This stratigraphic sequence includes a basal section of 150-200 meters of alluvial breccias and mass flow deposits, located at the south-west margin of the Ilgin Basin along the Sultandađı range, and channel conglomerates located further towards the center of the basin. Lateral equivalent is approximately 100 meters of yellow conglomerates, alternating with sandstones, carbonate-rich sandstones, clay beds and lacustrine limestones with gastropods. This sequence passes upwards into 250 to 300 meters of yellow sandstones, marls and relatively massive, lacustrine limestones. The sediments of these formations are deposited in a lacustrine to marginal (overbank) facies, intercalating with fluvial and alluvial conglomerates. The lower units of these formations are deposited unconformably on top of metamorphic basement rocks of the Sultandađı (Koçyiđit et al., 2000a, 2003; MTA Geological Map of Ilgin, scale: 1/100.000, 2009). The breccias and conglomerates and lacustrine sediments cover most of the Basin area and their intercalated occurrence makes it difficult to determine their lateral relationships and relative age. The alluvial fan deposits consist of clasts of mainly micaschists, quartzites and marble, derived from Paleozoic and Mesozoic metamorphic basement rocks of the basin margins. Some outcrops in the south of the Ilgin Basin near the village of Derbent show evidence of onlapping of conglomerates on basement rocks. At other outcrops, normal faults or brecciated zones indicate a tectonic boundary between the basin sediments and basement rocks. Imbricated pebbles observed at a few outcrops near the Sultandađı range at the south-west margin of the Ilgin basin indicate a direction of the mass flows towards the northeast and east.

Boray et al. (1985) initially proposed a Miocene-Pliocene age for the lacustrine sediments of similar formations studied at Köstere town in the central part of the Ilgin Basin, but no fossils were used for age dating. More recently, Koçyiđit et al. (2000a) studied the different types of macro- and micromammalian fossils (e.g., *Byzantinia bayraktepensis*, *Byzantinia*, Koçyiđit et al., 2000a) identified in several horizons of the same formations and found an early to middle Miocene age.

Middle- Late Miocene

Towards the south of the Ilgin basin, the middle Miocene sediments are unconformably overlain by middle to upper Miocene volcanic rocks of the Erenlerdağ Volcanic Complex. K-Ar age determinations of these mainly andesitic and dacitic rocks indicate ages of 10.9-8.8 Ma and 9.4-8.0 Ma (Besang et al., 1977). A younger age of 6.9 Ma is identified from basaltic and andesitic rocks at the southwest of the complex (Platzman et al., 1998). Another, much smaller volcanic terrane, i.e. the Sille Volcanic Complex, is situated in the Apa Basin southeast of the Ilgin Basin. K-Ar determinations of andesites and ignimbritic tuffs indicate an age of 11.45 ± 0.2 to 11.95 ± 0.2 Ma (Besang et al., 1977). A more recent study, using Ar-Ar dating of basalts and tuffs from the Sille volcanics indicate an age of 11.64 Ma (A. Koç, pers. comm.).

Stratigraphically on top of these volcanics lies an approximately 600 meter thick sequence of alternating mudstones, clay, and lacustrine limestones. These deposits change upwards and laterally into alluvial fan and mass flow deposits. Ar-Ar age determination of pumice particles, associated with the volcanics of the Erenlerdağ Volcanic Complex or Sille Volcanics to the south of the Basin are found in clay beds of these upper units and indicate an approximate age of 11 Ma (A.Koç, pers. comm.). In general, the upwards intercalating conglomerates are quite similar to the older, basal conglomerates of the i.e. Early-middle Miocene), but these conglomerates (studied at the Aşağıçiğil town) contain tuff clasts and are therefore younger (i.e. younger than ~11 Ma).

Pliocene-Quaternary

The fan deposits of the Middle-Late Miocene units pass upward into a 156 meter (estimated by the currently operating mining company, MTA) series of black, immature lignite, mudstone, limestones with gastropoda and unconformably overlying red marls with sand, clay, paleosoils (caliches) and conglomeratic channel beds. This sequence has been studied mainly in an open-pit mine in the north of the basin, near the Çhavuşgöl Fault zone (see next section). The lower series were likely deposited under lacustrine conditions, with the fine-grained clays and mud deposited in overbank settings. These facies change upwards and laterally into fluvial conditions with channelized streams and increasing clastic input. The upper parts of the red-bed sequence are mostly calcite-bearing paleosoils and are comparable to modern caliche or calcrete soils. The red colour suggests good drainage and an oxidizing early diagenetic regime. The slight alternation in yellow and red colors indicate the

development of different types of multiple soil profiles in response to changes in conditions (e.g. climatic fluctuations) through time. The presence of caliche horizons typically indicate arid to subhumid conditions where evaporate loss exceeded the supply of water to the surface by rainfall or flooding (Reading, 1996). Normal faults and associated, syn-sedimentary structures reflect unstable conditions under which the paleosoils developed. At the mine-pit located in the north of the Ilgin Basin, the deposits onlap onto metamorphic basement rocks (operating mining company, pers. comm.). However, at the center of the Ilgin Basin, only the upper red-bed sequence is recognized, and lies unconformably on top of early-middle to middle-late Miocene lacustrine limestones of the previously described units.

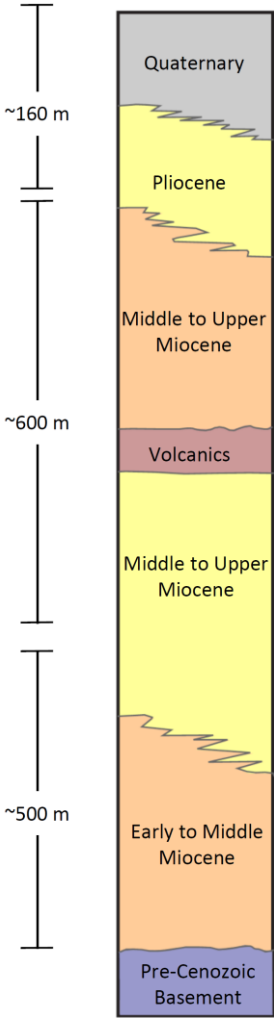


Figure 6. Generalized stratigraphic column of the Middle Miocene to Quaternary lacustrine and alluvial fan deposits of the Ilgin Basin.

General structural characteristics of the Ilgin Basin

The dominant deformation structures recorded are brittle structures such as joints and normal faults. These structures are present in Paleozoic and Mesozoic basement rocks and in the Miocene-Quaternary basin sediments, including consolidated and unconsolidated lacustrine deposits and conglomerates. Conglomerates identified along the southwest and southern margin of the Ilgin basin are generally mass-flow deposits with variable transport directions. Channelized conglomerates are more abundant towards the center of the basin. Normal faults are recognized as steeply dipping (i.e. dip angles $>50^\circ$) curved listric surfaces, with often steeper top parts and shallowing towards depth. At listric planes, the sedimentary sequences of the hanging wall are sometimes tilted towards the fault plane, where they bend into rollover anticlinal structures. Displacements vary from a few centimeters to meters in the center of the basin, to hundreds of meters at the Akşehir basin-bounding fault at the southwestern basin margin. Clay-rich layers at down-thrown sides are often found dragged along the fault contact (Figure 7 and 8). Less confined fault zones of brecciated rocks with tilted blocks are also present (Figure 9). Networks of fibrous white crystalline calcium carbonate, identified as travertine, are locally present in these highly deformed and brecciated zones.

Lineations on fault surfaces are all steeply dipping and parallel or sub-parallel within the slip planes. The rakes range from 50 degrees to almost vertical, indicative for a normal sense of hanging wall displacement with a minor oblique lateral shear component. Slickensides present on exposed fault surfaces locally show a downward stepping morphology but such observations are rare. The fault surfaces and lineations are often fractured into smaller planes, making it difficult to distinguish the sense of movement solely by fault-plane morphology. Nevertheless, the geometry of the steeply dipping fault planes and lineations, syn-sedimentary structures and the cross-cutting relationships of displaced beds all point to a last increment of normal-oblique slip displacement. Lineations are also frequently found on planar surfaces within intensely deformed metamorphic basement. Few of these are calcite slickensides, associated with fault-slip displacement but most of these slip-vectors are not distinguishable from intersection lineations associated with pre-Late Cenozoic deformation of the metamorphic basement rocks. In absence of other indicators for extensional deformation, these lineations are considered unreliable, hence unsuitable for fault-slip analysis.

Fault corrugations are mostly observed on clay-rich, steeply dipping fault planes situated in brecciated zones of unconsolidated sequences of generally clay, marl and lacustrine limestone (Figure 10). These structures commonly have a wavelength of a few centimeters. Similar corrugated surfaces can also form as a result of the swelling of clay in presence of water and can easily be mistaken for fault-slip indicators and corrugated surfaces were, therefore, carefully studied. Meter-scale corrugated surfaces are found at the Cavusgöl Fault zone, a few kilometers to the north of Ilgin town. The fault planes in this zone are nearly 2 m-high, steeply dipping scarps within a zone of unconsolidated limestone, marl and clay. The planes are straight or curved and show smooth surfaces of calcite slickensides. A few slip-planes have a polished finish, indicative for recent fault activity where 2 m-high planes are exposed by the last increment of displacement.



Figure 7. Steeply dipping ($\sim 70^\circ$) normal fault in middle to upper Miocene, lacustrine limestones, clay and marl sequence present in the southern part of the Ilgin basin, near the Debent Fault zone. (label q on figure 3) Brown clay layers are ~ 1 m displaced, are and slightly dragged at the down-thrown side of the fault. Note hammer for scale. Stereographic projection (equal area, lower hemisphere) of the same outcrop, showing orientations of normal faults and lineations, indicating \sim N-S directed extension.



Figure 8. Normal fault in middle to upper Miocene sediments at outcrop along road south of Ilgin town (near location indicated by label m on figure 3). Lacustrine limestones alternated with marls and clayey layers on left (i.e. up-thrown) side. Brown, clay and marl-rich, dragged sequence on down-thrown side. Note hammer (circle) for scale.

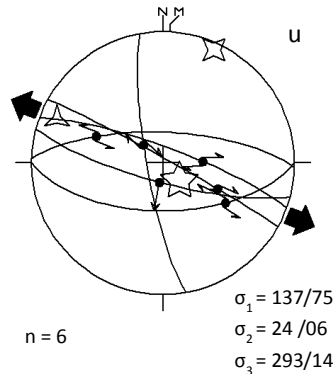
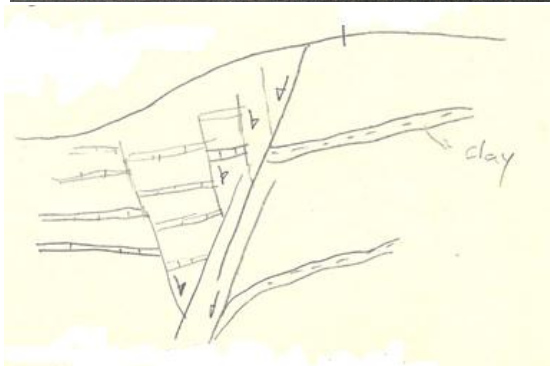
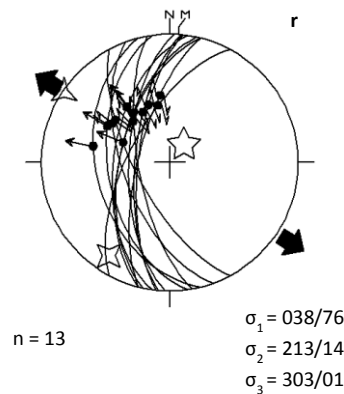


Figure 9. High angle, syn and antithetic normal faults in highly brecciated and unconsolidated sequence of alternating, Upper Miocene to Pliocene lacustrine limestone, clay and marls. Location of outcrop is indicated by label u on figure 3. Sketch illustrates the main structures observed in the same outcrop. Stereographic projection (equal area, lower hemisphere) shows the measured fault-slip planes, indicating a NW-SE direction of extension. Measured calcite veins (two) show no slip direction.



Figure 10. Normal faults and graben structure in Upper Miocene to Pliocene sequence of marls, clay and lacustrine limestones. Outcrop is located in the northern part of the basin at locality r, indicated in figure 3. Stereographic projection (equal area, lower hemisphere) showing normal fault planes and lineations, indicating a ~NW-SE directed extension.



Fault orientations and structural trends

Fault-slip data collected in the field are analyzed by the inversion technique initially developed by Angelier (1984, 1990, 1994) and combined with the structural trends identified on the DEM of the region. Fault exposures in the Ilgin Basin are scarce and, therefore, the amount of fault measurements obtained from the field is rather limited. Nevertheless, the fault orientations and their corresponding intermediate (σ_2) and minimum (σ_3) principle stress axes, largely correspond to the fault orientations and structural trends identified on the DEM. The results show that a multitude of fault orientations are found in both Pre-Late Cenozoic metamorphic basement rocks and the Miocene to recent basin sediments. For almost all fault slip data obtained from field-outcrops, the maximum principle stress axis (σ_1) is rather consistent and nearly vertical. Rather than large planar structures, faults are developed as variably oriented, cross-cutting segments and are often aligned into *zigzag* patterns, indicating a hard-linked and interlocking fault system (Figure 11-12). These patterns are observed both in outcrop-scale exposures and on km-scale observations from the DEM of region (Figure 13-14). Prominent and repetitively occurring structural lineaments are distinguished on the DEM by a slight difference in elevation of the ground surface. Most of the orientations of faults measured in the field correspond to the prominent and laterally continuous structural trends

observed on the DEM. The intersecting fault trends and lineaments form a semi-orthorhombic pattern in cross-sections observed at outcrops, and in plan view on maps and the DEM of the region. Clear cross-cutting relationships between the different fault trends are not identifiable which may be a result of severe overprinting of superimposed structures as a result of a history of successive phases of intense extensional deformation. Alternatively, the multiply oriented faults may have formed simultaneously, by accommodating extensional strain in variable directions. This is partly supported by the observation of quadrimodal fault sets, distinguished on outcrop-scale in the field (Figure 12). These polymodal fault sets are formed by the accommodation of three-dimensional strain, allowing the development of four sets of coeval fault planes (Oertel, 1965; Reches, 1978; 1983; Krantz, 1988). Rock failure by brittle deformation is commonly explained by deformation models that are generally based on Coulomb's 18th century) and Andersonian (1951) conventional models for brittle shear failure of isotropic material in two dimensions. Based on field observations of contemporaneous fault sets (Healy et al., 2006; Reches, 1978; 1983), it is apparent that faults can develop according to a quadrimodal fault system and are associated with simultaneous conjugate faulting in horizontal and vertical directions (Healy et al., 2006). The origin for the occurrence of three dimensional strain lies in the presence of pre-existing basement anisotropies and the linkage and interaction between intersecting faults.

Although highly variable in detail, a number of laterally persistent fault trends are distinguished from field observations in the Ilgin Basin and on the DEM image of the Ilgin Basin and adjacent region, including the Akşehir-Afyon, Apa, Yalvaç and Beyşehir Basins. These trends include NW-SE, E-W to WNW-ESE, NNE-SSW, NE-SW orientations. Key observations from the NW-SE Akşehir Fault zone, the ~E-W Derbent Fault and the NNE-SSW to NW-SE Çhavuşgöl Fault zones are described separately in the next subchapters.

NW-SE fault trends

The most prominent fault orientation is NW-SE, parallel to the main Akşehir-Afyon Basin and western margin of the Ilgin Basin. This trend is laterally persistent in the Ilgin Basin and on a more regional scale outside the study area. This NW-SE-trend includes the main boundary Akşehir Fault zone, located along the Sultandağı mountain range, and the Apa Fault zone, located to the east of the Ilgin Basin. Structures of the Apa Fault zone are previously analyzed in the field by A. Koç (pers. comm). The morphology and orientation of the Apa fault zone are analyzed in the present study by use of the DEM and geological maps of the region. The Akşehir and Apa Fault zones are eastward dipping, normal oblique-slip faults. In

plan view, these appear as laterally continuous, overstepping fault zones that are linked by nearly perpendicular (~E-W) orientated faults, located in the southern part of the Ilgin Basin. There are three separated blocks of metamorphic basement rocks located in the southeastern part of the Ilgin Basin. These blocks are bounded at their western margin by NW-SE-trending normal faults dipping to the south-west.

~E-W to WNW-ESE fault trends

An ~E-W trend is identified in the southern part of the Ilgin Basin, where faults of the Derbent Fault zone strike nearly perpendicular to the main NW basin trend. The Derbent Fault zone includes steep northward stepping fault scarps.

NNE-SSW fault trends

NNE-SSW fault trends are less prominent as compared to the other trends observed on the DEM and are mostly identified in the northern part of the Ilgin Basin and adjacent Akşehir-Afyon Basin. The Konya Fault zone at the south-eastern end of the Apa basin has a similar orientation. A detailed study of the Apa basin and Konya fault zone is, however, beyond the scope of this study. An important key outcrop studied in the north of the basin includes the Çhavuşgöl Fault zone. On plan view on the DEM of the region, this zone has an overall NNE-SSW orientation, but because the zone is segmented into multiple fault segments, the fault trend changes from NNE-SSW to ~N-S at its northern end, to NW-SE towards the south. The faults are mainly eastward dipping, normal-oblique.

NE-SW fault trends

NE-SW-striking faults are mainly located along basement blocks in the southern part of the Ilgin Basin and adjacent Apa Basin. Similar structural trends are present towards the west of the Sultandağı in the Yalvaç and Beyşehir Basins.



Figure 11. Plan view of cross-cutting faults and fractures in Middle to Upper Miocene lacustrine limestones (pencil for scale). Location of outcrop is at the center of the Ilgin basin, at locality o indicated in figure 3. Stereographic projection (equal area, lower hemisphere) showing normal fault planes and lineations, indicating ~NW-SE directed extension. Measured fault planes are perpendicular to square.



Figure 12. Quadrimodal fault set in middle Triassic to Jurassic basement limestones, adjacent to middle to upper Miocene basin sediments. Outcrop is located in the southeast of the Ilgin basin close to the Apa basin.

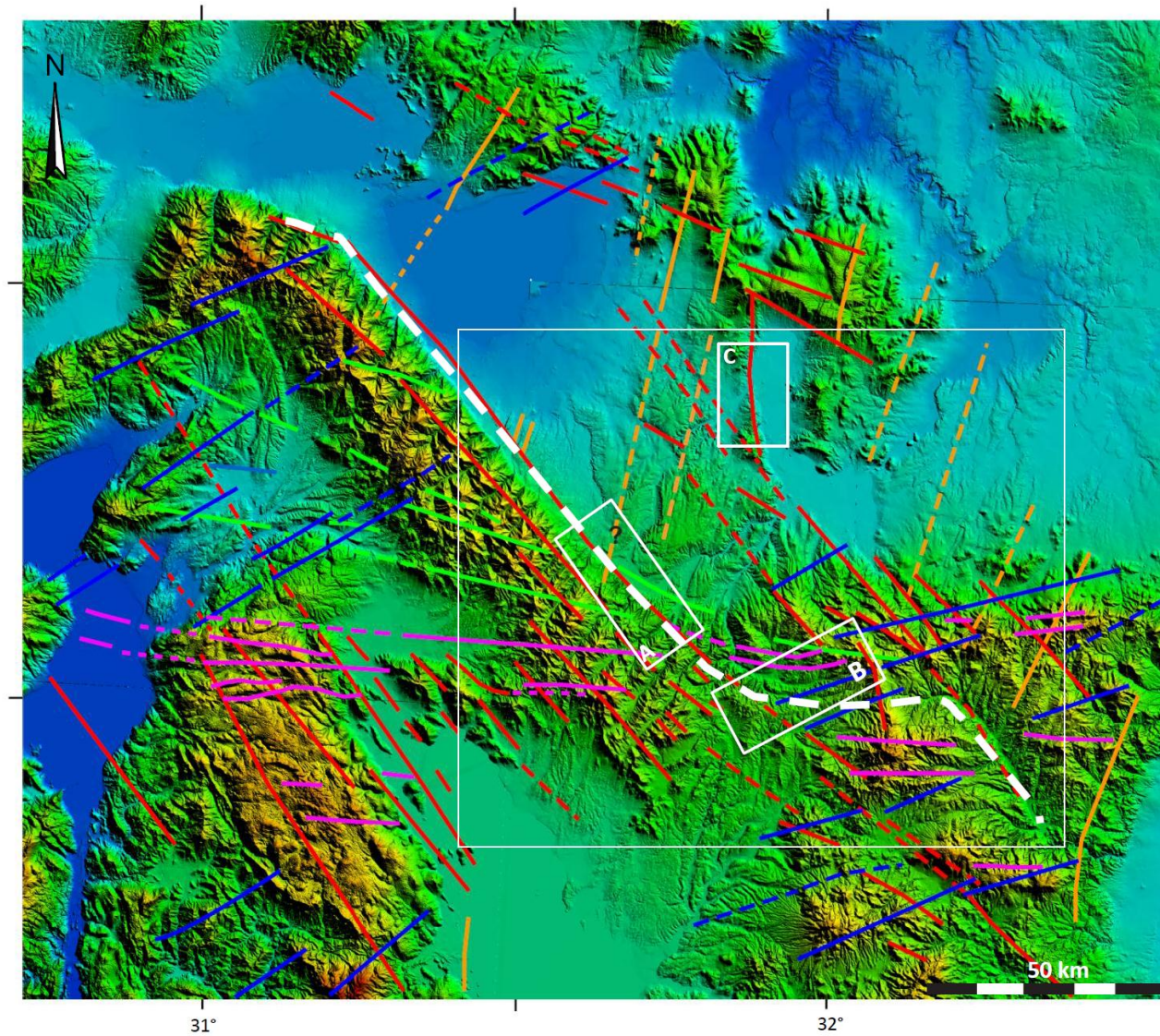


Figure 13. Digital Elevation Model of the same area illustrated in figure 3 showing the main fault orientations and structural trends: NW-SE (red), NNE-SSW (orange), NE-SW (blue), E-W (pink), WNW-ESE (green). White dashed line represents the horsetail geometry, typically found in transtensional fault systems. Smaller white boxes indicate the studied areas of the Akşehir (A), the Derbent (B) and Chavusgöl (C) Fault Zone.

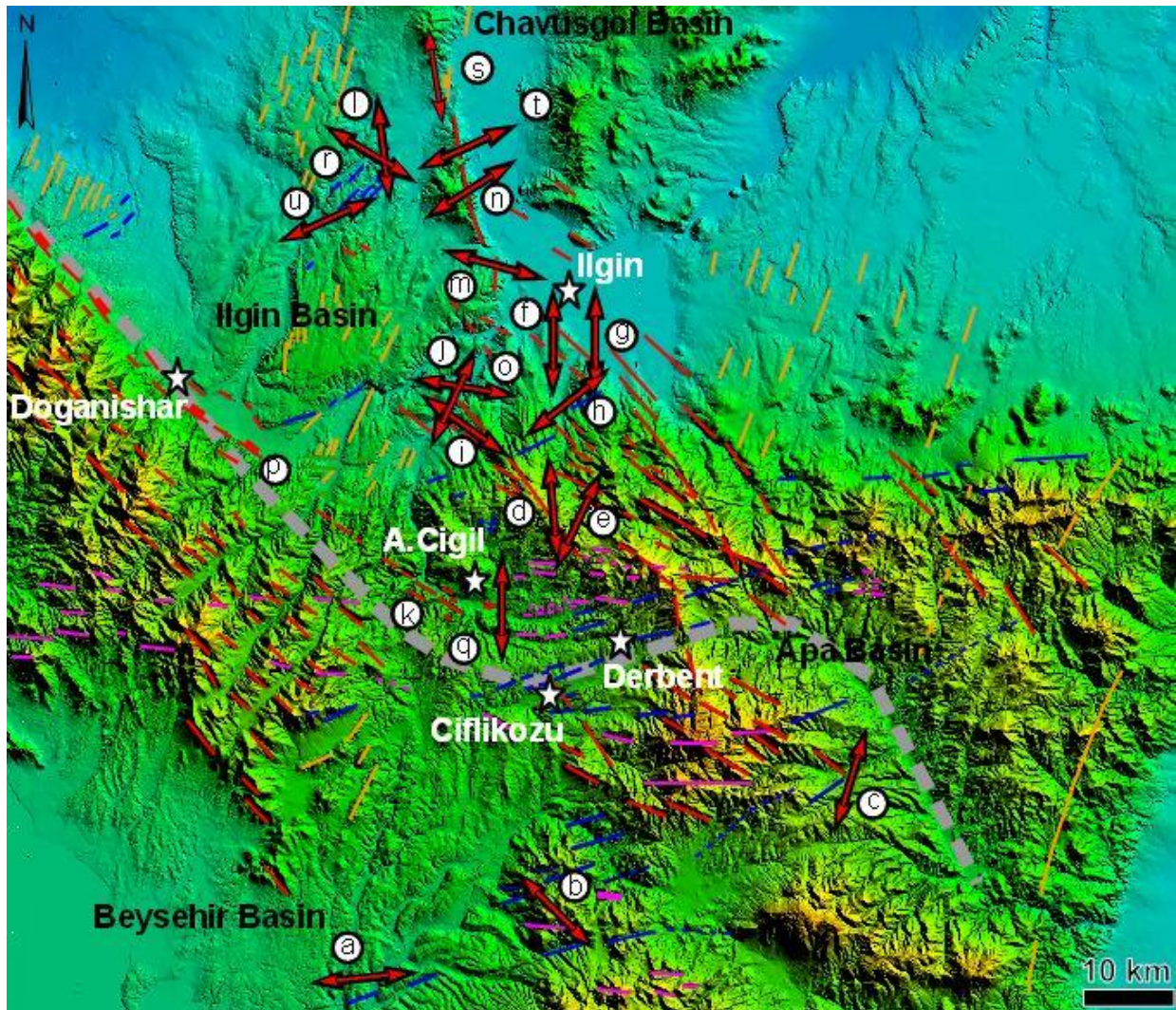
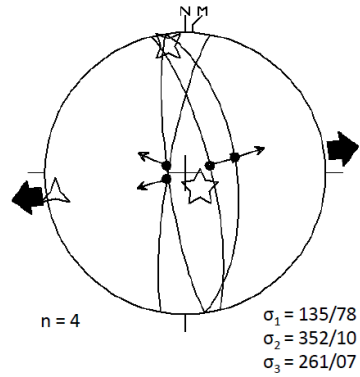
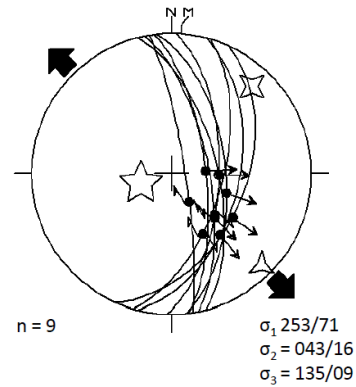


Figure 14. Inset figure indicated on figure 3, 13, and 15, showing a more detailed view of the DEM of the studied basin area. Different fault orientations indicated (same color code as in figures 13 & 15). Arrows indicate the orientation of minimum principle stress axis (σ_3) obtained from the measured faults at different localities (roman letters a-n). Stereographic projections (equal area, lower hemisphere) of measured localities are illustrated on next 2 pages. Dashed line indicates the horsetail basin geometry.

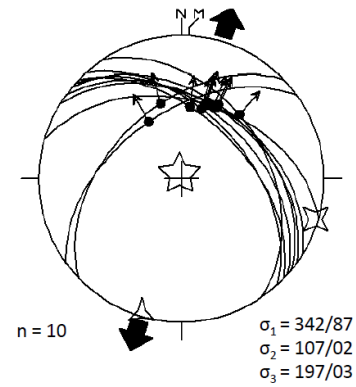
a) High-angle normal faults and lineations in Middle-Upper Miocene lacustrine limestone.



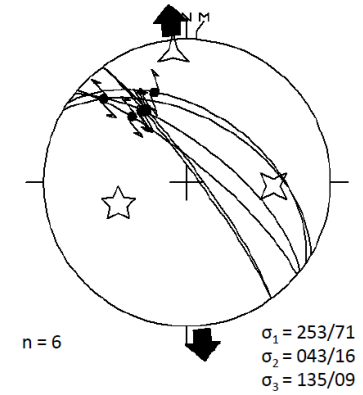
b) High-angle normal faults and lineations in Middle-Upper Miocene andesitic rocks of the Erenler Dagi Volcanic Complex.



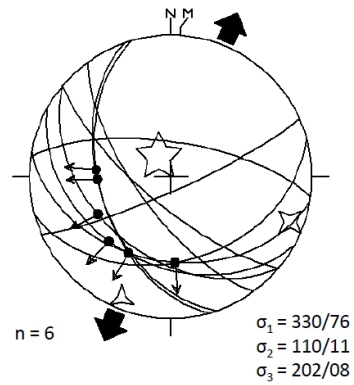
c) High-angle normal faults and lineations on Triassic basement adjacent to Lower - Middle Miocene lacustrine limestones.



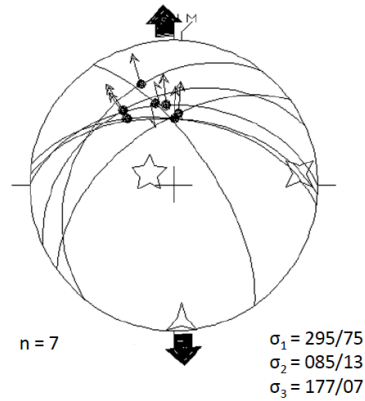
d) Lineations measured on basement metamorphic limestone, adjacent to Middle to Upper Miocene lacustrine basin sediments



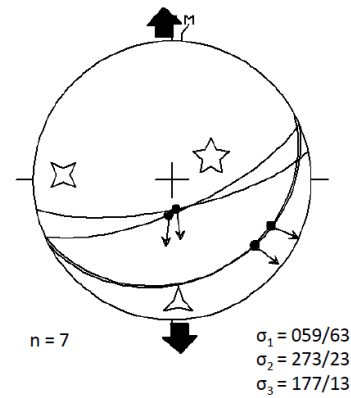
e) Lineations measured on basement metamorphic limestone, adjacent to Middle to Upper Miocene lacustrine basin sediments.



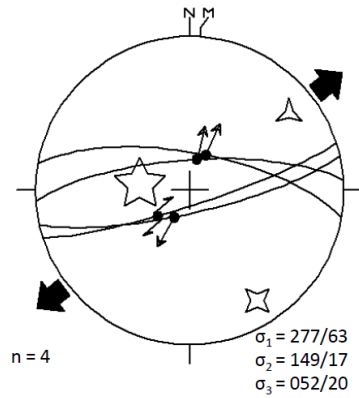
f) Lineations on lacustrine limestones at boundary zone between upper Miocene and Pliocene-Quaternary basin sediments.



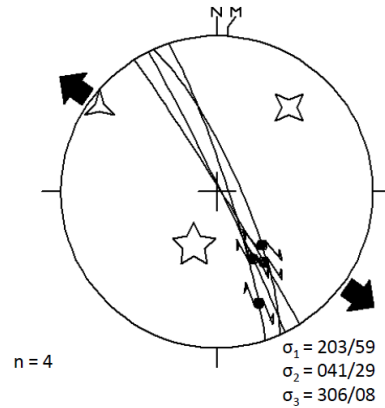
g) Lineations on lacustrine limestones in boundary zone between upper Miocene and Pliocene-Quaternary basin sediments.



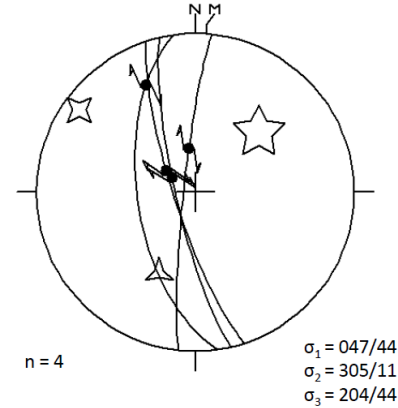
h) lineations on clay surface in Middle to Upper Miocene sequence with alternations of mudstones, clay and marls. Location is north-east of the Ilgin basin adjacent to Permian to lower Triassic metamorphic basement rocks.



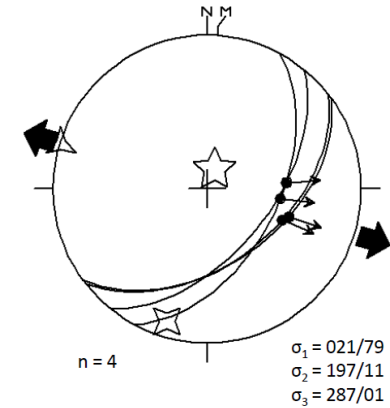
i) Lineations on Middle to Upper Miocene, lacustrine limestones, located in the center of the Ilgin basin.



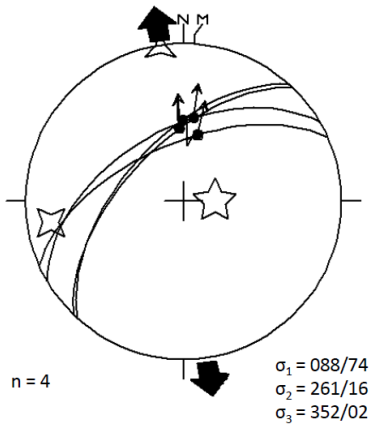
j) Lineations on Middle to Upper Miocene, lacustrine limestones located in the center of the Ilgin basin.



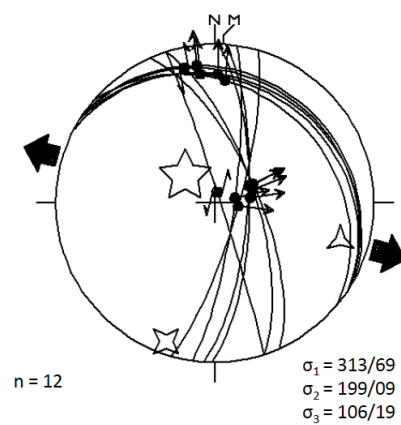
k) Weathered lineations on red conglomerates, located at the margin between the southern end of the Sultandagi and the Ilgin basin.



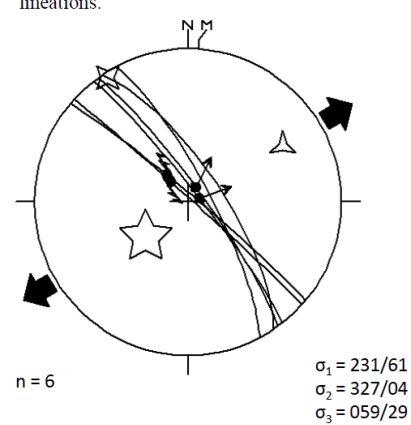
l) Lineations and corrugations on Upper Miocene to Pliocene clay surface, located in the northern part of Ilgin basin. Outcrop shows very incoherent sequence of alternating marl and clay.



m) Lineations on massive, veined limestones, most likely basement rocks (age unknown) adjacent to Upper Miocene or Pliocene-Quaternary basin marls and yellow sandstones.



n) Lineations on fault scarp of Carboniferous, quartzitic (greenschist facies?) basement rocks adjacent to Pliocene-Quaternary basin sediments. Outcrop is located at the Chavusgöl Fault zone. Two fault planes show no lineations.



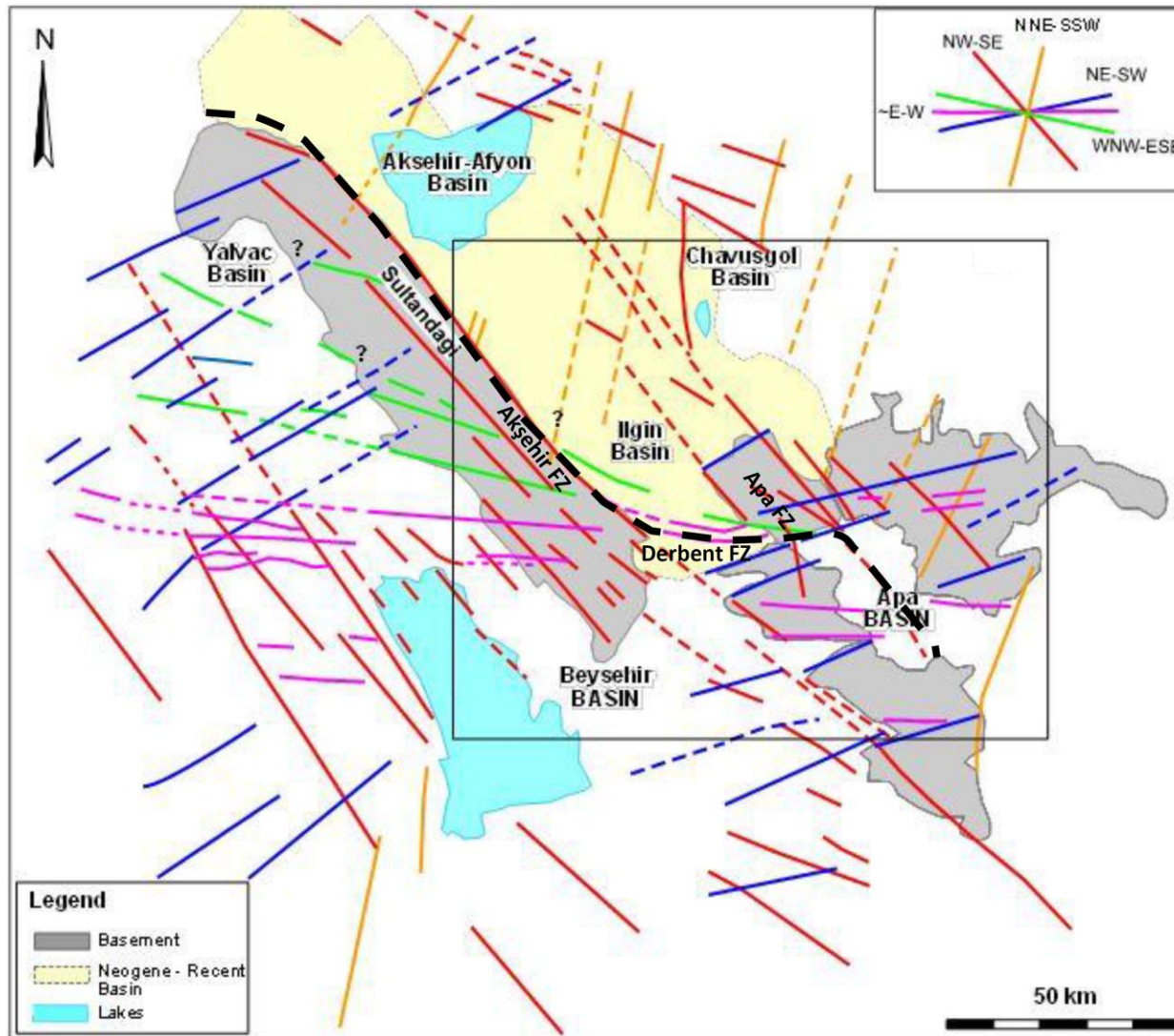


Figure 15. Structure map of the same area illustrated in figures 3, 13 and 14, showing the main basement highs and adjacent Akşehir-Afyon and Ilgin Basins and the prominent, intersecting structural trends identified on the DEM and from field observations of the Ilgin Basin area.

Akşehir Fault Zone

The approximately 2 km high and 100 km long Sultandağı mountain range is a very prominent structure and easily recognizable on the DEM of the area by the abrupt elevation difference between the Sultandağı and the adjacent Akşehir-Afyon and Ilgin basins. The boundary between this NW-SE trending basement range and basin floor is defined by the sinusoidal (or ‘z-shaped’) geometry of the Akşehir Fault zone. The Sultandağı range and the Akşehir-Afyon and Ilgin basins form a typical horst-and-graben type of structure, also referred to as the Akşehir-Afyon Graben (AAG; Koçyiğit et al., 2000; 2003). Koçyiğit et al (2000; 2003) studied the Akşehir Fault zone and the eastern graben-boundary fault, the Karaköztepe Fault zone, in the very northern part of the Akşehir-Afyon Basin. When studied in more detail, it is apparent that the Akşehir Fault is actually a zone of numerous closely spaced, synthetic normal fault faults or scarps, distinguished by the swarm of typical triangular facets or so-called ‘flat irons’. The resulting structure is a typical *range-front morphology*, characteristic for normal fault activity (McCalpin et al., 2009) but reverse-fault range fronts and rapidly growing anticlines can also develop such faceted spurs (McCalpin et al., 2009). In general, fault scarps are considered as primary geomorphic indicators of paleoearthquakes and can vary from thousands of meters high bedrock cuts along mountain fronts, or decimeter-scale scarps in Quaternary alluvium and colluvium (McCalpin et al., 2009). The swarms of parallel facets along the Sultandağı are associated with normal-oblique displacements. The slight decrease in elevation between the facets from the inner part of the range towards its eastern margin indicate that the main (active) fault is located at the basin margin and ‘secondary’ and ‘tertiary’ faults of previous events are located further interior within the mountain range.

The Akşehir fault zone has been interpreted earlier by several authors (Şaroğlu et al. (1987) as a thrust fault but more recent studies (e.g., present study) point to a recent normal-oblique sense of displacement. There are NW-SE trending thrusts within the inner zones of the Sultandağı mountain range indicated on the geological map (Geological map of Ilgin, scale: 1/100.000, MTA, General Directorate of Mineral Research & Exploration, 2009). These are most likely old, pre-Cenozoic structures associated with the formation of the Sultandağı. Normal-oblique fault activity along the margin of the Sultandağı is supported by outcrop observations of nearly vertical, down-stepping slickensides on footwall basement rocks (Koçyiğit et al., 2003). The fault geometry from seismic and GPS data of the northern end of the Akşehir fault (Ergin et al., 2009; Aktuğ et al., 2010) also indicate normal-oblique faulting. This is in agreement with outcrop observations from present study near the southern

end of the Akşehir Fault (i.e. at the southwestern margin of the Ilgin basin) where fault planes dip towards the east at angles of 70 to 80 ° and slickensides are nearly vertical.

Hanging valleys present at the range front of the basin (i.e. the Sultandaği) also indicate recent normal fault displacement. These structures can be recognized on the DEM, at the boundary between the Sultandaği and the basin floor (Figure 16), and indicate recent normal fault activity at the outer facets of the fault trace (i.e. at the basin margin). A hanging valley can be recognized by a step or nickpoint in a stream channel at the fault trace. This abrupt step in elevation forms when river channels that erode through the fault scarp are displaced by normal fault movement. If the base level of a stream is suddenly lowered by normal fault displacement, stream incision is expected to occur from the up-thrown side towards the downthrown blocks, creating a gradual channel profile. Subsequent faulting creates a scarp across the stream channel and increases the height of the preexisting fault scarp. The abrupt increase in channel height across the fault trace indicates recent fault activity along the Akşehir Faults zone and little erosion.

Apart from (relative) uplift, range-front morphology is also controlled by other factors such as climate, lithology and structure. For example, in very humid climates, high erosion rates are expected to play an important role in degradation of the scarps, and a more rapid uplift rate is necessary to maintain the typical range-front morphology (McCalpin et al., 2009). In case of the northern part of the Sultandaği range, the elevation difference between range and basin is relatively abrupt. In the south of the AAG and at the Ilgin basin, there is a more gradual change in elevation but this will be discussed later. Few small alluvial wedges along the Sultandaği in the north indicate a rather ‘starved’ range front, where little sediment accumulates into the basin. The abrupt change in elevation, the multiple, parallel faceted segments along the range front, and the few small alluvial fans all point to a relative large cumulative displacement along the Akşehir Fault zone. McCalpin et al. (2009) describe the typical scarp evolution when consolidated bedrock is exposed on a scarp face and subsequent displacement and scarp height increases by the following three stages: with increasing displacement and scarp height, the upper scarp face becomes a stripped erosional surface and only little colluvium is formed. The downslope scarp is less steep and, while the slope above the fault becomes steeper and higher, the downslope part of the scarp profile transforms from a site of deposition to a site of transport. This means that particles that would previously stop downslope of the fault to form a colluvial wedge, will now keep moving towards the toe of the scarp or into the basin. As this process continues, the scarp becomes a fully bedrock-cored fault scarp with the fault plane nearly at the toe, with a relatively small colluvial wedge at the

basin front compared with the size of the scarp. As a result of the occurrence of many successive paleo-earthquakes, a typical faceted range-front of bedrock-cored fault scarps develops (McCalpin et al., 2009).

The increasing number of faulting events and thereby the increasing height of fault scarps can initiate a large enough gravitational potential to start slope instability. This may create landslides, but also coseismic fault refraction towards the scarp face. The type of landslide occurring depends on the type of material, the moisture content, and by the type of movement, e.g. if the material topples, slides, slumps or spreads. Many classifications and landslide studies have been published to identify landslide structures (McCalpin et al., 2009). In this study, soft sediment structures have been identified in an approximately 4 m² outcrop of red beds, at the southern end of the Akşehir Fault zone (Figure 17). These structures show an internal stratification of intensely folded (slumps) of fine grained, clay-rich layers. These intensely deformed red beds are situated within a larger sequence of relatively undeformed and flat lying, red alluvial fan deposits. The underlying and partially intercalating white lacustrine clay beds and limestones are also relatively horizontal and show no structures of intense folding. The outcrop with the folded red-beds forms an isolated structure, enclosed by horizontal stratified layers. The structures are cm-scale, recumbent folds with horizontal or slightly inclined axial planes. Faults cross-cutting part of the folded sequence show a slight normal sense of displacement. Such slumped structures may be the result of earthquake triggering. Similar morphological features are identified by stability analyses of landslides and indicate that sliding along low-angle basal shear surfaces more easily occurs under the influence of earthquake shaking than in other conditions (McCalpin et al., 2009). Liquefaction of subsurface layers may also cause landsliding, and are also likely to form seismically.

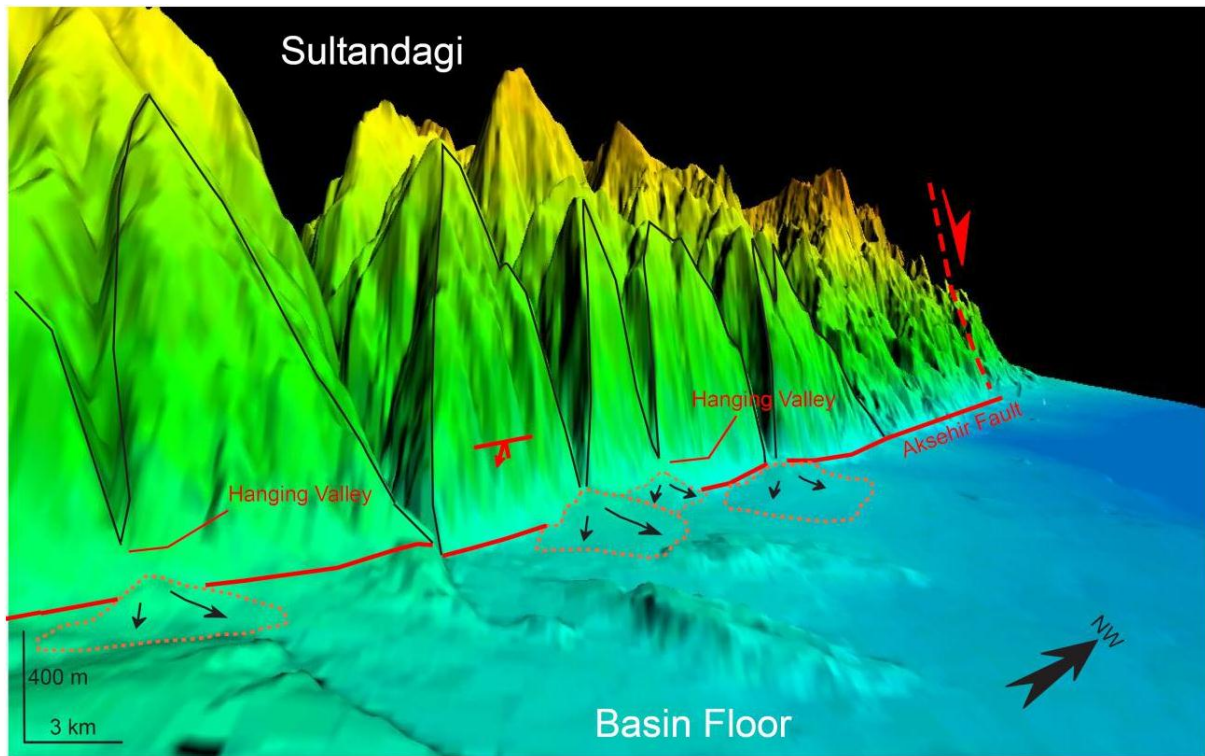


Figure 16. DEM snapshot showing a 3D view of hanging valleys at the Sultandağı Mountain front with the triangular facets associated with normal-oblique slip displacement along the NE dipping Akşehir Fault Zone at the Ilgin Basin margin. Trace of the fault is indicated by red lines. Dashed lines: alluvial fans (see figure 3 for location).



Figure 17. Soft sediment (slump) structures in red clay-rich layers, alternated with thinner coarser-grained quartzitic, layers. Location of outcrop is ~10 km to the southwest of location p (indicated in figure 3), along the Sultandağı mountain range.

From northwest to southeast, there is a lateral change in elevation between the Sultandađı range and the graben floor, indicating a difference in total down-throw displacement along the Akşehir Fault zone. This is apparent from the topography which shows an abrupt change in elevation between the basin and basement in the northwest compared to the southeast, where there is a more gentle, terraced change in topography (e.g. Figure 13). In the northwest the elevation changes abruptly from the basement footwall at nearly 1800 meter to the hanging wall sediments in the basin at 980 meter. Similarly, Koçyiđit et al. (2003) found a total throw of 870 meter at the Yakasenek town in the northwestern end of the Akşehir-Afyon Basin, along the Akşehir Fault zone. This is obtained from borehole data of Pleistocene fan-apron deposits accumulated on the hanging wall (Koçyiđit et al., 2003) and from the total amount of down-cutting of river channels (Ođdum et al, 1991). Lithological analyses from the borehole data showed that the same stratigraphic formation found at 570 meter above the graben floor (980 meter) is also found at a depth of 320 meter below the graben floor. From this, Koçyiđit et al. (2003) estimated a total throw of the Akşehir Fault zone in the northwest of 870 meter, comparable to the 750-1100 meter estimated from the down-cutting of streams (Ođdum et al, 1991).

Observations during the present study of the southern part of the Akşehir Fault zone, at the western margin of the Ilgin basin, show that the Sultandađı basement range has a down-stepping, terraced geometry and has therefore a more gentle change in topography than in the northwest. At the village of Ayaslar, few kilometers south of Doganishar, the footwall basement is cut by several, synthetic normal faults and shows a downthrown, stepping decrease in elevation from approximately 1600 meter to 1400 meter and from 1300 to 1200 meter (Figure 5). In plan view, these stepping normal faults are curved into splays, giving the southern end of the Akşehir Fault zone a typical horsetail shape. These faults appear to bifurcate off from the main Akşehir Fault and curve into a nearly east-west orientation, parallel to the Derbent Fault zone. This ~E-W trend is also recognized on the DEM and continues towards the east into the Apa Basin (Figure 13-15).

At the western margin of the Ilgin basin, along the southern part of the Sultandađı basement range, mass flow conglomerates are exposed along several outcrops. These mass flows, deposited on the hanging-wall of the Akşehir fault (i.e. basinward), are normal faulted and dragged along the fault planes. Figure 5 (photo A) shows these deposits at Tekkeköy town near Doganishar. The Tekkeköy conglomerates are exposed along a 200 meter long and 50 meter high outcrop, and are found alternating with marls and brecciated zones of conglomerates and quartzite basement blocks of the Sultandađı. The conglomerates show

extensional deformation structures: a few shallow dipping faults and younger, steeply dipping, syn- and antithetic normal faults. Some of the steeper, N-S to NW-SE striking normal faults seem to cut and displace the older, shallower dipping normal faults, but because of adjacent marls and brecciated zones the cross-cutting relationships are somewhat unclear. P-shear foliations adjacent to a steeply dipping fault plane also indicate a normal sense of fault displacement (Figure 18). The bedding has a variable dip angle, and rotates progressively from relatively steep orientations in the southwestern part (i.e. towards the Sultandađı range) to nearly horizontal orientations in the northeastern part of the outcrop (i.e. towards the basin). In the southwestern part, steep normal faults are often found parallel or nearly parallel to the steeply dipping bedding. The structure suggests that transtension/extension was accommodated by normal-oblique faulting and by down-thrown dragging of the Tekkeköy conglomerates along the normal faults. Fault-slip directions could not be defined because of the lack of fault-slip indicators such as slickensides and striations. Nevertheless, the orientations of the steeply dipping fault planes suggest a NE-SW direction of extensional deformation. Koçyiđit et al. (2003) studied the structures of similar flow conglomerates in the same region at Doganishar town, and suggests these deposits are normal faulted and terraced during Late Pliocene to Quaternary.

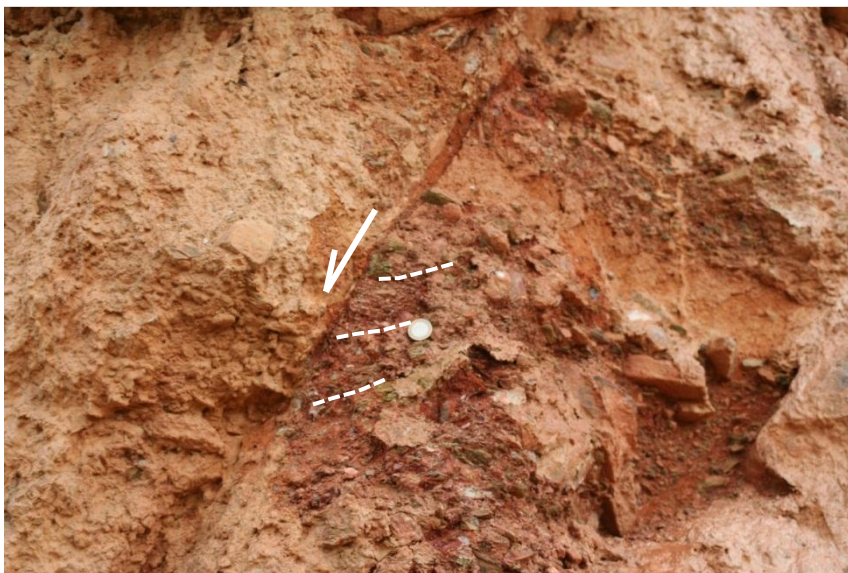


Figure 18. Normal fault at Tekkeköy outcrop (location p indicated on figure 3), dipping to the SW. P-shear foliation in (white dashed lines) are consistent with normal fault displacement of hanging-wall block.

Derbent Fault Zone

Splay faults bifurcate off from the NW-SE trending Akşehir Fault zone and bend into series of parallel, ~E-W to WNW-ESE normal faults of the Derbent Fault zone (Figure 13-15). These faults have downthrown blocks towards the north. Parallel to this zone is the prominent Çifliközü fault scarp, located to the south. This ~E-W striking scarp is recognized in the field by the abrupt change in topography from the lower, relatively horizontal hanging wall and the higher footwall range (Figure 19). Alluvial fan deposits cover the scarp trace and are cut by few faults but these structures were only viewed from a distance of the scarp. Hanging valleys present at the toe of fault scarp suggest a relatively recent fault activity. The parallel striking faults located further to the north of the Derbent Fault zone are not clearly visible in the field but can be observed from 3D view of the DEM by the stepping geometry and tilted blocks between the north dipping faults (Figure 20). The faults are identified by the continuous alignment of multiple segments, crossing the entire width of the southern part of the Ilgin basin towards the east, into the Apa basin. From east to west, the faults segments are laterally traceable over almost 40-50 kilometers of basin width. Large fault scarps and the steeply dipping ground surface between these parallel stepping faults indicate significant throw accumulation. Due to a lack of exposure, only few fault measurements could be obtained from the field. The stereographic projection of figure 7 (locality q, indicated in figure 3 and 14) indicate N-S directed extension.

Towards the east and south of the Derbent Fault zone, a NE-SW (i.e. blue fault trend in figures 13-15) trend becomes more prominent. These faults cross-cut basement rocks of the western margin of the Apa basin and form the boundaries between the basement and the adjacent Neogene basin sediments. From analysis of the DEM it seems that these ~E-W to NE-SW striking, and the less abundant WNW-ESE striking faults form a linkage between the NW trending Akşehir Fault zone and Apa Fault zone. The ~E-W faults of the Derbent Fault zone connect the overstepping area or *relay zone* between the NW-SE-striking and eastward dipping Akşehir and Apa faults zones. River channels parallel to the Derbent Fault zone suggests that the ~E-W striking faults control the drainage of the Ilgin Basin towards the Apa Basin.

At the Akşehir Fault zone, the dominant NW-SE orientation of normal-oblique faults in Late Miocene to Pliocene alluvial fan deposits indicate a general hanging-wall displacement towards the N to NE. Along the southern part of the fault zone and Ilgin basin, along the Derbent Fault zone, normal faults in Late Miocene to recent sediments indicate a hanging-

wall displacement towards the N to NNW. These structures indicate contemporaneous NE-SW and ~N-S direction of extension. There are no outcrop-scale observations of clear cross-cutting relationships between these two fault sets. However, from observation of the Çifliközü fault scarp in the field (Figure 19), it seems that this ~ENE-WSW trending structure cross-cuts a smaller ~NW-SE fault scarp (also indicated on the geological map of the Ilgin area, scale: 1/500.000). Fault patterns and lineations analyzed on the DEM and geological maps show that the main basin trend (i.e. NW-SE) is a more dominant trend than the ~E-W Derbent fault trend and continues outside the study area towards the adjacent basins regions to the west and south (i.e., Beyşehir and Yalvaç Basins and adjacent basement lithologies). The lateral extent of both fault trends may indicate that these structures belong to an older fault set or basement fabric that became reactivated during recent deformation.



Figure 19. ~E-W trending fault scarp at the Derbent Fault Zone near Çifliközü town (see figure 3). Lines and arrows show ~N-ward transport direction of alluvial fans along the scarp trace

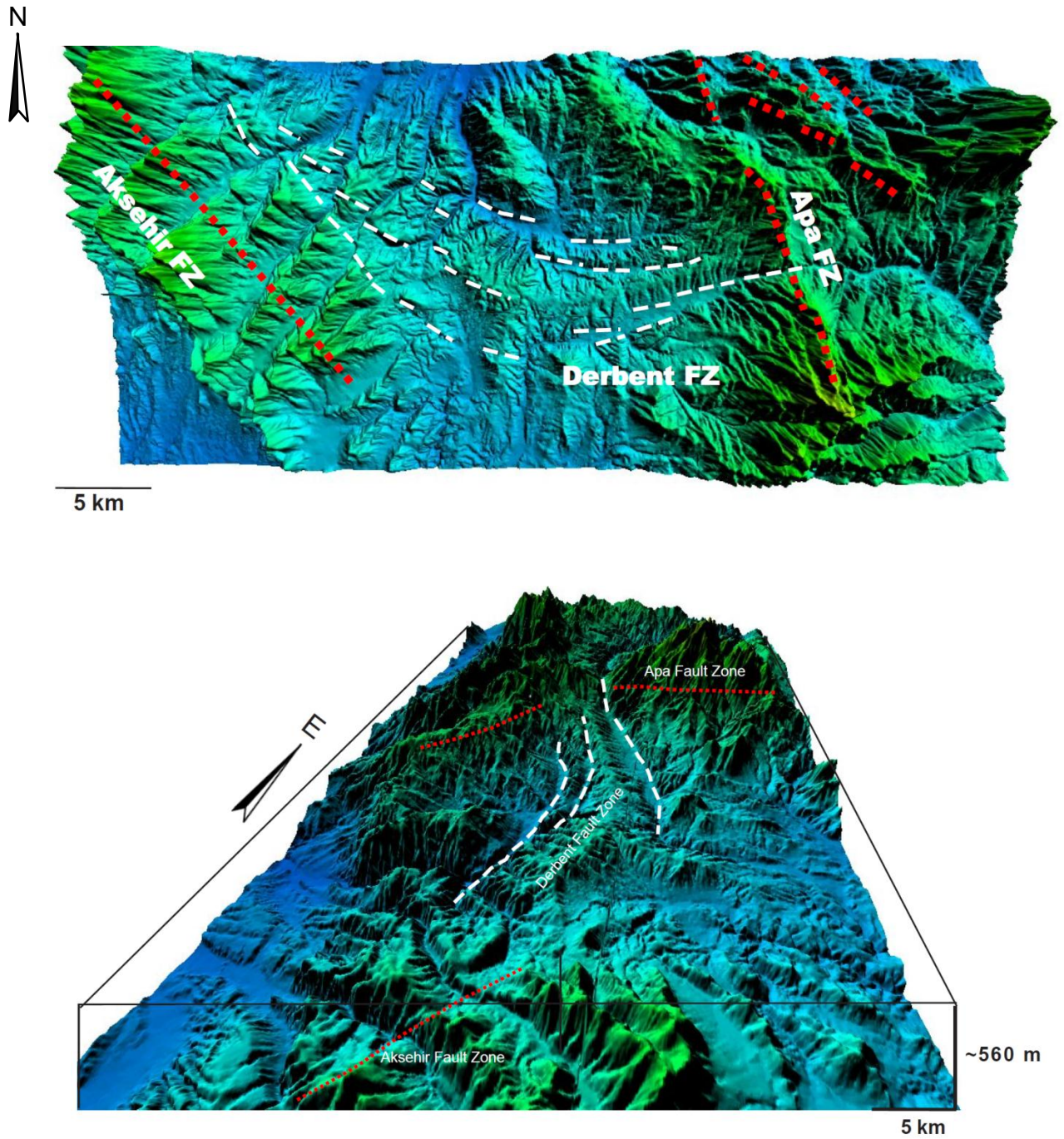


Figure 20. DEM plan view (top figure) and semi 3D view (lower figure) showing the ~E-W Derbent Fault Zone (FZ, white lines) at the southern margin of the Ilgin Basin. Arrays of faults bifurcate off from the southern end of the NW-SE Akşehir FZ in the west and form a ~E-W breaching fault zone (i.e. the Derbent FZ), crossing the relay between the Akşehir and Apa FZ (red lines).

Çhavuşgöl Fault Zone

The structures and tectono-stratigraphy of the Çhavuşgöl Fault zone are studied at three localities, represented by labels s, n and t, indicated on the map of figures 3 and 14. The fault-slip data of normal-oblique faults measured at these localities are represented by the stereographic projections in Figure 21, 14 and 26, respectively.

The structures of locality s are studied at a lignite, open-pit mine, where ~15 m of Quaternary, red alluvium is exposed. These sediments form the upper part of a ~156 m thick, Pliocene to Quaternary sedimentary cover, situated on top of Triassic or older, metamorphic basement rocks (pers. comm. Akpınar Madencilik Company). The upper red-beds are exposed along two, ~E-W and ~N-S orientated trench sections of 50m and ~10m in length, respectively. Syn- and antithetic, normal-oblique faults present in both sections are recognized by their steeply (60-80°) dipping planes and the almost vertical displacements of nearly horizontal bedding planes. The fault planes have slightly listric geometries at downthrown-ends while the upper parts are straighter and steeper. The normal fault indicated in Figure 21 cuts through most of the exposed red-bed sequence. The fault seems listric, but this is an effect of angle of observation; it is rather straight, planar and is slightly curved at its downthrown end. Steeply inclined corrugations and slickensides occur at the lower end of the fault plane (stereographic projection in figure 21). The slickensides are polished grey to greenish minerals, which are most likely iron-oxides. Towards the top, the fault branches upward into a zone of smaller faults, which nearly cut the top surface. Separation of traceable bed-horizons indicates nearly one meter of net displacement along the fault. Smaller faults in the same section show fault-slips of a few centimeters. The amount of fault displacement is only a rough estimate because of the variable bed thickness and slight thickening of beds at down-thrown ends of the fault planes. The thickening at down-thrown sides indicates syn-sedimentary deposition during fault displacement.

The N-S orientated trench located next and perpendicular to the previously described trench (i.e. the E-W orientated trench section, Figure 21), shows meter-scale horst-and-graben structures with dragged layers at the downthrown-sides of the boundary growth faults (Figure 22) The beds show a displacement of ~0.5-1 m. The orientation of these faults is approximately E-W. The orientations of the growth faults in both trenches indicate that both, ~E-W and N-S fault sets were active during the Quaternary. Such polymodal fault-sets are associated with the accommodation of extension in three-dimensions (Healy et al., 2006).

Despite some dragging and minor rotations of bedding planes adjacent to the normal-oblique faults in both trench sections, the stratigraphy is rather horizontal. At the western side

of the E-W trench, the bedding changes orientation from horizontal to ~20 degrees dip to the west. This structure may indicate the development of a hanging-wall rollover anticline of the stratigraphy adjacent to a listric normal fault. The structure could also represent a monocline, where a 'blind' normal fault typically underlies the center of the folded stratigraphy. In this case, slip propagation along the deeper situated fault plane will result in the bending and flexure of superimposed beds bent over the fault. Compared to the overall horizontal upper red-bed sequence, the underlying white limestone, dark clays and lignite series contain only few normal faults and are slightly folded into very open, meter-scale folds. This bending and flexure of bedding planes is also identified on a larger scale (i.e. basin-scale) in the center of the Ilgin Basin (Figure 4). There are no folds nor thrusts that might indicate deformation associated with compression.

There is a rather remarkable structure in the E-W trench of the open-mine pit that can easily be mistaken for a thrust fault (Figure 23). This structure is a relatively high-angle, i.e. 60-70° westward dipping fault, that appears to off-set the strata by a reversed sense of displacement. The beds at the up-thrown side of the fault seem to be thrust over the corresponding beds of the downthrown block. This structure suggests compressional deformation but this seems very unlikely, since there are no other indications or structures associated with compressional deformation in the Ilgin Basin. Compression is commonly accommodated by broader zones of intense folding and thrusting.

Tectonically induced changes in the principle stress field

The basic concepts and methods of mechanics of tectonic faulting of Mandl (1988) can provide insights on the structures observed in the open mine pit at the Çhavusgöl Fault zone. Explained by the concepts of Mandl (1988), it is apparent that there is a significant difference in differential stress between fault failure in compression or extension. Because of this difference, the material subjected to tectonic shortening by thrust faulting will generally be much more intensely deformed than in extension by normal faulting. It is thus likely that thrust faults will be found embedded in a wider zone of pre-faulting deformation than normal faults (Mandl, 1988). The single fault in Figure 23, seems to represent a reversed fault, but is enclosed by nearly horizontal bedding markers and folds or intense deformation zones are absent. Mandl (1988) proposed an alternative explanation for the development of such (precursor) fault structures under extension. They recognized that the effects of tectonically induced changes in the stress field associated with the formation of these structures are important controlling factors. Changes in principle stress directions are thought to be very

common, because of frictional stresses along the base or lateral boundaries of a deforming rock mass. In contrast with normal faulting, these effects are better pronounced in low-angle thrusting where large strains, accompanied by the build-up of a large differential stress, precedes the formation of the fault. To illustrate this, Mandl (1988) gives an example of the formation of a low-angle thrust in a horizontally shortened strata that have a frictional contact with underlying, undeformed basement. Before the formation of the actual thrust fault, basal shear stresses will deflect the σ_1 -trajectories and enable the thrust fault to develop a listric shape. In contrast, a normal fault may develop in brittle rocks on a rigid basement that is rifted apart, or on a substratum that is locally stretched. The strains preceding normal faulting will remain small and the associated basal shear stresses may have only little effect on the σ_1 -trajectories (Mandl, 1988). These concepts illustrate that in general, strain accommodation in extension is much 'easier' (i.e. requires less work) than in compression.

Mandl (1988) compared the results of computational fault simulations with results of sandbox experiments. The results illustrate that strong changes in principle stress directions related to normal faulting in overburden sediments may occur as a result of movements along vertical faults in a basement substratum. In case of a uniform brittle overburden and initial stress isotropy ($\sigma_1 = \sigma_3$), vertical movements in the basement is accommodated along a plane of maximum shear strain and shear stress in the overburden, forcing the σ_1 -trajectories to intersect that plane at 45° (Figure 24 and 25). Because of the partial unloading of the subsiding basement block, σ_1 -trajectories will form a 'stress arch' that transfers overburden load to the higher basement block (i.e. footwall). Consequently, the faults in the overburden may have a character of downward-concave reverse faults (Mandl et al., 1988).

In a case of a model representative for a more natural situation, Mandl (1988) studied the effect of a multilayered overburden by analyzing the influence of weak bedding planes on the directions of principle stresses and associated faults. In this model, the assumption is made that before the onset of faulting, the layers are flexed, and the frictional resistance of the densely spaced bedding planes is ignored. In this situation, the σ_1 principle stress trajectories will initially be perpendicular to the bedding plane, and the first normal fault will develop where the flexure, induced by extension of the bedding, is greatest. The faults now have a character of normal faults, dipping towards the down-thrown block. The stress trajectories will be changed by shearing, induced by flexural slip of the beds. Because of the sliding of upper beds over underlying beds, towards the point of greatest curvature, the bedding-parallel shear stresses are directed towards the faults (indicated by dotted arrows in figure 25). The σ_1 principle stresses are now no longer perpendicular, but make acute angles with the beds and

open against the relative slip directions. The σ_1 -trajectories widen and the upward-convex faults will be more strongly curved. According to this model, normal graben bounding faults are expected to form first instead of a reverse fault. In more natural situations, changes in fault shape and orientation will depend on many tectonic and non-tectonic factors which are not included in the models of Mandl (1988). Non-tectonic factors may include strength anisotropies, compaction by overburden weight, and high pore pressures. Tectonic events, affecting the shape of an incipient or fully developed fault are related to changes in the stress field, which is often thought to be linked to changes in far-field stresses (i.e. stress-field on a more regional-scale) caused by regional-scale tectonic processes. Another important factor is the influence of pre-existing basement structures that form weak zones of leading to strength anisotropies. Such weak zones are easily reactivated and may interact with newly developed faults. Prominent structural trends present in the Ilgin Basin and adjacent regions on a larger scale are likely old, inherited basement trends that may have strongly influenced the orientation and style of newly developed faults. The conceptual models of Mandl (1988) described earlier provide insights on the mechanics of faulting in the alluvial red beds at the open-mine pit, and may explain the kinematic style of faulting to some extent. The model does not however, include the effect of fault interaction between interconnected faults and the influence of basement strength anisotropies.

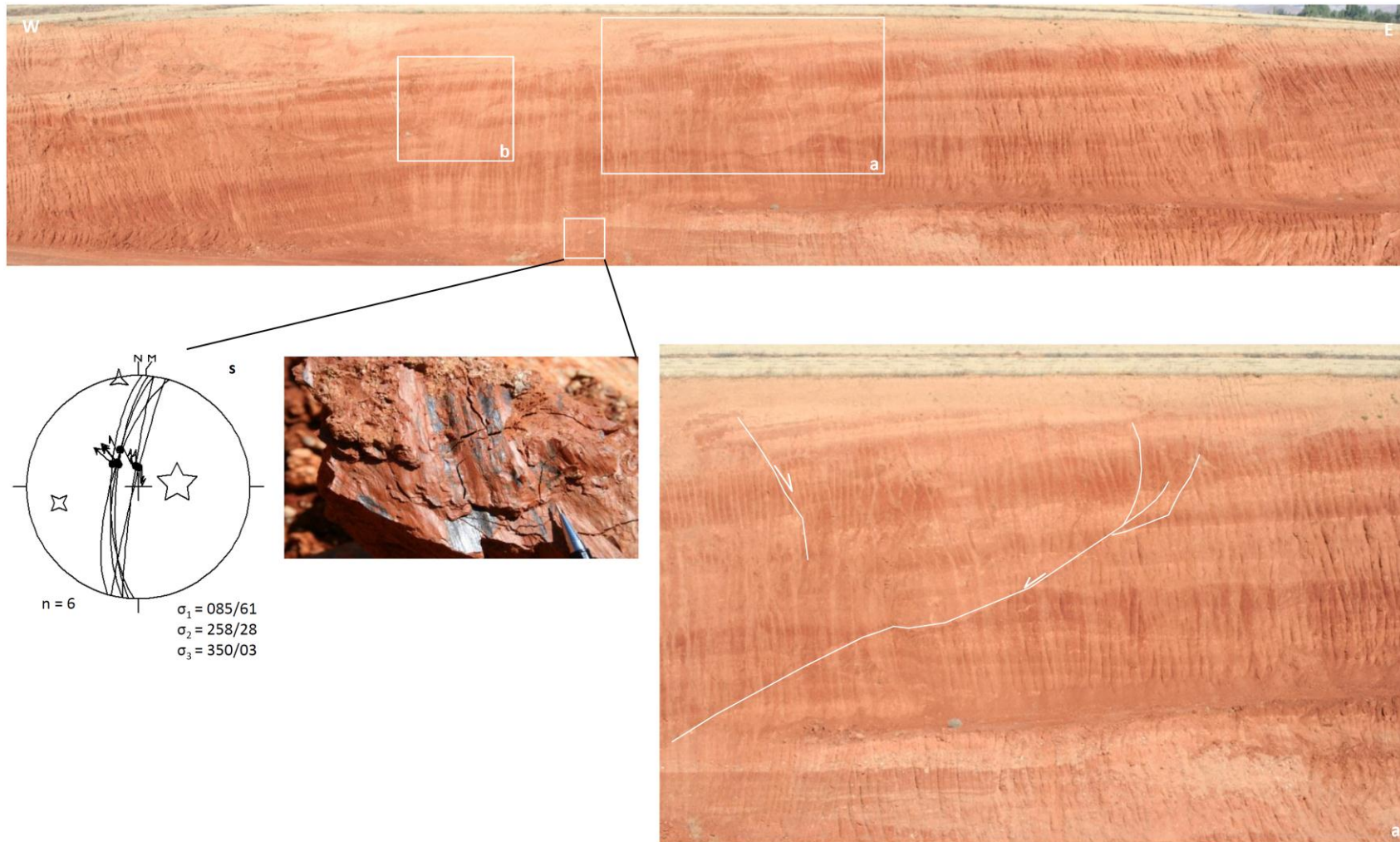


Figure 21. Normal faults dipping ~E and W in Quaternary red alluvium with caliche horizons at the Çhavusgöl Fault zone. Most faults show thickening of bedding at downthrown sides, indicating fault growth during deposition. Stereographic projection (equal area, lower hemisphere) showing fault slip data, indicating NNW-SSE directed extension. Square indicates location of measured fault plane and lineations. Length of section is approximately 50 m, and height 15 m. **Figure a:** Enlargement of part of the trench section showing normal faults dipping west.

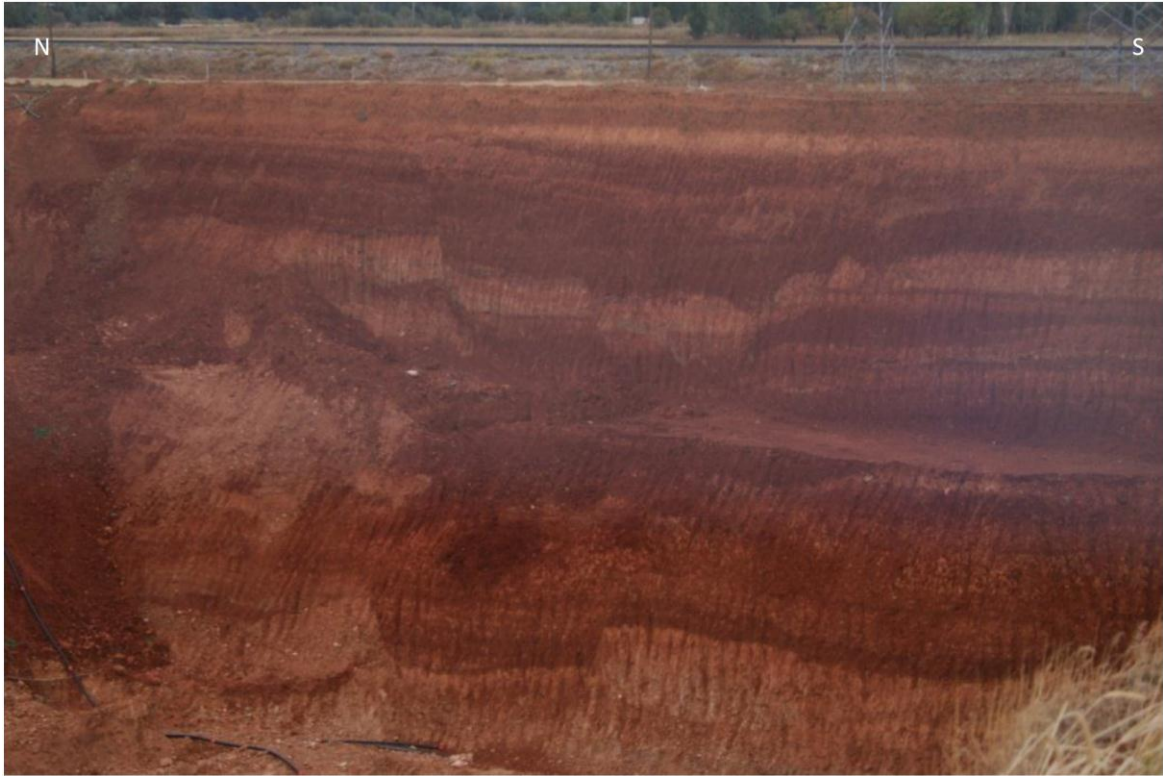


Figure 22. 10x10m section perpendicular, i.e. ~N-S, to the section of Figure 21, showing graben structures with growth faults dipping N and S.



Figure 23. Enlargement of part of the trench section indicated by large square (b) in Figure 21, showing a precursor fault structure (Top left of photo; Mandl. 1988).

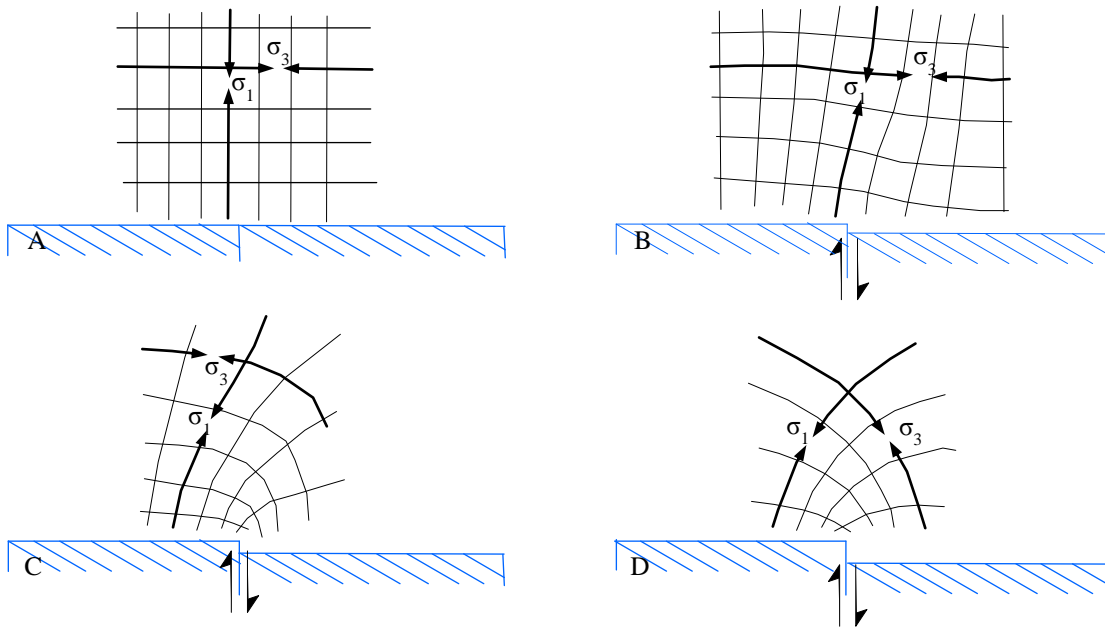


Figure 24. Principle stress field above a vertical basement fault. Initial stress field (A) will deflect with increasing vertical displacement (B-D). Modified after Mandl (1988)

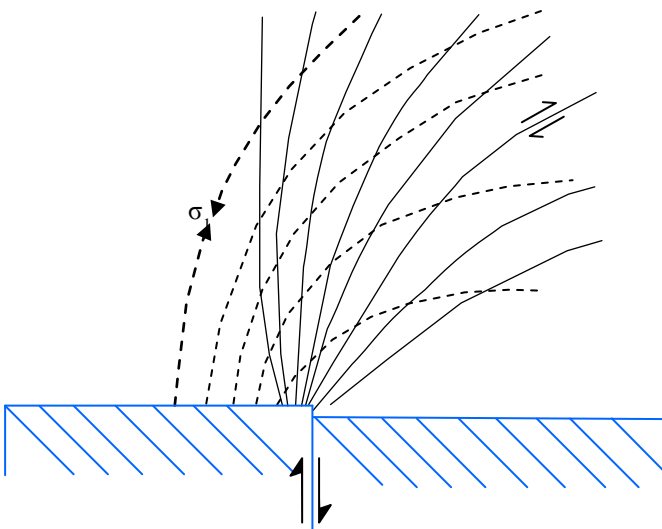


Figure 25. Schematic illustration of precursor faults above a vertical basement offset at low confining stress conditions. Stress field is similar to situation in figure 24D. Modified after Mandl (1988).

A few kilometers to the south of the lignite mine, ~2 m² fault scarps are exposed along a 15-20 meter long road section (indicated by label t on figure 3). These prominent scarps are also observed on the DEM. The scarps are separated by blocks of basement limestones, alternating with zones of unconsolidated breccia and red marls (Figure 26). The basement metamorphic rocks consist of calcite veins and are intensely fractured and brecciated. Adjacent to the individual fault planes, the brecciated zones of marl and clay contain angular clasts of variable sizes that are frequently coated with white, carbonate precipitate rims. This coating is often found as a network of cement between the clasts, forming zones of slightly more consolidated breccias. These are most likely travertine networks, which indicate the precipitation of carbonate minerals from solution in ground, surface or geothermal water. As hot springs are common in the region, these travertines are likely formed by upward percolation of geothermal water through cracks and fractures.

The eastward dipping fault scarps are straight or corrugated and vary in strike from ~N-S to NNE-SSW, with dips between 60 and 80 degrees to the east. Striations on the fault surfaces are generally steeply plunging white calcite slickensides, occasionally down-stepping, indicating a normal sense of displacement. These calcite slickensides tend to completely cover the exposed fault surfaces, giving the planes a polished finish. Few of these planes have less continuous, more fractured lineations. The rakes of the slickensides vary from 60-80°, to shallower values of 30-45° and indicate a left-lateral sense of shear. Stereographic projection (equal-area, lower hemisphere, figure 26) of the combined fault-slip data show a NE-SW directed transtension. The adjacent clastic-rich red marls are in composition similar to the alluvial fan deposits located at the open-mine pit to the north, suggesting a comparable, i.e. Quaternary age for the deposits. The fault scarps, formed within these sediments indicates recent fault activity. In addition, the fresh appearance of the scarps at the road section (location t) suggests a quite recent increment of slip along these planes.



Figure 26. Road section showing fault scarps (white squares) at the Chavusgöl Fault zone. The scarps are almost planar (a) or curved and corrugated (b) and consist of steeply dipping lineations and striations. Stereographic projection (equal area, lower hemisphere) showing fault slip data of the three left planes of the section, indicating NE-SW directed extension.

Fault slip data from the Çhavuşgöl Fault Zone and their significance

The direction of oblique-slip vectors along the fault planes, and thereby the orientation of the principle stress axes, is not consistent throughout the outcrop. The directions of slickensides are rather variable and the fault scarp of figure 27 is highly curved and corrugated. Multiple sets of slip vectors are often typically interpreted to develop by multiple, successive events of tectonic deformation by which each event or ‘phase’ of deformation corresponds to a differently oriented set of slip vectors and consequently indicate different orientated stress fields (e.g. Angelier, 1983, 1994). The change in orientation of principle stress axes are often linked to far-field stresses related to changes in regional-scale, tectonic plate configuration. These inversion methods use the assumption that the direction of slip is constant over each fault plane and occurs in the direction of maximum resolved shear stress, and thereby ignoring the significant effects of fault interactions or fault geometry. The curved fault scarp in figure 27, consists of curved corrugations and slickensides suggesting that the assumption of parallelism between maximum resolved shear stress and slip vectors, assumed for the inversion methods, is not satisfied. Instead, the curved plane may suggest that the direction of local principle stresses changed during the formation of the fault along the fault plane, and thereby changing the geometry of the fault plane. Variations in slip directions and fault shape are explained by, e.g. Willemse et al. (1996) and Maerten et al. (1999, 2000), by mechanical interaction between coeval linked faults and are thought to be closely related to local stress/strain perturbations (Willemse et al., 1996).



Figure 27. Curved and corrugated fault scarp at the Chavusgol Fault zone (indicated by square b in figure 26).

4. Basin geometry and kinematics: discussion

The southwestern margin of the Ilgin basin is controlled by the main NW-SE trending Akşehir Fault zone. In southeasterly direction a ~30 km long zone of W-E trending splay faults form the Derbent Fault zone, which is interpreted as an overstepping link between the Akşehir Fault zone and the NW-SE trending Apa Fault zone to the East of the Ilgin Basin (Figure 13). River channels parallel to the Derbent Fault zone suggests that these structures control the drainage of the Ilgin basin towards the Apa basin. The Derbent Fault zone has a terraced geomorphology with large fault scarps dipping towards the N to NE. The steeply dipping ground surface between these E-W to WSW-ENE, parallel faults indicate significant accumulated normal to oblique throw. Such splay faults or breaching fault geometries are typically associated with the development of relay ramps (Goguel, 1952; Larsen, 1988; Peacock et al., 2002) or monoclinial ramps (Macdonald; 1957; Peacock et al., 2002). Peacock et al. (2002) and Peacock and Sanderson (1991, 1994) consider a relay ramp (Figure 28) typical for transfer of displacement between overstepping, normal faults, connecting the footwall of one fault or zone of faults, with the hanging-wall of another.

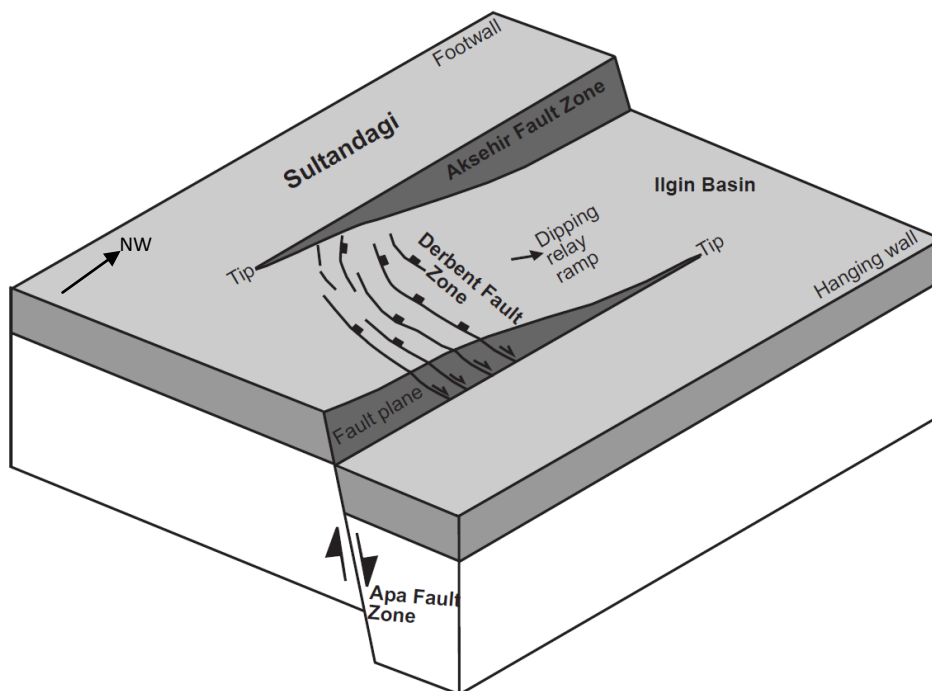


Figure 28. Block diagram showing the main structures of the breached relay ramp located in the southern region of the Ilgin Basin between the overstepping Akşehir and Apa Fault zone. The northward stepping faults of the Derbent Fault zone accommodate displacement between the overstepping fault zones (Figure modified from Peacock, 2003)

Relay ramps with variable geometries and scales are identified in many regions, for example: the East African Rift (e.g., Griffiths, 1980; Morley et al., 1990; Ebinger et al., 1989; Nelson et al., 1992), the British Isles (Peacock and Sanderson, 1991; Huggins et al., 1995; Peacock, 2003), Hawaii (e.g., Peacock and Parfitt, 2002), the Basin and Range (e.g., Machette et al., 1991; Anders, 1995; Ferril et al., 1999). The scale of these relay ramps can range from cm-scale to hundreds of kilometers in variably important structures that control the shape and discontinuity of extensional (rift) systems. (e.g. Ancocella et al., 2005). The variable geometry of relays may indicate different evolutionary stages of fault linkage (e.g. Peacock and Sanderson, 1991, 1994; Peacock et al., 2002). Based on the degree of interaction and linkage between fault segments, Peacock et al. (2002) and Peacock & Sanderson (1994a) identified four general stages of relay ramp evolution (Figure 29). *Stage 1* is characterized by normal fault segments that do not interact. These structures are identified as sub-parallel, non-coplanar, possibly underlapping fault segments. In this early evolutionary stage the zone between the faults shows gentle dips and little or no internal faulting. During *Stage 2*, interaction between fault segments initiate and tilted beds between two interacting faults form a relay ramp or monoclin ramp (Macdonald, 1957). The dip of the ramp increases with increasing down-throw along the bounding overstepping faults. It is important to realize that the faults may seem unconnected at the surface, whereas they can be connected at depth. During *Stage 3*, the relay ramp is being ruptured by connecting fractures that progressively evolve into a zone of larger faults. This stage includes the formation and linkage of breaching syn- and antithetic faults within the relay zone. At *Stage 4*, the relay ramp is completely breached and destroyed by through-going faults cutting across the entire relay ramp. These four stages can develop through time or spatially with depth along the fault zone (Peacock et al., 2002). Hanging-wall rollover, with folding of the fault blocks can occur progressively through these stages, for example by decreasing dips of the bounding faults at depth (i.e. listric fault geometries). Cracks in the hanging-wall will partly accommodate hanging-wall rollover and continue to propagate into larger fractures and faults. The gentle bedding dips (~10-20°) and large-scale (i.e. basin-scale) flexure of the basin sediments observed in the Ilgin Basin can be a result of large-scale bending and hanging-wall rollover at the Akşehir Fault zone. Also ~N-S monoclin folding at the relay ramp before the formation of breaching faults of the Derbent Fault Zone, as well as blind faults present at depth may be responsible for the gentle dipping stratigraphy.

In general, relay ramps that develop as unbreached slopes between stepping faults and extensional fractures, are also referred to as ‘soft-linked’ accommodation zones (e.g, Walsh

and Watterson, 1991), i.e., *Stage 2* of Peacock et al. (2002). ‘Hard linkage’ of accommodation zones (Walsh and Watterson, 1991) occurs when fault interaction continues, and faults grow by the coalescence of multiple cracks or fractures within the relay ramp (i.e. comparable to *Stage 3 and 4* of Peacock et al., 2002).

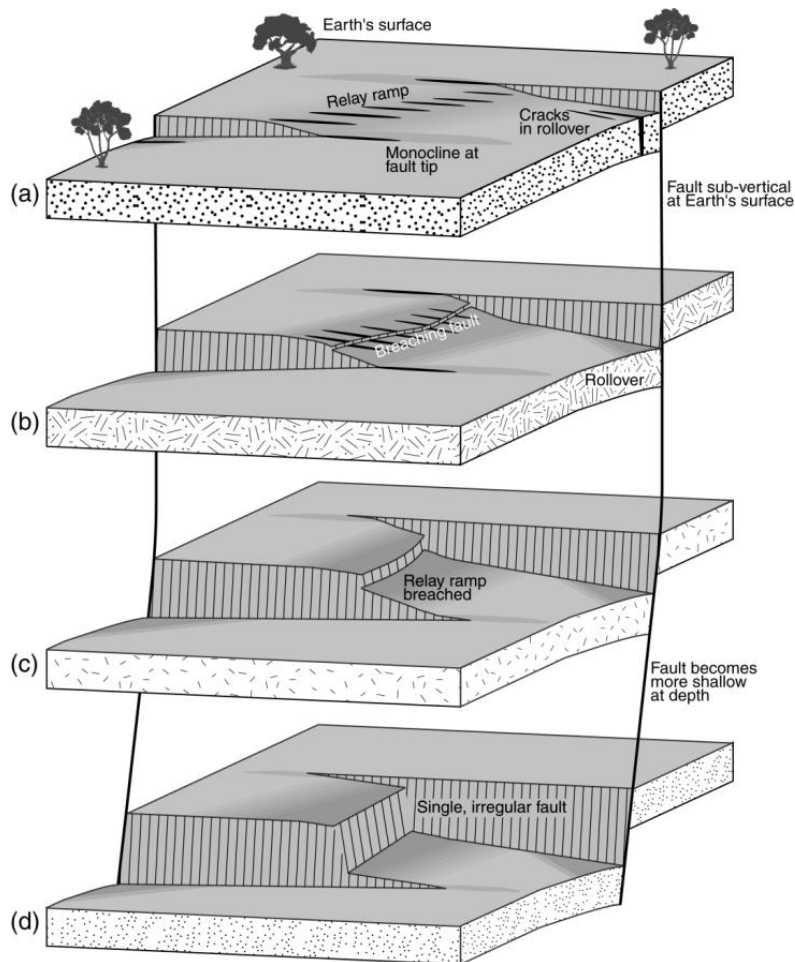


Figure 29. Block diagram showing the temporal and spatial evolution of overstepping faults and relay breaching. Three evolutionary stages of relay ramps can be identified. (a) Bounding faults understep but may be connected by an echelon cracks. (b) The relay ramp develops as the faults overstep and become connected by a breaching fault as displacement increases. The breaching fault cuts across the center of the relay ramp. (c) The relay ramp is breached. The layer in (d) shows a single, irregular fault. Four stages may be identified in the propagation of individual fault segments. (1) A monocline develops above a dipping normal fault (the sub-surface lateral continuation of a fault seen at the surface). (2) Vertical cracks occur bounding and within the monocline. (3) Hanging wall rollover develops as throw increases along the overstepping fault probably because the normal faults are listric. Rollover is partly accommodated by cracks in the hanging wall. Figure adapted from Peacock et al. (2002).

The model of relay ramp formation of Peacock et al. (2002) provides insights regarding the interaction of faults, and how zones of overstepping faults can progressively evolve into hard-linked, interconnected networks of variable orientated faults, such as observed in the Ilgin Basin and adjacent regions. According to the evolutionary stages of relay ramp development, the breaching faults of the Derbent Fault zone are formed during a later stage (i.e. stage 3 or 4) and are relatively younger than the basin-boundary faults. However, clear cross-cut relations between the bounding Akşehir and Apa Fault zones and the nearly perpendicular striking Derbent Fault Zone cannot be identified. Moreover, cross-cutting relationships between the other fault trends present in the Ilgin Basin are also not determinable on outcrop scale nor on plan view maps and the DEM of the region. The interaction and linkage of coeval faults of variable orientations and the presence of pre-existing basement structures may explain why the inter-relationships between faults are obscured.

NW-SE striking faults form the most dominant structural trend in the Ilgin Basin, as well as in the adjacent Beyşehir and Yalvac Basins, and even further to the west in the inner flanks of the Isparta triangle. This prominent trend of regional importance is probably an old, pre-existing basement grain that was reactivated during Neogene to recent basin development. This trend would suggest a basin-scale, NE-SW direction of extension during the formation of these basins. However, the presence of the nearly E-W and WNW-ESE trending faults would indicate ~N-S to NNE-SSW extension in the southern zone of the Ilgin basin. This could suggest that a local stress field with a ~N-S orientated minimum principle stress axis (σ_3) acts on the domain of the Derbent Fault zone, and a more regional-scale (i.e. basin-scale) stress field with a NE-SW orientated σ_3 acting on the Akşehir and Apa Fault trends. In this scenario, partially overlapping stress domains result in extensional deformation accommodated in both, NE-SW and N-S directions. However, this proposition does not explain the presence of the other, NNE-SSW and NE-SW striking fault trends in the Ilgin Basin region. It is possible that under the overlapping stress domains as previously described, pre-existing faults with different orientations are hard-linked at depth and susceptible to coeval reactivation. Slip along one fault plane can trigger slip on a cross-cutting (set of) fault(s). Although the prominent structural trends suggest that pre-existing basement structures may play a significant role in the development of the deformation pattern in the region, the conspicuous 'horsetail' basin architecture cannot be explained by a kinematic 'end-member' model of pure extension in NE-SW or ~N-S directions. The curvature in fault trends from the Akşehir Fault zone to the northward stepping Derbent faults give the Ilgin Basin its typical geometry. The

typical right-stepping horsetail observed in plan view on the DEM and maps of the region suggest that a transtensional kinematic system with a minor left-lateral slip component may have controlled the deformation on the Ilgin Basin, and possibly even larger, regional scale.

Fault patterns modeled by analogue sandbox experiments provide information on the possible orientations and kinematics of newly developed faults under a specific applied stress field. The development of the horsetail structures under transtensional deformation is confirmed by analogue sandbox experiments where oblique-slip along a steeply dipping (i.e. $\sim 60^\circ$) basement fault occurs under left-lateral transtension with a moderate strike-slip to dip-slip component. Figure 30 shows the structures that develop under such conditions in an isotropic sand medium. The faults are slightly right-stepping and few are connected, creating the typical tail-structures. Relays develop between overstepping faults. The experiment uses an isotropic overburden sand medium and is therefore not representative for natural conditions where anisotropic inherited basement structures are involved. Although such sandbox models are limited by boundary conditions due to their experimental set-up and the isotropic medium, they do show the range of possible fault orientations and structural geometries that may develop under specific stress conditions. Experimental analogues that include pre-existing basement anisotropies are poor but the presence of weak, distributed basement trends are believed to play a significant controlling role on the reactivation of pre-existing faults and development and linkage of new faults (DePaola et al., 2005; An and Sammis, 1996; Jones et al., 2005). Previous studies on regions with rift related deformation recognized that the directions of divergence are oblique to the main boundaries of transtensional strain (Harland, 1971; Withjack and Jamison, 1986; Woodcock, 1986; Smith and Durney, 1992; Dewey et al., 1998; Dewey, 2002; DePaola et al., 2005). Three-dimensional, non-coaxial strains at regional-scale can relate to deformation caused by oblique lithospheric plate motions and/or intrabasinal faults, which results in reactivation of pre-existing structures with an orientation oblique to the maximum extension direction. The first case of oblique plate separation assumes a homogeneous transtensional model (Sanderson and Marchini, 1984; Dewey et al., 1998). The second case describes how bulk strain by transtension is split up in local domains of partitioned transtension where the location and orientation of structures are controlled by pre-existing anisotropies, such as lithological contacts, faults and shear zones structural basement (Tikoff and Teyssier, 1994; Jones and Tanner, 1995; Jones et al., 2005; DePaola et al., 2005). Thus, instead of a localized zone of bulk strain, accommodation occurs over a wide zone where pre-existing structures preferentially take up components of the bulk transtensional strain. Progressive brittle

deformation by transtension in the Ilgin Basin and adjacent region may have resulted in the development of partitioned domains of variable kinematic significance that continued to develop, creating an interconnected network of faults and thereby increasing structural complexity.

Figure 31 illustrates the concept of the significance of distributed pre-existing structural trends, mainly based on the results and conclusions from analogue sandbox experiments by An and Mannis (1996) and Richard et al. (1995). The top figure (A) shows an end-member model of left-lateral, simple shear along one basement trend assuming an isotropic overburden. This scenario represents the most ideal isotropic conditions under which arrays of right-stepping shear fractures (c.f. Riedel, 1929) develop. In case of multiple basement trends, simple shear is distributed over a wider zone and accommodated by syn- and antithetic shear fractures and by (hybrid) transtensional fractures, indicating an increasing component of extensional (B) opening of hybrid cracks perpendicular to the maximum principle stress axis). Under progressive transtensional deformation (C), extension along the right-stepping fractures continues and normal-oblique faults are formed. The syn- and antithetic shear fractures are no real strike-slip Riedels (i.e. in the sense of Riedel, 1929) but rather oblique-slip normal faults with a significant dip-slip component. Both syn- and antithetic faults continue to grow along the multiple parallel basement trends and will start to coalesce into larger faults with variable orientations. The direction of far-field extension acting on the wide zone (i.e. basin-scale or a larger regional scale) does no longer correspond to the orientations of normal-oblique faults because strain is accommodated preferentially along the pre-existing fractures and faults which have variable orientations. Continued transtension leads to the formation of a completely interconnected framework of oblique-slip faults (D). If transtension continues even further, subsidence and collapse will lead to the formation of a basin or rift complex with a subsidence axis perpendicular to the far field minimum principle stress axis (σ_3). Note that for the kinematic models illustrated in Figure 31 only a set of parallel trending basement anisotropies is involved, whereas in more realistic natural conditions, the basement structural trends are variable and will consequently lead to a highly variable fault pattern in the overburden.

The multitude of intersecting basement trends identified in the Ilgin Basin and adjacent regions confirm that neotectonic deformation is probably strongly controlled by the pre-existing structures. It is likely that these trends are reactivated under regional ~NE-SW extension in an overall left-lateral transtensional system (Figure 32) that acts not only on basin scale but probably on a much larger, regional scale. This kinematic system is

comparable to the system represented by figure 31D and shows that the interaction of structural anisotropies in the Ilgin Basin may explain the presence of active faults that have an adverse to unfavourable orientation with respect to the ~NE-SW far field minimum stress axis (σ_3).

Individual domains of finite strain at measured outcrop-scale or basin sub-areas may therefore not display the same orientation as the bulk strain that acts on a regional-scale or even plate-tectonic scale. Consequently, fault-slip data collected from an area as large as possible is required to be able to relate outcrop-scale or basin-scale structures and the associated stress axes to global-scale tectonic processes (Jones et al., 2005).

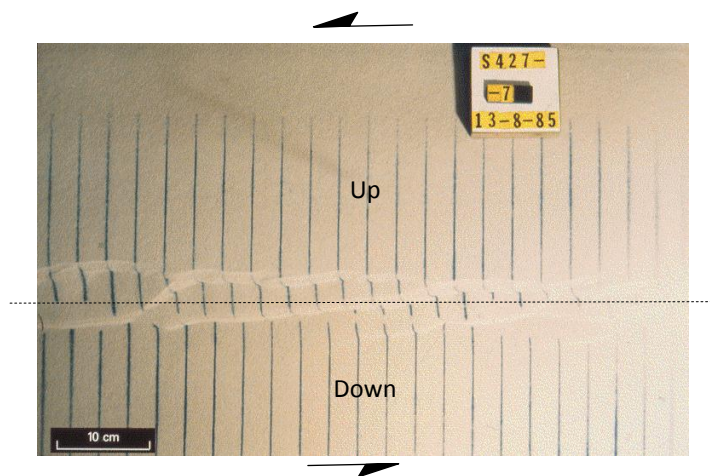


Figure 30. Sandboc experiment (plan view) showing the fault patterns in an isotropic overburden as a result of oblique-slip on a steeply dipping basement fault (dashed line) with a minor left-lateral strike-slip/dip-slip ratio. The right-stepping fault patterns and 'horsetailing' indicate a left-lateral component of displacement (modified from Richard et al., 1995)

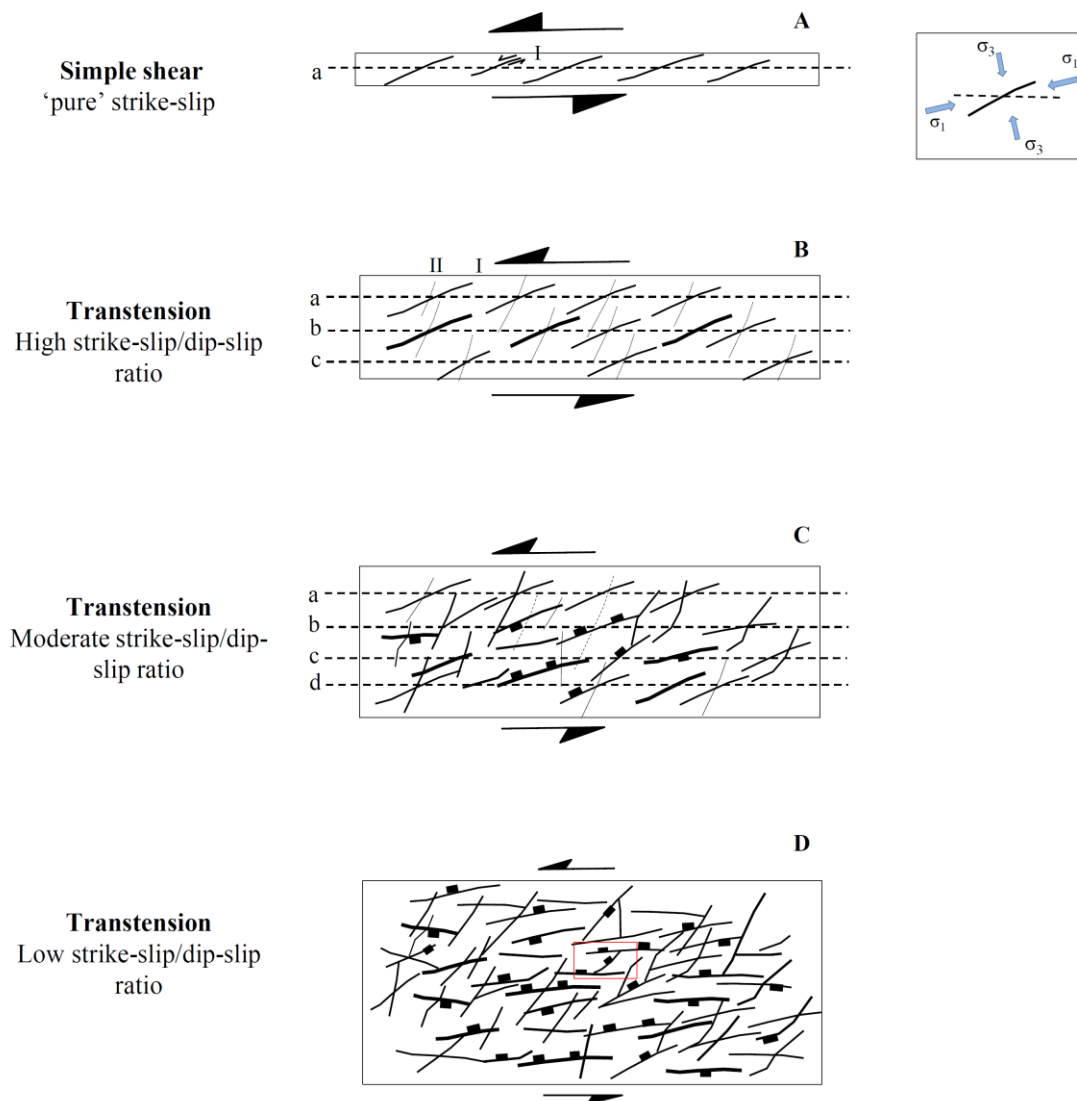


Figure 31. Schematic illustrations of four kinematic models showing fault patterns and orientation of faults typically formed under simple shear (A) along one pre-existing basement anisotropy (horizontal dashed line a) and under left-lateral transtension with increasing influence of basement anisotropies from model B-D. Orientation of applied stress field is the same for all models. Model A represents an end-member model of strike-slip (i.e. most isotropic scenario), where synthetic Riedel shears (I; antithetic Riedels: II) develop along a narrow shear zone. With increasing number of basement anisotropies (dashed lines b-d), strike-slip/dip-slip ratio decreases and left-lateral transtension is accommodated along a wide zone of normal-oblique faults. Hybrid model D illustrates a wide zone of intersecting normal-oblique faults with orientations predominantly parallel to the (re-activated) pre-existing basement trends, forming a hard-linked, semi-orthorhombic fault pattern. Note that in these models the basement trends are parallel, but in more realistic and natural scenarios, there are multiple, variable basement trends, which will result in more chaotic, hard-linked fault pattern than illustrated in figure D. The kinematic stress system of the Ilgin Basin can be considered as a small domain (red square in figure D) in a much larger overall left lateral transtensional stress system with a minor strike-slip component. Figures are based on results and conclusions from An & Sammis (1996) and Richard et al. (1995).

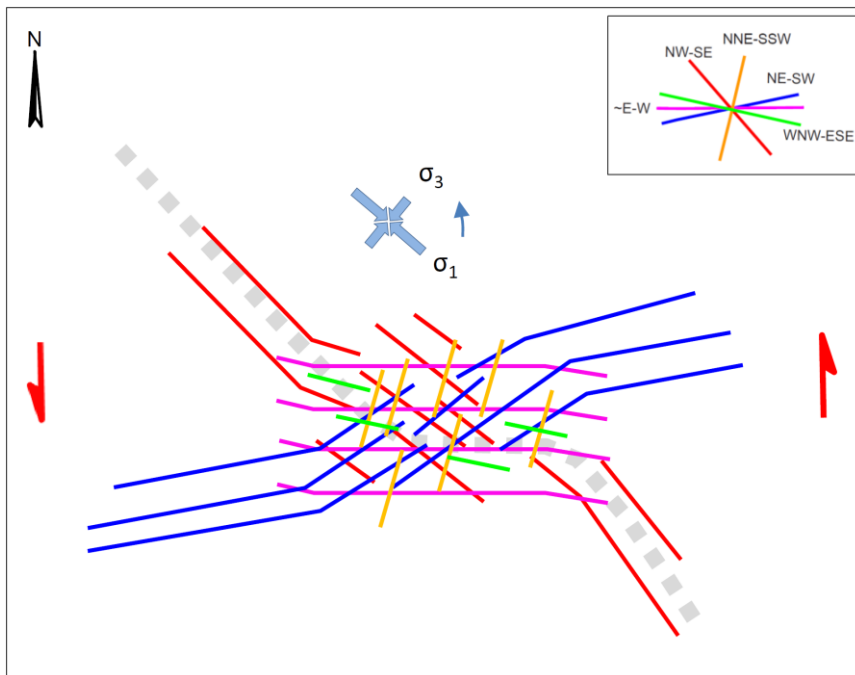


Figure 32. Schematic kinematic model showing the typical, right-stepping horsetail geometry of the Ilgin Basin area and the intersecting structural trends. The basin geometry indicates a left-lateral transtensional (neotectonic) kinematic fault system under a far field stress domain with ~NE-SW minimum (σ_3) and NW-SE maximum (σ_1) principle stress axes.

5. Implications of present study

Implications for the stress Inversion Method

Many outcrop-based studies in a large variety of structural settings and regions worldwide use the results obtained by the (paleo) stress inversion method (Angelier, 1979; 1984, 1990, 1994) to extrapolate to regional/basin-scale analyses and plate tectonic models. As for any brittle deformation structure, strain increments related to the formation of faults are associated with the magnitude and direction of stresses exceeding the bulk strength of the rocks involved. So, faults can provide information about the nature of paleo-stresses acting on the bulk rocks involved. On the basis of these general presumptions, the inversion method assumes that the direction of slip along each fault plane is constant and occurs in the direction of maximum resolved shear stress (Carey and Brunier, 1974; Wallace, 1951; Bott, 1959; Etchecopar et al., 1981; Angelier, 1979, 1984, 1990, 1994; Petit and Laville, 1985; Means, 1987; Reches, 1987; Krantz, 1988; Lisle, 1987; Doblas, 1998). Moreover, a spatially and temporally single homogeneous tectonic stress field is assumed to be responsible for the direction of slip on fault planes. Applying these paleo-stress inversion principles, the fault slip data obtained from the Ilgin basin would provide an estimation of the orientation of local principal stress axes acting on single fault segments. However, it is important to realize that strains observed in a relatively limited, outcrop-scale domain do not necessarily equal the bulk finite strain at basin-scale or plate-tectonic scale. Therefore, data must be collected from areas as large as possible to relate local structures to a regional kinematic system, or to plate-tectonic scale (Jones et al., 2005). The Ilgin Basin is moderately exposed and fault-slip data for the inversion method are limited. The integration of fault-slip measurements from the field and the structural analysis using the DEM is therefore essential to reconstruct their meaning in terms of kinematic evolution of the Ilgin Basin. The interconnectivity and interference between cross-cutting faults in the Ilgin Basin and probably also the adjacent basin regions are prominent complications to the application of the stress inversion method.

As typically done in stress inversion studies, the variably distributed slip vectors (i.e. slickensides) on normal fault planes are often related to multiple phases of slip during successive episodes of regional-scale (extensional) deformation. Thus, each set of slickenside striations are related to a 'phase' of deformation. However, the intersecting contemporaneous fault sets observed in the Ilgin Basin on outcrop and basin-scale, both on maps and in cross-

sections, indicate that faults form an interconnected, hard-linked network of fault segments with synchronous activity. Several studies have documented slip distributions on fault planes that show multiple slip maxima near the intersection line of two crossing faults (Walsh and Waterson, 1991; Childs et al., 1993; Mansfield and Cartwright, 1996; Nicol et al., 1996; Maerten et al., 1999; Maerten, 2000). These slip characteristics are explained by the mechanical interaction between intersecting coeval faults. Analysis of the fault slip direction show that the direction of slip along a fault plane is especially influenced in zones adjacent to fault intersections and illustrate that the assumption of parallelism between maximum resolved shear stress and slip vector used in stress inversion methods are not satisfied (Maerten; 2000). This implies that, if known, the strike of the faults and their vertical dimensions can be used to estimate the area adjacent to fault intersections, where fault slip data should not be used in stress inversion analyses. Examples of curved fault plane geometries observed in outcrops in the north of the Ilgin Basin (i.e. the Çhavüsgöl Fault Zone) also indicate that stress along such planes is accommodated by slip into variable directions, leading to the curvature of slickenside striations.

Regional implications of the Ilgin basin kinematics

The regional extent of the NW-SE trending overall left-lateral transtensional system that acts on the Ilgin Basin is unclear. However, prominent hard-linked basement trends continue towards the southwest of the Sultandağı mountain range and extend further west into the inner eastern flank of the Isparta Angle. This suggests that the early (i.e. Pre-Cenozoic) deformation history of the region and the formation of the basement trends must have been similar. A structural and kinematic study of the Beyşehir and Yalvaç basin regions immediately adjacent to the west of the Sultandağı may provide more insights to the lateral extent of the transtensional domain of the Ilgin Basin.

Koçyiğit et al. (2003) studied the Early Miocene to Quaternary tectono-stratigraphy of the Akşehir-Afyon graben to the northwest of the Ilgin Basin and proposed a multistage evolutionary history. The lower, Early – Middle Miocene fluvio-lacustrine sediments of the basin are folded and thrust and unconformably overlain by a relatively horizontal Pliocene – present-day fluvio-lacustrine sequence, locally faulted by oblique-normal faults. Koçyiğit et al. (2003) propose that the ~300 m thick Early – Middle Miocene sequence is deformed during a period of compression between a first and second phase of extensional deformation. Folds of this sequence are series of WNW-trending, (sub-) parallel anti- and synclines.

Folds or thrust or any indications for compressional deformation in the Ilgin Basin region are absent. The observations made by Koçyiğit et al. (2003) described earlier were obtained from outcrops in the Akşehir-Afyon Basin, almost 100 km to the NW of the Ilgin Basin, along the Sultandağı range. Extrapolation of these observations in southeastern direction towards the Ilgin basin can be considered speculative. It is possible that the Early-Middle Miocene sediments of the Akşehir-Afyon Basin are only locally folded as a result of partitioning of strain accommodating local transpression along the Akşehir Fault zone adjacent to the Sultandağı range.

The left-lateral transtensional kinematic model inferred for the Ilgin Basin is not aligned and therefore difficult to correlate with the deformation kinematics of Late Cenozoic fault zones to the east and northeast. The Eskişehir Fault zone, located at ~200 km to the northeast of the Ilgin and Akşehir-Afyon basins (see Figure.), has a parallel, NW-SE to WNW-ESE trend (Ocakoglu, 2007). Very little is known about the structural style and deformation kinematics of this fault zone, and its southern end in particular seems to be largely unexplored. The Eskişehir Fault zone (also called the İnönü-Eskişehir Fault zone) seems to be a branch from the dextral North Anatolian Fault Zone (NAFZ) and consists of arrays of NW-SE trending dextral strike-slip faults, as well as E-W to WNW-ESE segments (Ocakoglu, 2007). Other major fault zones in Central Anatolia are the NW-SE trending Tuzgölü, Cihanbeyli and Yeniceoba Fault zones (e.g., Gorur et al., 1984; Çemen et al., 1999). These presumably extensional to transtensional fault zones and the development of the large, extensional or transtensional Tuzgölü Basin have their origin in the Late Maastrichtian (e.g., Görür et al., 1984; Çemen et al., 1999), and continued their activity into Miocene time (Dellaloğlu and Aksu, 1984; Pasquare et al., 1988; Dirik and Goncuoğlu, 1996). The Tuzgölü Fault zone is reported as a 200 km long, right-lateral strike-slip fault, consisting of an en-echelon pattern of fault segments (e.g., Dirik and Goncuoğlu, 1996) and has been repeatedly reactivated, with the most recent normal to right-lateral displacements recorded for the post-Eocene (Çemen et al., 1999).

Both the major NW-SE trending Eskişehir and Tuzgölü (and smaller Chanbeyli and Yeniceoba) Fault zones are reported as extensional to transtensional fault systems with right-lateral displacements. The trends of these fault zones are parallel to the Akşehir Fault zone extending along the Ilgin and Akşehir-Afyon basins. The main question is how the left-lateral transtensional boundary fault system of the Ilgin Basin (likely continuous into the fault zone of the Akşehir-Afyon basin) fits with the right-lateral Eskişehir and Tuzgölü fault zones. Structural basement inheritance and the effects of strain partitioning discussed earlier must

have significant impacts on the kinematics and fault patterns in Central Anatolia. Accordingly, extrapolation of interpretations from one 'nested' structural domain to the next, to regional Anatolian scale or plate-tectonic scale, is a challenging step prone to unjustified interpretations. Taking into account the speculative character of such extrapolations, an attempt is made below to explain the findings of the Ilgin Basin in a regional structural context.

After the southern branch of Neotethys reached its maximum size at some time in the middle Cretaceous (e.g., Şengör et al., 1981; Dewey et al., 1989), convergence initiated between the African-Arabian plate moving north with respect to the southern boundary of Eurasia. The northern margin, characterized by , old, relatively cold continental crust is a major constraint on the structural setting of the Late Cenozoic Ilgin Basin. It is likely that the continental margin of the approaching Africa-Arabian plate was not a straight but rather irregular boundary, with a major embayment at the African-side in the west and a major salient at the Arabian-side in the east. The broad promontory of Arabian continental crust acted as a prominent collisional indenter to the active plate margin of Eurasia, including the Anatolian assembly, which forms the basement of the Ilgin Basin. Together with the Isparta Angle, the location of the Ilgin Basin and its continuation into the Akşehir-Afyon Basin coincides with the longitude of the lateral boundary between embayment and salient of the involved northern Gondwana continental margin.

The initial geometry of the continental margin of Gondwana has implications for inherited structural trends and deformation kinematics in Eastern and Central Anatolia, including the Ilgin Basin region. Because of the irregularities between continental and oceanic crust along the plate margins, continent-continent collision between Arabia and Eurasia initiated during the Miocene (Keskin, 2003; Facenna et al., 2006; Hafkenscheid et al., 2006; Hüsing et al., 2009), while oceanic crust is still subducting along the oceanic margin of the African plate. At this side, an increasingly land-locked oceanic basin is formed (e.g., van Hinsbergen et al., 2009).

Relative northward movement of the irregular indenter of buoyant continental Arabia has a prominent impact on the Late Cenozoic to present-day kinematics of the Ilgin Basin. Collision between the Gondwana continental crust and its variably segmented fragments along Anatolia takes place in the course of the Late Cenozoic, leading to the major Bitlis-Zagros Suture Zone. The Arabian continental boundary and its inherent basement anisotropies have imposed a significant right-lateral strike-slip sense of motion, particularly resolved on NW-SE structural trends. This right-lateral sense of shear accommodates the differential plate

movement of Africa and Arabia with respect to Eurasia. The relatively northward motion of Arabia imposes continent-continent collision, coeval with ongoing subduction of the African plate under the Eurasian assembly, including Central Anatolia.

It is possible that the NW-SE basement trends, including the Eskişehir, Tuzgölü and Akşehir Fault zones located in Central Anatolia are signatures of this early continent-continent collisional process during the Oligo-Miocene. The North Anatolian and East Anatolian Fault zones, and most likely also the Central Anatolian Fault Zone are formed much later, during the Pliocene, and accommodate the westward, lateral extrusion of Anatolia with respect to Eurasia in response to continuing convergence between the Arabian continental promontory and Eurasia. Northward oceanic subduction at the African oceanic embayment resulted in roll-back of a southerly advancing, curved Hellenic Arc causing back-arc extensional/transensional collapse in the Aegean region and West Anatolia (e.g., van Hinsbergen et al., 2009, 2010).

Well before the Late Cenozoic (Late Miocene to recent) evolution of the Ilgin basin, the effects of roll-back in the west and continent-continent collision in the east have a profound effect on Central Anatolia. The right-lateral effects along the NW-SE trends along the Tozgolü, Cihanbeyli and Yeniceoba Fault zones are well explained by the kinematics of this differential advance in major continent-continent collision. Similar right-lateral effects are still acting today, in the strain partitioning of right-lateral strike-slip along the NW-SE Zagros deformation belt (e.g., Tavakoli et al., 2008). The westward lateral escape of Anatolia in (e.g. van Hinsbergen et al., 2009), largely accommodated along the NAFZ and the EAFZ initiated at some time in middle to late Miocene (Dewey & Sengör, 1979) or during the latest Miocene to Early Pliocene (e.g., Barka et al., 2000) and is an important accelerator to extension, controlling accommodation space in the local Ilgin Basin setting. A progressive northward advancing, left-lateral shear zone associated with the opening of the Red Sea between Africa and Arabia, initiated (or was reactivated) during the same period and is still active at present. This Late-Miocene – present timing of interference and overlap in regional-scale kinematics may be regarded as a major factor contributing to the left-lateral relay in the Ilgin Basin.

6. Conclusions

The Ilgin Basin is a Late Cenozoic transtensional, fault-controlled depression developed on top of Late Mesozoic-Early Cenozoic substratum in Central Anatolia. Fault geometries and kinematic analysis indicate that the basin is influenced by a small (but geometrically significant) left-lateral shear component. It is difficult to interpret this lateral shear component in the regional setting of the basin because of the presence of a multitude of contemporaneous, hard-linked fault trends and the effects of strain partitioning. The origin for the multitude of prominent structural trends in both Pre-Cenozoic basement and Late Miocene to recent lacustrine basin sediments lies in the presence of pre-existing basement structures giving rise to anisotropy and mechanical interaction between intersecting faults systems.

Conventional inversion methods are commonly used to reconstruct the paleo-stress history of regions in Central Anatolia, similar to the Ilgin Basin setting. The present study leads to conclude that extrapolations of paleostress data to larger regional or plate tectonic scales should be made with caution.

Acknowledgements

I thank Prof. Dr. Reinoud L. M. Vissers and N. Kaymakci for their support in the field and for their constructive comments and discussions. I am grateful for the assistance of A. Koç and E. Gulyuz in the field and I thank N. Kaymakci for his hospitality. This study was financed by the Molengraaff Fonds from the TU Delft.

References

- Acocella, V., Morvillo, P., Funicello, R. 2005. What controls relay ramps and transfer faults within rift zones? Insights from analogue models. *Journal of Structural Geology* 27, 397-408.
- Aktuğ, B., Kaypak, B., Çelik, R. N. 2010. Source parameters for the Mw = 6.6, 03 Februari 2002, Çay Earthquake (Turkey) and aftershocks from GPS, Southwestern Turkey. *J. Seismol* 14, 445-456. DOI 10.1007/s10950-009-9174-y.
- Alçıçek, M. C. 2001. Sedimentological investigation of Çameli Basin (Late Miocene–Late Pliocene, Denizli, SW Anatolia). PhD thesis, Ankara University, Ankara, Turkey.
- Alçıçek, M. C., Kazancı, N., Özkul, M. 2005. Multiple rifting pulses and sedimentation pattern in the Çameli Basin, southwestern Anatolia, Turkey. *Sedimentary Geology*, 173, 409-431.
- Altunel, E., Barka, A. & Akyüz, S. 1999. Paleoseismology of the Dinar fault, SW Turkey. *Terra Nova* 11, 297-302.
- An, L., Sammis, C. G. 1996. A cellular automaton for the development of crustal shear zones. *Tectonophysics* 253, 247-270.
- Anderson, E. M. 1951. *The Dynamics of Faulting and Dyke Formation with Applications to Britain*, Oliver and Boyd, Edinburgh.
- Angelier, J. 1979. Determination of the mean principal directions of stress for a given fault population. *Tectonophysics* 56, T17– T26.
- Angelier, J. 1984. Tectonic analysis of fault-slip data sets. *Journal of Geophysical Research* 89, 5835–5848.
- Angelier, J. 1990. Inversion of field data in fault tectonics to obtain regional stress. III. A new rapid direct inversion method by analytical means. *Geophysical Journal International* 103, 363–376.
- Angelier, J. 1994. Fault slip analysis and paleostress reconstruction. In: Hancock, P.L. (Ed.), *Continental Deformation*. Pergamon Press, Oxford, pp. 53–100.
- Barka, A. A., Reilinger, R. E., Şaroğlu, F. & Şengör, A.M.C. 1995. Isparta Angle: its importance in the neotectonics of the Eastern Mediterranean Region. In: Pişkn, D., Ergün, M., Savaşın, M.Y. & Tarcan, G. (eds), *International Earth Science Colloquium on the Aegean Region Proceedings*, 3-18.
- Barka, A. A., Reilinger, R. 1997. Active tectonics of the Mediterranean region: deduced from GPS, neotectonic and seismicity data. *Annali di Geophys.* XI, 587–610.
- Barka, A. A., Serdar, Akyüz, H. S., Cohen, H. A., Watchorn, F. 2000. Tectonic evolution of the Nixsar and Tasova-Erbaa pull-apart basins, North Anatolian Fault Zone: their significance for the motion of the Anatolian block. *Tectonophysics* 322, 243-264.
- Becker-Platen, J. D. 1970. *Lithostratigraphische Untersuchungen im Känozoikum Südwest Anatoliens (Türkei)-(Känozoikum und Braunkohlen der Türkei)-Beihefte zum. Geol. Jahrb.* 97. 244 pp., Hannover.
- Besang, C., Eckhardt, F. J., Harre, W., Kreuzer, H. & Müller, P. 1977. Radiometrische Altersbestimmungen an Neogenen eruptivgesteinen der Türkei. *Geologisches Jahrbuch* B25, 3–36.
- Boray, A., Şaroğlu, F. & Emre, Ö. 1985. Isparta Büklümünün kuzey kesiminde D-B daralma için bazı veriler [Evidence for E-W shortening in the north of Isparta Angle]. *Jeoloji Mühendisliği* 23, 9-20.
- Bott, M. H. P. 1959. The mechanics of oblique slip faulting, *Geol. Mag.*, 96, 109-117.

- Bozkurt E., Koçyiğit A. 1996. The Kazova basin: an active negative flower structure on the Almus Fault Zone, a splay fault system of the North Anatolian Fault Zone, Turkey, *Tectonophysics* 265, 239–254.
- Bozkurt, E. 2000. Timing of extension on the Büyük Menderes Graben, western Turkey, and its tectonic implications. In: Bozkurt, E., Winchester, J. A., Piper, J. D. A. (eds.), *Tectonics and Magmatism in Turkey and the Surrounding Area*, Spec. Pub. Geological Society vol. 173. Blackwell, London, pp. 385–403.
- Bozkurt, E. 2001. Neotectonics of Turkey – a synthesis. *Geodynamica Acta* 14, 3–30.
- Bozkurt, E. & Oberhänsli, R. 2001. Menderes Massif (Western Turkey): structural, metamorphic and magmatic evolution - a synthesis. *International Journal of Earth Sciences*, 89, 679–708.
- Blumenthal, M. 1963. Le système structural du taurus sudanatolien. In: livre à la mémoire du professeur Paul Fallot. *Mém. Hors-sér.-Soc. géol. Fr.*, 611 – 662.
- Carey, E., Brunier, B. 1974. Analyse théorique et numérique d'une modèle mécanique élémentaire appliqué à l'étude d'une population de failles. *Comptes Rendus de l'Académie des Sciences Series D* 279, 891–894.
- Çemen, I., Gönüoğlu, M. C., Dirik, K. 1999. Structural Evolution of the Tüzgözü Basin in Central Anatolia, Turkey. *The Journal of Geology* 107, 693–706.
- Childs, C., S. J. Easton, B. C. Vendeville, M. P. A. Jackson, S. T. Lin, J.J. Walsh, and J. Watterson. 1993. Kinematic analysis of faults in a physical model of growth faulting above a viscous salt analogue, *Tectonophysics*, 228, 313–329.
- Coulomb, C. A. 1773. Sur une application des règles de Maximis et Minimis a quelques problèmes de statique relatifs à l'Architecture, *Acad. Roy des Sciences de math et de physique par divers savans*, vol. 7, pp. 343–382.
- Dellaloğlu, A., Aksu, R., 1984. Geology and hydrocarbon potential of Kulu, Sereflikochisar and Aksaray. Turkish Petroleum Corporation Report 2020.
- DeMets, C., Gordon, R. G., Argus, D. F., Stein, S. 1990. Current plate motions. *Geophys. J. Inter.* 102, 425–478.
- DeMets, C., Gordon, R. G., Argus, D. F., Stein, S. 1994. Effects of recent revisions to the geomagnetic reversal time scale on estimates of current plate motions. *Geophys. Res. Lett.* 21, 2191–2194.
- DePaola, N., Holdsworth, R. E., McCaffrey, K. J. W., Barchi, M. R. 2005. Partitioned transtension: an alternative to basin inversion models. *Journal of Structural Geology* 27, 607–625.
- Dewey, J. F. & Sengör, A. M. C. 1979. Aegean and surrounding regions: Complex multiplate and continuum tectonics in a convergent zone. *Geological Society of America Bulletin*, 90, 84–92.
- Dewey, F. J., Hempton, M. R., Kidd, W. S. F., Şaroğlu, F. & Şengör, A. M. C. 1986. Shortening of continental lithosphere: the neotectonics of eastern Anatolia – a young collision zone. In: Coward, M. P. & Ries, A. C. (eds) *Collision Tectonics*, Geological Society, London, Special Publication, 19, 3–36.
- Dewey J. F., Helman M. L., Turco E., Hutton D. H. W., Knott S. D. 1989. Kinematics of the western Mediterranean, in: Coward M.P., Dietrich D., Park R.G. (Eds.), *Alpine Tectonics*, Geological Society Special Publication no. 45, Geological Society, London, pp. 265–283.
- Dewey, J. F., Holdsworth, R. E., Strachan, R. A. 1998. Transpression and transtension zones, in: Holdsworth, R.E., Strachan, R.A., Dewey, J.F. (Eds.), *Continental Transpressional and Transtensional Tectonics* Geological Society, London, Special Publications, 135, pp. 1–14.
- Dewey, J. F. 2002. Transtension in arcs and orogens. *International Geology Review* 44, 402–439.

- Dilek, Y. & Altunkaynak, S. 2009. Geochemical and temporal evolution of Cenozoic magmatism in western Turkey: Mantle response to collision, slab breakoff, and lithospheric tearing in an orogenic belt. In: Van Hinsbergen, D. J. J., Edwards, M. A. & Govers, R. (eds) *Geodynamics of collision and collapse at the Africa–Arabia–Eurasia subduction zone*. Geological Society, London, Special Publications, 311, 000–000.
- Dirik, K., Goncuoğlu, M. C. 1996. Neotectonic characteristics of central Anatolia *International Geology Review* 38, 807–817.
- Doblas, M. 1998. Slickenside kinematic indicators. *Tectonophysics* 295, 187–197.
- Dupoux, B. 1983. Etude comparée de la tectonique néogène des bassins du sud de Chypre et du bassin d'Antalya (Turquie). Unpublished PhD thesis, Université de Paris-Sud Centre Orsay.
- Ebinger, C. J. 1989a. Tectonic development of the western branch of the East African Rift System. *Geological Society of America Bulletin* 101, 885–903.
- Ebinger, C. J. 1989b. Geometric and kinematic development of border faults and accommodation zones, Kivu–Rusizi Rift, Africa. *Tectonics* 8, 117–133.
- Edwards, M. A. & Grasemann, B. 2009. Mediterranean snapshots of accelerated slab retreat; subduction instability in stalled continental collision. In: Van Hinsbergen, D. J. J., Edwards, M. A. & Govers, R. (eds) *Geodynamics of collision and collapse at the Africa–Arabia–Eurasia subduction zone*. Geological Society, London, Special Publications, 311, 000–000.
- Erakman, B., Meşhur, M., Gül, M. A., Alkan, H., Öztaş, Y., Akpınar, M. 1982. Toros projesine bağlı Kalkan-Köyceğiz-Çameli-Tefenni arasında kalan alanın jeolojisi ve hidrokarbon olanakları raporu. Natural Oil and Gas Company of Turkey (TPAO), Technical Report no 1732, Ankara, Turkey.
- Ergin, M., Aktar, M., Özalaybey, S., Tapirdamaz, M. C., Selvi, O., Tarancıoğlu, A. 2009. A high-resolution aftershock seismicity image of the 2002 Sultandağı-Çay earthquake (Mw = 6.2), Turkey. *J. Seismol* 13, 633–646. DOI 10.1007/s10950-009-9155-1.
- Etchecopar, A., Vasseur, G., Daignieres, M. 1981. An inverse problem in microtectonics for the determination of stress tensors from fault striation analysis. *Journal of Structural Geology* 3, 51–65.
- Faccenna, C., Bellier, O., Martinod, J., Piromallo, C. & Regard, V. 2006. Slab detachment beneath eastern Anatolia: A possible cause for the formation of the North Anatolian Fault. *Earth and Planetary Science Letters*, 242, 85–97.
- Flecker, R., Robertson, A. H. F., Poisson, A., Müller, C. 1995. Facies and tectonic significance of two contrasting Miocene basins in south coastal Turkey. *Terra Nova* 7, 221–232.
- Flecker, R., Poisson, A., Robertson, A.H.F., 2004. Facies and palaeogeographic evidence for the Miocene evolution of the Isparta Angle in its regional eastern Mediterranean context. *Sedimentary Geology* 173, 277–314.
- Frizon de Lamotte, D., Poisson, A., Aubourg, C., Temiz, H. 1995. Chevauchements post-tortonien vers l'ouest puis vers le sud au coeur de l'angle d'isparta (taurus, turquie). conséquences géodynamiques. *Bull. Soc. Géol. Fr.* 161 (1), 59–67.
- Gautier, P., Brun, J. P. & Jolivet, L. 1993. Structure and kinematics of Upper Cenozoic extensional detachment on Naxos and Paros. *Tectonics*, 12, 1180–1194.
- Gautier, P. & Brun, J. P. 1994. Ductile crust exhumation and extensional detachments in the central Aegean (Cyclades and Evvia Islands). *Geodinamica Acta*, 7, 57–85.
- Geological map of Ilgin – L27 & L28 quadrangle, scale 1:100.000, MTA, General Directorate of Mineral Research and Exploration, 2009.
- Geological map of Turkey, scale: 1/500.000, General Directorate of Mineral Research and Exploration 2002.

- Gessner, K., Ring, U., Johnson, C., Hetzel, R., Passchier, C. W. & GÜngör, T. 2001. An active bivergent rolling-hinge detachment system: Central Menderes metamorphic core complex in western Turkey. *Geology*, 29, 611–614.
- Glover, C. P., Robertson, A. H. F. 1998a. Role of regional extension and uplift in the Plio–Pleistocene evolution of the Aksu Basin, SW Turkey. *J. Geol. Soc. (Lond.)* 155, 365–387.
- Glover, C. P., Robertson, A. H. F. 1998a. Neotectonic intersection of the Aegean and Cyprus tectonic arcs: extensional and strike-slip faulting in the Isparta Angle, SW Turkey. *Tectonophysics* 298, 103–132.
- Glover, C. P., Robertson, A. H. F. 1998b. Role of regional extension and uplift in the Plio–Pleistocene evolution of the Aksu Basin, SW Turkey. *J. Geol. Soc. (Lond.)* 155, 365–387.
- Goguel, J. 1952. *Traité de Tectonique*. Masson, Paris. Translated by Thalmann, H.E. (1962). *Tectonics*. Freeman, San Francisco.
- Görsöy, H., Piper, J. D. A., Tatar, O. 2003. Neotectonic deformation in the western sector of tectonic escape in Anatolia: palaeomagnetic study of the Afyon region, central Turkey. *Tectonophysics*, 374, 57–79.
- Görür, N., Oktay, F.Y., Seymen, I., Sengor, A.M.C. 1984. Palaeotectonic evolution of the Tuzgözü Basin complex, central Turkey: sedimentary record of a Neotethyan closure. In: Dixon, J.E., Robertson, A.H.F. (Eds.), *The Geological Evolution of the Eastern Mediterranean*. Geological Society, London, Special Publications 17, pp. 467–482.
- Govers, R. & Wortel, M. J. R. 2005. Lithosphere tearing at STEP faults: Response to edges of subduction zones. *Earth and Planetary Science Letters*, 236, 505–523.
- Griffiths, P. S. 1980. Box-fault systems and ramps: atypical associations of structures from the eastern shoulder of the Kenya Rift. *Geological Magazine* 117, 579–586.
- Hafkenscheid, E., Wortel, M. J. R. & Spakman, W. 2006. Subduction history of the Tethyan region derived from seismic tomography and tectonic reconstructions. *Journal of Geophysical Research*, 111, B08401, doi: 10.1029/2005JB003791.
- Hancock, P.L., 1985. Brittle microtectonics: principles and practice. *Journal of Structural Geology* 7, 437–457.
- Harland, W. B. 1971. Tectonic transpression in Caledonian Spitzbergen. *Geological Magazine* 108, 27–42.
- Healy, D., Jones, R. R., Holdsworth, R. E. 2006. New insights into the development of brittle shear fractures from a 3-D numerical model of microcrack interaction. *Earth and Planetary Science Letters* 249, 14–28.
- Hubert-Ferrari, A., Armijo, R., King, G., Meyer, B. & Barka, A. 2002. Morphology, displacement, and slip rates along the North Anatolian Fault, Turkey. *Journal of Geophysical Research*, 107, 2235, doi: 10.1029/2001JB000393.
- Hubert-Ferrari, A., King, G., Vand der Woerd, J., Villa, I., Altunel, E. & Armijo, R. 2009. Long-term evolution of the North Anatolian Fault: new constraints from its eastern termination. In: Van Hinsbergen, D. J. J., Edwards, M. A. & Govers, R. (eds) *Geodynamics of collision and collapse at the Africa–Arabia–Eurasia subduction zone*. Geological Society, London, Special Publications, 311, 000–000.
- Huggins, P., Watterson, J., Walsh, J. J., Childs, C. 1995. Relay zone geometry and displacement transfer between normal faults recorded in coal-mine plans. *Journal of Structural Geology* 17, 1741–1755.
- Hüsing, S. K., Van Zachariasse, W. J., Van Hinsbergen, D. J. J., Krijgsman, W., Inceöz, M., Harzhauser, M., Mandic, O. & Kroh, A. 2009. Oligocene–Miocene basin evolution in SE Anatolia, Turkey: constraints on the closure of the eastern Tethys gateway. In: Van Hinsbergen, D. J. J., Edwards, M. A. & Govers, R. (eds) *Geodynamics of collision and collapse at the Africa–Arabia–Eurasia subduction zone*. Geological Society, London, Special Publications, 311, 000–000.

- İlgar, A., Nemec, W., 2004. Early Miocene lacustrine deposits and sequence stratigraphy of the Ermenek Basin, Central Taurides, Turkey. *Sediment. Geol.* 173.
- Jolivet, L. 2001. A comparison of geodetic and finite strain pattern in the Aegean, geodynamic implications. *Earth and Planetary Science Letters*, 187, 95–104.
- Jolivet, L., Facenna, C., Goffé, B., Burov, E. & Agard, P. 2003. Subduction tectonics and exhumation of high-pressure metamorphic rocks in the Mediterranean orogen. *American Journal of Science*, 303, 353–409.
- Jones, R. R., Tanner, P. W. G. 1995. Strain partitioning in transpression zones. *Journal of Structural Geology* 17, 793–802.
- Jones, R. R., Holdsworth, R. E., McCaffrey, K. J. W., Clegg, P., Tavarnelli, E. 2005. Scale dependence, strain compatibility and heterogeneity of three-dimensional deformation during mountain building: a discussion. *Journal of Structural Geology* 27, 1190-1204.
- Karabıyıkoglu, M., Çiner, A., Monod, O., Deynoux, M., Tuzcu, S., Örcen, S. 2000. Tectonosedimentary evolution of the Miocene Manavgat Basin, western Taurides, Turkey. In: Bozkurt, E., Winchester, J. A., Piper, J. D. A. (Eds.), *Tectonics and Magmatism in Turkey and the Surrounding Area*, Spec. Pub.-Geological Society vol. 173. Blackwell, London, pp. 271–294.
- Kaymakci, N., White, S. H., van Dijk, P.M. 2000. Paleostress inversion in a multi-phase deformed area: kinematic and structural evolution of the Çankırı Basin (Central Turkey): Part 1. In: Bozkurt, E., Winchester, J. A., Piper, J. (Eds.), *Tectonics and Magmatism in Turkey and its Surroundings*. Geological Society London, Special Publication 173, pp. 445–473.
- Kaymakci, N., White, S. H., van Dijk, P. M. 2003b. Kinematic and structural development of the Çankırı Basin (Central Anatolia Turkey): a paleostress inversion study. *Tectonophysics* 364, 85–113.
- Kaymakci, N. 2006. Kinematic development and paleostress analysis of the Denizli Basin (Western Turkey): implications of spatial variation of relative paleostress magnitudes and orientations. *Journal of Asian Earth Sciences* 27, 207-222.
- Kaymakci, N., Ozelik, Y., White, S. H. & Van Dijk, P. M. 2009. Tectono-stratigraphy of the Çankırı Basin: Late Cretaceous to Early Miocene evolution of the Neotethyan suture zone in Turkey. In: Van Hinsbergen, D. J. J., Edwards, M. A. & Govers, R. (eds) *Geodynamics of collision and collapse at the Africa–Arabia–Eurasia subduction zone*. Geological Society, London, Special Publications, 311, 000–000.
- Kazancı, N., Nemec, W., İleri, Ö., Karadenizli, L., Christian, B.H. & Briseit, H. 1997. Palaeoclimatic significance of the Late Pleistocene deposits of Akşehir Lake, west-central Anatolia. In: *An International Symposium on the Late Quaternary in the Eastern Mediterranean*, Programme and Abstracts. General Directorate of Mineral Research and Exploration (MTA) Publications, 58-59.
- Keskin, M. 2003. Magma generation by slab steepening and breakoff beneath a subduction-accretion complex: An alternative model for collision-related volcanism in Eastern Anatolia, Turkey. *Geophysical Research Letters*, 30, 8046, doi: 10.1029/2003GL018019.
- Koçyiğit, A. 1996. Lakes region graben-horst system, SW Turkey: differential stretching and commencement age of the extensional neotectonic regime. In: Görür, N. (coordinator), *National Marine Geological and Geophysical Programme, Workshop-1, Istanbul, Extended Abstracts*, 99-103.
- Koçyiğit, A., Yusufoglu, H., Bozkurt, E. 1999. Evidence from the Gediz graben for episodic two-stage extension in western Turkey. *J. Geol. Soc. (Lond.)* 156, 605–616.
- Koçyiğit, A., Ünay, E., Saraç, G. 2000. Episodic graben formation and extensional neotectonic regime in west Central Anatolia and the Isparta Angle: a case study in the Akşehir-Afyon Graben, Turkey. In: Bozkurt, E., Winchester, J.A., Piper, J. D. A. (eds.),

- Tectonics and Magmatism in Turkey and the Surrounding Area, Spec. Pub. Geological Society vol. 173. Blackwell, London, pp. 405– 421.
- Koçyiğit, A., Özacar, A. 2003. Extensional Neotectonic Regime through the NE Edge of the Outer Isparta Angle, SW Turkey: New Field and Seismic Data. *Turkish Journal of Earth Sciences*, 12, 67-90.
- Krantz, R.W. 1988. Multiple fault sets and three-dimensional strain: theory and application. *J. Struct. Geol.* 10, 225– 237.
- Larsen, P. H. 1988. Relay structures in a Lower Permian basement involved extension system, East Greenland. *Journal of Structural Geology* 10, 3– 8.
- Lisle, R.J. 1987. Principal stress orientations from faults: an additional constraint. *Ann. Tecton.* 1, 155– 158.
- Lister, G., Banga, G. & Feenstra, A. 1984. Metamorphic core complexes of Cordilleran type in the Cyclades. Aegean Sea, Greece. *Geology*, 12, 221–225.
- Macdonald, G. A. 1957. Faults and monoclines on Kilauea Volcano, Hawaii, *Bulletin of the Geological Society of America* 68, 269-271.
- Maerten, L., J. M. Willemsse, D. D. Pollard, and K. Rawnsley. 1999. Slip distribution on intersecting normal faults, *J. Struct. Geol.*, 21, 259-271.
- Maerten, L. 2000. Variations in slip on intersecting normal faults: Implications for paleostress inversion. *Journal of Geophysical Research* 105, 25553-25565.
- Mandl, G. 1988. *Mechanics of tectonic faulting, Models and Basic Concepts. Developments in Structural Geology*, 1. Elsevier Science Publishers. ISBN: 0-444-42946-8.
- Mansfield, C. S., and J. A. Cartwright. 1996. High resolution fault displacement mapping from three-dimensional seismic data: Evidence for dip linkage during fault growth, *J. Struct. Geol.*, 18, 249-263.
- McCalpin, J. P. 2009. *Paleoseismology – 2nd edition*. Vol 95, International Geophysics Series. ISBN: 978-0-12-373576-8.
- Means, W.D. 1987. A newly recognized type of slickenside striation. *J. Struct. Geol.* 9, 585– 590.
- Meşhur, M., Akpınar, M., 1984. Yatağan-Milas-Bodrum-Karacasu-Kale-Acıpayam-Tavas civarlarının jeolojisi ve petrol olanakları. Natural Oil and Gas Company of Turkey (TPAO), Technical report, no1963, Ankara, Turkey.
- Morley, C. K., Nelson, R. A., Patton, T. L., Munn, S. G. 1990. Transfer zones in the East African rift system and their relevance to hydrocarbon exploration in rifts. *Bulletin of the American Association of Petroleum Geologists* 74, 1234-1253.
- Nelson, R. A., Patton, T. L., Morley, C. K. 1992. Rift segment interaction and its relation to hydrocarbon exploration in rift systems. *Bulletin of the American Association of Petroleum Geologists* 76, 1153–1169.
- Nicol, A., J. Watterson, J. J. Walsh, and C. Childs. 1996. The shapes, major axis orientations and displacement patterns of fault surfaces, *J. Struct. Geol.*, 18, 235-248.
- Ocakoğlu, F. 2007. A re-evaluation of the Eskişehir Fault Zone as a recent extensional structure in NW Turkey. *Journal of Asian Earth Sciences* 31, 91-103.
- Oertel., G. 1965. The mechanism of faulting in clay experiments, *Tectonophysics* 2, 343–393.
- Öğdüm, F., Kozan, T., Bircan, A., Bozbay, E. & Tüfekçi, K. 1991. Sultandağları ile Çevresindeki Havzaların Jeomorfolojisi ve Genç Tectoniği [Geomorphology and Neotectonics of Basins in and around Sultandağları]. General Directorate of Mineral Research and Exploration (MTA) Report No. 9123.
- Oral, M. B., Reilinger, R. E., Toksöz, M. N., Kong, R. W., Barka, A. A., Kınık, İ., Lenk, O. 1995. Global positioning system offers evidence of plate motions in eastern Mediterranean. *EOS Transac.* 76 (9).

- Papanikolaou, D., Gouliotis, L. & Triantaphyllou, M. 2009. The Itea—Amfissa detachment: A pre-Corinth rift Miocene extensional structure in central Greece. In: Van Hinsbergen, D. J. J., Edwards, M. A. & Govers, R. (eds) *Geodynamics of collision and collapse at the Africa–Arabia–Eurasia subduction zone*. Geological Society, London, Special Publications, 311, 000–000.
- Pasquare, G., Poli, S., Vezzoli, L., Zanchi, A. 1988. Continental arc volcanism and tectonic setting in Central Anatolia. *Tectonophysics* 146, 217–230.
- Peacock, D. C. P., Sanderson, D. J. 1991. Displacements, segment linkage and relay ramps in normal fault zones. *Journal of Structural Geology* 13, 721–733.
- Peacock, D. C. P., Sanderson, D. J. 1994. Geometry and development of relay ramps in normal fault systems. *Bulletin of the American Association of Petroleum Geologists* 78, 147–165.
- Peacock, D. C. P., Parfitt, E. A. 2002. Active relay ramps and normal fault propagation on Kilauea Volcano, Hawaii. *Journal of Structural Geology* 24, 729–742.
- Peacock, D. C. P. 2003. Scaling of transfer zones in the British Isles. *Journal of Structural Geology* 25, 1561–1567.
- Pearce, J. A., Bender, J. F., De Long, S. E., Kidd, W. S. F., Low, P. J., Guner, Y., Şaroğlu, F., Yilmaz, Y., Moorbath, S. & Mitchell, J. G. 1990. Genesis of collision volcanism in Eastern Anatolia, Turkey. *Journal of Volcanology and Geothermal Research*, 44, 189–229.
- Pe-Piper, G. & Piper, D. J. W. 2002. *The igneous rocks of Greece. The anatomy of an orogen*. Berlin-Stuttgart, Gebrüder Borntraeger.
- Petit, J.-P., Laville, E. 1985. Morphology and microstructure of hydroplastic slickensides in sandstone. Program. Conference on Deformation Mechanisms in Sediments and Sedimentary Rocks. University College, London. Abstract.
- Platzman, E. S., Tapirdamaz, C. & Sanver, M. 1998. Neogene anticlockwise rotation of central Anatolia (Turkey): preliminary palaeomagnetic and geochronological results. *Tectonophysics* 299, 175–189.
- Poisson, A. 1977. *Recherches géologiques dans le Taurus occidental. Turquie. Thèse d'Etat*, Univ. Paris-Sud, Orsay.
- Poisson, A. 1984. The extension of the Ionian trough into southwestern Turkey. In: Dixon, J.E., Robertson, A. H. F. (eds.), *The Geological Evolution of the Eastern Mediterranean*, Spec. Publ.-Geol. Soc. Lond., vol. 17, pp. 241–250.
- Poisson, A., Wernli, R., Sagular, E. K., Temiz, H. 2003a. New data concerning the age of the Aksu Thrust in the south of the Aksu Valley, Isparta Angle (SW Turkey): consequences for the Antalya Basin and the eastern Mediterranean. *Geol. J.* 38 (3–4), 311–327.
- Price, S. P., Scott, B. C. 1991. Pliocene Burdur Basin, SW Turkey: tectonics, seismicity and sedimentation. *J. Geol. Soc. (Lond.)* 148, 345–354.
- Price, S. P., Scott, B. 1994. Fault-block rotations at the edge of a zone of continental extension; southwest Turkey. *J. Struct. Geol.* 16, 381–392.
- Reading, H. G. 1996. *Sedimentary Environments: Processes, Facies and Stratigraphy* – 3rd edition. Chapter 3. Blackwell Publishing company. ISBN: 978-0-6320-3627-1.
- Reches, Z. 1978. Analysis of faulting in three-dimensional strain field, *Tectonophysics* 47, 109–129.
- Reches, Z. 1983. Faulting of rocks in three-dimensional strain fields II. Theoretical analysis, *Tectonophysics* 95, 133–156.
- Reches, Z. 1987. Determination of the tectonic stress tensor from slip along faults that obey the Coloumb yield criterion. *Tectonics* 6, 849–861.
- Reilinger, R.E., McClusky, S. C., Oral, M. B., King, W., Toksöz, M. N. 1997. Global Positioning, System measurements of present-day crustal movements in the Arabian–Africa–Eurasia plate collision zone. *J. Geophys. Res.* 102, 9983–9999.

- Richard, P. D., Naylor, M. A., Koopman, A. 1995. Experimental models of strike-slip tectonics. *Petroleum Geoscience*, Vol 1, pp.71-80.
- Riedel, W. 1929. Zur Mechanik Geologischer Brucherscheinungen. *Zentralblatt für Mineralogie, Geologie und Paleontologie B*, 354–368.
- Ring, U. & Reishmann, T. 2002. The weak and superfast Cretan detachment, Greece: exhumation at subduction rates in extruding wedges. *Journal of the Geological Society of London*, 159, 225–228.
- Robertson, A. H. F., Woodcock, N. H. 1982. Sedimentary history of the south–western segment of the Mesozoic–Tertiary Antalya continental margin, south–western Turkey. *Ecolgae Geol. Helv.* 75, 517– 562.
- Robertson, A. H. F., Dixon, J.E. 1984. Introduction: aspects of the geological evolution of the eastern Mediterranean. In: Dixon, J.E., Robertson, A.H.F. (Eds.), *The Evolution of the Eastern Mediterranean*, Spec. Pub. Geological Society, vol. 17. Blackwell, London, pp. 1 – 74.
- Robertson, A. H. F., Clift, P. D., Degnan, P. J., Jones, G. 1991. Palaeogeographic and palaeotectonic evolution of the eastern Mediterranean Neotethys. *Palaeogeogr. Palaeoclimatol. Palaeoecol.* 87, 289– 343.
- Robertson, A.H.F. 1993. Mesozoic–Tertiary sedimentary and tectonic evolution of neotethyan carbonate platforms, margins and small ocean basins in the Antalya Complex, of southwest Turkey. *Spec. Publ. Int. Assoc. Sedimentol.* 20, 415–465.
- Robertson, A. H. F. 2000. Mesozoic-Tertiary tectonic-sedimentary evolution of a south Tethyan oceanic basin and its margins in southern Turkey. In: Bozkurt, E., Winchester, J. A. & Piper, J. D. A. (eds) *Tectonics and Magmatism in Turkey and the Surrounding Area*. Geological Society, London, Special Publications, 173, 97-138.
- Robertson, A. H. F., Parlak, O. & Ustaömer, T. 2009. Melange genesis and ophiolite emplacement related to subduction of the northern margin of the Tauride-Anatolide continent, central and western Turkey. In: Van Hinsbergen, D. J. J., Edwards, M. A. & Govers, R. (eds) *Geodynamics of collision and collapse at the Africa–Arabia–Eurasia subduction zone*. Geological Society, London, Special Publications, 311, 000–000.
- Sanderson, D. J., Marchini, W. R. D. 1984. Transpression. *Journal of Structural Geology* 6, 449–458.
- Şaroğlu, F., Emre, Ö. & Boray, A. 1987. Türkiye'nin Diri Fayları ve Depremselliği [Seismicity and Active Faults of Turkey]. General Directorate of Mineral Research and Exploration (MTA) Report No. 8174.
- Satur, N., Hurst, A., Cronin, B. T., Kelling, G., Gürbüz, K. 2000. Sand body geometry in a sand-rich, deep-water clastic system, Miocene Cingöz Formation of southern Turkey. *Mar. Pet. Geol.* 17, 239– 252.
- Sen, S. & Seyitoğlu, G. 2009. Magnetostratigraphy of early-middle Miocene deposits from E-W trending Alaşehir and Büyük Menderes grabens in western Turkey, and its tectonic implications In: Van Hinsbergen, D. J. J., Edwards, M. A. & Govers, R. (eds) *Geodynamics of collision and collapse at the Africa–Arabia–Eurasia subduction zone*. Geological Society, London, Special Publications, 311, 000–000.
- Şengör, A. M. C., Yılmaz, Y. 1981. Tethyan evolution of Turkey: a plate tectonic approach. *Tectonophysics* 75, 181– 241.
- Şengör, A. M. C., Görür, N., Şaroğlu, F. 1985. Strike-slip faulting and related basin formation in zones of tectonic escape: Turkey as a case study. In: Biddle, K.T., Christie-Blick, N. (eds) *Basin Formation and Sedimentation*, Society of Economic Paleontologists and Mineralogists Special Publications, 37, 227–264.

- Şengör, A. M. C., Özeren, S., Genç, T. & Zor, E. 2003. East Anatolian high plateau as a mantle support, North–South shortened domal structure. *Geophysical Research Letters*, 30, doi: 10.1029/2003GL017858.
- Sengör, A.M. C., Tüysüz, O., Imren, C., Sakinc M., Eyidogan, H., Görür, N., Le Pichon, X. & Rangin C. 2005. The North Anatolian Fault: a new look. *Annual Reviews in Earth and Planetary Sciences*, 33, 37–112.
- Seyitoğlu, G., Scott, B. C. 1996. The cause of N–S extensional tectonics in western Turkey: tectonic escape vs. back-arc spreading vs. orogenic collapse. *J. Geodyn.* 22, 145– 153.
- Seyitoğlu, G., 1997. Late Cenozoic tectono-sedimentary development of Selendi and Uşak–Güre basins: a contribution to the discussion on the development of east–west and north-trending basins in western Turkey. *Geol. Mag.* 134, 163–175.
- Smith, J.V., Durney, D. W. 1992. Experimental formation of brittle structural assemblages in oblique divergence. *Tectonophysics* 216, 235–253.
- Tanar, Ü., Gökçen, N. 1990. Mut-Ermenek tersiyer istifinin stratigrafisi ve paleontolojisi. *Bull. Miner. Res. Explor. Turkey* 110, 175– 181.
- Tatar O., Piper J. D. A., Gürsoy H. 2000. Palaeomagnetic study of the Erciyes sector of the Eceemis, Fault Zone: neotectonic deformation in the eastern part of the Anatolian Block. In: Bozkurt E., Winchester J. A., Piper J. D. A. (eds.), *Tectonics and magmatism in Turkey and the surrounding area*, Geological Society Special Publication no. 173, Geological Society, London, pp. 423–440.
- Tavakoli, F., Walpersdorf, A., Authemayou, C., Nankali, H .R., Hatzfield, D., Tatar, M., Djamour, Y., Nilforoushan, F., Cotte, N. 2008. Distribution of the right-lateral strike-slip motion from the Main Recent Fault to the Kazerun Fault System (Zagros, Iran): Evidence from present-day GPS velocities. *Earth and Planetary Science Letters* 275, 342-347.
- Taymaz, T. & Tan, O. 2001. Source parameters of June 6, 2000 Orta-ankırı (Mw=6.0) and December 15, 2000 Sultandaği-Akşehir (Mw=6.0) earthquakes obtained from inversion of teleseismic PandSH-body-waveforms. *Symposia on Seismotectonics of the North-Western Anatolia-Aegean and Recent Turkish Earthquakes*, Istanbul, Extended Abstracts, 96-107.
- Temiz, H., Poisson, A., Andrieux, J., Barka, A. 1997. Kinematics of the Plio-Quaternary Burdur–dinar cross-fault system in SW Anatolia. *Ann. Tecton.* 11 (1–2), 102– 113.
- ten Veen, J.H. 2004. Extension of Hellenic forearc shear zones in SW Turkey: the Pliocene–Quaternary deformation of the Eşen Çay Basin. *Journal of Geodynamics* 37, 181–204.
- ten Veen, J.H., Kleinspehn, K.L. 2002. Geodynamics along an increasingly curved convergent plate margin: Late Miocene–Pleistocene Rhodes, Greece. *Tectonics* 21, 8-1–8-21.
- Tikoff, B., Teyssier, C. 1994. Strain modelling of displacement field partitioning in transpressional orogens. *Journal of Structural Geology* 16, 1575–1588.
- Tirel, C., Gautier P., Van Hinsbergen, D. J. J. & Wortel, M. J. R. 2009. Sequential development of interfering metamorphic core complexes: numerical experiments and comparison with the Cyclades, Greece. In: Van Hinsbergen, D. J. J., Edwards, M. A. & Govers, R. (eds) *Geodynamics of collision and collapse at the Africa–Arabia–Eurasia subduction zone*. Geological Society, London, Special Publications, 311, 000–000.
- Uysal, Ş. 1995. Graben formation in the collisional belts: an example from SW Anatolia, Eşençay graben. In: Pişkin, Ö, Ergün, M., Savaşçın, M. Y. & Tarcan, G. (eds), *International Earth Sciences Colloquium on the Aegean Region Proceedings* 1, 273-287.
- van Hinsbergen, D. J. J. & Boekhout, F. 2009. Neogene brittle detachment faulting on Kos (E Greece): implications for a southern break-away fault of the Menderes metamorphic core complex (western Turkey). In: Van Hinsbergen, D. J. J., Edwards, M. A. & Govers, R. (eds) *Geodynamics of collision and collapse at the Africa–Arabia–Eurasia subduction zone*. Geological Society, London, Special Publications, 311, 000–000.

- van Hinsbergen, D. J. J., Edwards, M. A. & Govers, R. 2009. Geodynamics of collision and collapse at the Africa-Arabia-Eurasia subduction zone – an introduction. In: Van Hinsbergen, D. J. J., Edwards, M. A. & Govers, R. (eds) *Collision and Collapse at the Africa–Arabia–Eurasia Subduction Zone*. The Geological Society, London, Special Publications, 311, 1–7.
- van Hinsbergen, D.J.J., Dekkers, M.J., Bozkurt, E., Koopman, M. 2010b. Exhumation with a twist: paleomagnetic constraints on the evolution of the Menderes metamorphic core complex (western Turkey). *Tectonics* 29, TC3009. doi: 10.1029/2009TC002596.
- Verhaert, G., Similox-Tohon, D., Vandycke, S., Sintubin, M., Muechez, P. 2006. Different stress states in the Burdur-Isparta region (SW Turkey) since Late Miocene times: a reflection of a transient stress regime. *Journal of Structural Geology* 28, 1067-1083.
- Waldron, J. W. F. 1984. Evolution of carbonate platforms on a margin of the Neotethys ocean: Isparta Angle, southwestern Turkey. *Ecolgae Geol. Helv.* 77, 553– 582.
- Wallace, R. E. 1951. Geometry of shearing stress and relation to faulting, *J. Geol. Chicago*, 59, 118-130.
- Walsh, J.J., Watterson, J. 1991. Geometric and kinematic coherence and scale effects in normal fault systems. In: Roberts, A.M., Yielding, G., Freeman, B. (Eds.), *The Geometry of Normal Faults*. Geological Society Special Publications, vol. 56, pp. 193– 203.
- Willemsse, J. M., D. D. Pollard, and A. Aydin. 1996. Three-dimensional analyses of slip distribution on normal fault arrays with consequences for fault scaling, *J. Struct. Geol.*, 18, 295-309.
- Withjack, M. O., Jamison, W. R. 1986. Deformation produced by oblique rifting. *Tectonophysics* 126, 99–124.
- Woodcock, N. H., Robertson, A. H. F. 1977. Origins of some ophiolite-related metamorphic rocks of the ‘Tethyan’ belt. *Geology* 3, 373– 376.
- Woodcock, N. H. 1986. The role of strike-slip fault systems at plate boundaries. *Philosophical Transaction of the Royal Society of London A317*, 13–29.
- Yilmaz, A., Yilmaz, H., 2006. Characteristic features and structural evolution of a post collisional basin: The Sivas Basin, Central Anatolia, Turkey. *Journal of Asian Earth Sciences* 27, 164-176.
- Zanchi, A., Kissel, C., TapVrdamaz, C. 1993. Late Cenozoic and Quaternary brittle continental deformation in western Turkey. *Bull. Soc. Géol. Fr.* 164, 507–517.